

KAMILA CABRAL MIELKE

**SUGARCANE STRAW BIOCHAR AND COW BONECHAR: PHYSICAL-
CHEMICAL CHARACTERIZATION AND INTERFERENCE ON THE BEHAVIOR OF
METRIBUZIN IN SOIL AND WATER**

Thesis submitted to the Crop Science
Graduate Program of the Universidade
Federal de Viçosa in partial fulfillment of the
requirements for the degree of *Doctor
Scientiae*.

Adviser: Kassio Ferreira Mendes

**VIÇOSA - MINAS GERAIS
2023**

**Ficha catalográfica elaborada pela Biblioteca Central da Universidade
Federal de Viçosa - Campus Viçosa**

T

M631s
2023 Mielke, Kamila Cabral, 1993-
Sugarcane straw biochar and cow bonechar:
physical-chemical characterization and interference on the
behavior of metribuzin in soil and water / Kamila Cabral Mielke.
– Viçosa, MG, 2023.

1 tese eletrônica (71 f.): il. (algumas color.).

Texto em inglês.

Inclui anexo.

Orientador: Kássio Ferreira Mendes.

Tese (doutorado) - Universidade Federal de Viçosa,
Departamento de Agronomia, 2023.

Inclui bibliografia.

DOI: <https://doi.org/10.47328/ufvbbt.2023.520>

Modo de acesso: World Wide Web.

1. Fitorremediação. 2. Solos - Movimento de herbicidas.
3. Solos - Descontaminação. I. Mendes, Kássio Ferreira, 1990-.
II. Universidade Federal de Viçosa. Departamento de
Agronomia. Programa de Pós-Graduação em Fitotecnia.
III. Título.

CDD 22. ed. 628.55


KAMILA CABRAL MIELKE

SUGARCANE STRAW BIOCHAR AND COW BONECHAR: PHYSICAL-CHEMICAL CHARACTERIZATION AND INTERFERENCE ON THE BEHAVIOR OF METRIBUZIN IN SOIL AND WATER


Thesis submitted to the Crop Science Graduate Program of the Universidade Federal de Viçosa in partial fulfillment of the requirements for the degree of *Doctor Scientiae*.

APPROVED: July 25, 2023.

Assent:

Documento assinado digitalmente
 **KAMILA CABRAL MIELKE**
Data: 28/08/2023 18:08:01-0300
Verifique em <https://validar.iti.gov.br>

Kamila Cabral Mielke
Author

Documento assinado digitalmente
 **KASSIO FERREIRA MENDES**
Data: 28/08/2023 18:43:30-0300
Verifique em <https://validar.iti.gov.br>

Kassio Ferreira Mendes
Adviser

*To God, my parents and brothers for their
teachings and my friends for their support
I dedicate.*

ACKNOWLEDGEMENTS

To God, for my life, and for helping me overcome all the obstacles encountered along the way.

To my parents, Lucy Moreira Cabral Mielke and José Antônio Mielke, for all the teachings, understanding, and support in difficult times, and for understanding my absence while I dedicated myself to fulfilling my dreams.

To my siblings and all other family members, for their support and affection. To all the professors and staff at UFV, for their assistance and teachings. In particular, to Professor Kassio Ferreira Mendes, for his friendship, guidance, and trust during my doctoral studies. The completion of this cycle was only possible thanks to his guidance and dedication.

To all the members of the Integrated Weed Management group, for the companionship, friendship, and assistance during the execution of the experiments. I have undoubtedly learned a lot from all of you and I am very proud to have been part of this group.

To the Federal University of Viçosa, for the opportunity to complete the postgraduate course.

This research was funded by Coordination for the Improvement of Higher Education Personnel (CAPES - 88887.479265/2020-00).

To the Foundation for Research Support of the State of Minas Gerais (FAPEMIG - 2070.01.0004768/2021-84).

To the National Council for Scientific and Technological Development (CNPq - 404240/2021-6).

ABSTRACT

MIELKE, Kamila Cabral, D.Sc., Universidade Federal de Viçosa, July 2023. **Sugarcane straw biochar and cow bonechar: physical-chemical characterization and interference on the behavior of metribuzin in soil and water.** Advisor: Kassio Ferreira Mendes.

The pyrolysis temperature in biochar production and the application rate in soil can influence the sorption, desorption, and degradation of herbicides, as well as soil fertility. The objective of the study was to investigate the effect of soil amendment with different pyrolysis temperature-produced sugarcane straw biochar application rates on the behavior of metribuzin and soil fertility. A second objective was the production of a cellulose acetate film with cow bonechar as a viable alternative for metribuzin removal from water. The treatments for the sorption-desorption and degradation studies of metribuzin consisted of three pyrolysis temperatures (BC350 °C, BC550 °C, and BC750 °C) and seven application rates (0, 0.1, 0.5, 1, 1.5, 5, and 10 % w/w). The treatments for the metribuzin removal from water study consisted of 2 and 3 g of bonechar fixed in the cellulose acetate film, pure powdered bonechar (2 g), and a control (without bonechar addition). Metribuzin quantification in soil and water was performed using High Performance Liquid Chromatography (HPLC). The amended soil with different application rates showed a reduction in H + Al and an increase in pH, OC, P, K, Ca, Mg, Fe, Mn, CEC, and BS. Metribuzin sorption and desorption coefficient (K_f) were 1.42 and 0.78 $\text{mg}^{(1-1/n)} \text{L}^{1/n} \text{Kg}^{-1}$, respectively, for the unamended soil. Biochar application rates <1 % sorbed ~23 % and desorbed ~15 % of metribuzin, similar to the unamended soil, for all pyrolysis temperatures. Amended soil with a 10 % application rate of BC350 °C, 550 °C, and 750 °C sorbed 63.8 %, 75.5 %, and 89.4 % and desorbed 8.3 %, 5.8 %, and 3.7 % of metribuzin, respectively. The values of degradation half-life time, DT_{50} and DT_{90} , for metribuzin in unamended soil were 7.37 and 24.94 days, respectively. The soil amended with 10% of BC350 °C increased metribuzin DT_{50} from 7.35 to 17.32 days and DT_{90} from 24.41 to 57.26 days compared to the unamended soil. The lower application rates (0.1 to 1.5 %) of BC550 °C and BC750 °C decreased metribuzin DT_{50} to ~4.05 and ~5.41 days, respectively. The amended soil with BC350 °C at high application rates (5 and 10 %) provided high microbial respiration rate (C-CO₂), low carbon fixation of microbial biomass (MBC) and

high metabolic rate ($q\text{CO}_2$). The addition of 2 and 3 g of bonechar fixed in the cellulose acetate film sorbed 40 % and 60 %, respectively, of metribuzin at lower concentrations (0.25, 0.33, and 0.5 mg L⁻¹). At higher concentrations of 1.0 and 2.0 mg L⁻¹, sorption was 16% and 50% of metribuzin for the addition of 2 and 3 g of bonechar fixed in the cellulose acetate film, respectively. High pyrolysis temperature and application rates of sugarcane straw biochar demonstrate the ability to immobilize metribuzin, improve soil fertility, and increase metribuzin degradation in soil, which can influence weed control effectiveness. The acetate film with bonechar was efficient in metribuzin removal, with only a loss of sorptive capacity compared to pure bonechar observed.

Keywords: Environmental remediation. Herbicide. Natural polymer. Carbonaceous material. Behavior.

RESUMO

MIELKE, Kamila Cabral, D.Sc., Universidade Federal de Viçosa, julho de 2023. **Sugarcane straw biochar and cow bonechar: physical-chemical characterization and interference on the behavior of metribuzin in soil and water.** Orientador: Kassio Ferreira Mendes.

A temperatura de pirólise na produção de *biochar* e a taxa de aplicação no solo podem influenciar na sorção, dessorção e degradação dos herbicidas e na fertilidade do solo. O objetivo do estudo foi investigar o efeito de modificações no solo com taxas de aplicação do *biochar* de palha de cana-de-açúcar produzido em diferentes temperaturas de pirólise sobre o comportamento do metribuzin e fertilidade do solo. Um segundo objetivo foi a produção de um filme de acetato de celulose com *bonechar* como uma alternativa viável para remoção do metribuzin da água. Os tratamentos dos estudos de sorção-dessorção e degradação do metribuzin foram três temperaturas de pirólise (BC350 °C, BC550 °C e BC750°C) e sete taxas de aplicação (0; 0,1; 0,5; 1; 1,5; 5 e 10 % p p⁻¹). Os tratamentos do estudo da remoção do metribuzin da água foram compostos por 2 e 3 g de *bonechar* fixado no filme de acetato de celulose, *bonechar* puro em pó (2 g) e um controle (sem adição do *bonechar*). A quantificação do metribuzin no solo e na água foi realizada em *High Performance Liquid Chromatography* (HPLC). O solo modificado com diferentes taxas de aplicação mostrou redução de H + Al e aumento do pH, OC, P, K, Ca, Mg, Fe, Mn, CTC e SB. A sorção e a dessorção do metribuzin foram 1,42 e 0,78 mg^(1-1/n) L^{1/n} Kg⁻¹ respectivamente, para o solo não modificado. Taxa de aplicação <1 % do *biochar* sorveu ~23 % e dessorveu ~15 % do metribuzin, similar ao solo não modificado, para todas as temperaturas de pirólise. Solo modificado com taxa de aplicação de 10 % do BC350 °C, 550 °C e 750 °C sorveu 63,8; 75,5 e 89,4 % e dessorveu 8,3; 5,8; e 3,7 % do metribuzin, respectivamente. Os valores da DT₅₀ e DT₉₀ do metribuzin no solo não modificado foram de 7,37 e 24,94 dias, respectivamente. O solo modificado com 10 % do BC350 °C aumentou a DT₅₀ do metribuzin de 7,35 para 17,32 dias e a DT₉₀ de 24,41 para 57,26 dias em relação ao solo não modificado. As menores taxas de aplicação (0,1 a 1,5 %) do BC550 °C e BC750 °C diminuíram o DT₅₀ do metribuzin para ~ 4,05 e ~ 5,41 dias, respectivamente. O solo corrigido com BC350 °C em altas taxas de aplicação (5 e 10 %) proporcionou alta taxa de respiração microbiana (C-

CO₂), baixa fixação de carbono da biomassa microbiana (CBM) e alta taxa metabólica (qCO₂). A alta temperatura de pirólise e as taxas de aplicação do *biochar* de palha de cana-de-açúcar mostram uma capacidade de imobilizar o metribuzin, melhorar a fertilidade do solo e aumentar a degradação do metribuzin no solo, o que pode influenciar a eficácia no controle das plantas daninhas. A adição de 2 e 3 g do *biochar* fixado no filme de acetato sorveu 40 e 60 %, respectivamente, do metribuzin nas menores concentrações (0,25; 0,33 e 0,5 mg L⁻¹). Nas maiores concentrações de 1,0 e 2,0 mg L⁻¹, a sorção foi em 16 e 50 % do metribuzin para adição de 2 e 3 g do *biochar* fixado no filme de acetato, respectivamente. A elevada temperatura de pirólise e as taxas de aplicação do *biochar* de palha de cana-de-açúcar demonstram a capacidade de imobilizar o metribuzin, melhorar a fertilidade do solo e aumentar a degradação do metribuzin no solo, o que pode influenciar a eficácia do controle das plantas daninhas. O filme de acetato de celulose com *biochar* foi eficiente na remoção de metribuzin, tendo sido observada apenas uma perda de capacidade de absorção em comparação com o *biochar* puro.

Palavras-chave: Remediação ambiental. Herbicida. Polímero natural. Material carbonáceo. Comportamento de herbicida.

SUMMARY

1. GENERAL INTRODUCTION.....	11
2. REFERENCES.....	13
Pyrolysis Temperature and Application Rate of Sugarcane Straw Biochar Influence Sorption and Desorption of Metribuzin and Soil Chemical Properties	17
1. Introduction.....	17
2. Materials and Methods.....	19
2.1 Sugarcane Straw Biochar	19
2.2 Soil Collection and Analysis	19
2.3 Sorption–Desorption Studies	20
2.4 Freundlich Model for Sorption–Desorption and Apparent Coefficient.....	21
3. Results and Discussion.....	22
3.1 Biochar Characterization	22
3.2 Characterization of Biochar-Amended and Unamended Soils.....	23
3.3 Sorption–Desorption Metribuzin in Biochar-Amended and Unamended Soils	25
4. Conclusions.....	30
5. References	31
6. Attachment.....	36
Pyrolysis Temperature vs. Application Rate of Biochar Amendments: Impacts on Soil Microbiota and Metribuzin Degradation.....	38
1. Introduction.....	38
2. Results	40
2.1. Metribuzin Degradation.....	40
2.2. Respiration Rate of the Microbial Rhizosphere	42
3. Discussion.....	46
4. Materials and Methods.....	50
4.1. Soil Collection and Analysis.....	50
4.2. Sugarcane Straw Biochar	50
4.3. Soil Preparation and Application of Metribuzin.....	50
4.4. Extraction of Metribuzin	51
4.5. Chromatographic Conditions	51
4.6. Degradation Kinetics of Metribuzin in Soil.....	52
4.7. Respiration Rate of the Microbial Rhizosphere	52
4.8. Statistical Analysis	52
5. Conclusions.....	53

6. References	53
Cellulose Acetate Film Containing Bonechar for Removal of Metribuzin from Contaminated Drinking Water	57
1. Introduction.....	57
2. Materials and Methods.....	59
2.1 <i>Drinking Water Samples</i>	59
2.2 <i>Bonechar and Cellulose Acetate Film</i>	59
2.3 <i>Sorption–Desorption Metribuzin</i>	60
2.4 <i>Freundlich Model for Sorption–Desorption and Apparent Coefficient</i>	60
3. Results and Discussion.....	61
3.1 <i>Synthesis of the Acetate Film with Added Bonechar</i>	61
3.2 <i>Removal (Sorption/Desorption) of Metribuzin</i>	62
4. Conclusions.....	67
5. References	67
GENERAL CONCLUSIONS.....	71

1. GENERAL INTRODUCTION

Biochar is a carbon-rich material derived from the partial carbonization of vegetable waste (hydrochar, biochar, lignochar) and animal waste (bonechar) under controlled conditions with little or no oxygen and relatively low temperatures (LEHMANN; JOSEPH, 2015). The variability in the physical and chemical properties of biochar depends on the feedstock used and the temperatures reached during the pyrolysis process (LEHMANN; JOSEPH, 2015). These two factors modify the specific surface area (SSA), polarity, atomic ratio, pH, elemental composition, and therefore the overall surface property of biochar (RONSSE et al., 2013; AHMAD et al., 2014).

The use of biochar in agricultural soils as a fertilizer and soil conditioner has been frequently reported by researchers (BIEDERMAN; HARPOLE, 2013; GLASER et al., 2015; LEHMANN; JOSEPH, 2015). The increase in crop yield is a commonly recognized benefit of biochar application. However, crop responses are highly variable and depend on the type of biochar, application rates, soil properties, and climatic conditions (HUSSAIN et al., 2017).

The distinct characteristics of high sorption capacity, SSA, microporosity, and ion exchange (AHMAD et al., 2014) make biochars potential immobilizers of various soil and water contaminants, including herbicides. The ability to immobilize herbicides has been reported by different authors (CABRERA et al., 2014; HUANG et al., 2018; SZMIGIELSKI et al., 2018; MENDES et al., 2019a; MIELKE et al., 2022). The pyrolysis temperature of biochar influences the efficiency of herbicide sorption, and in general, the efficiency of biochars is increased with higher temperatures (SHAABAN et al., 2018). This can be explained by the electrostatic attractions between organic pollutants and charged surfaces of biochar (SHAABAN et al., 2018; ZHAO et al., 2018).

The addition of biochar to the soil also influences the degradation of herbicides. Some authors have indicated that biochar reduces the biodegradation of herbicides in soils due to its high sorption capacity (TATARKOVÁ et al., 2013; KHORRAM et al., 2016). On the other hand, the addition of biochar influences the structure and microbial diversity of the soil, improving microbial balance and, therefore, promoting greater microbial degradation (ZHANG et al., 2005; MENG et al., 2019).

The herbicides have the soil as a temporary and/or final destination after application in pre- or post-emergence. Herbicides with high leaching potential, such as metribuzin [4-amino-6-tert-butyl-4,5-dihydro-3-methylthio-1,2,4-triazin-5-one] (INOUE

et al., 2003), pose a risk of environmental contamination. Metribuzin is a selective systemic herbicide belonging to the Photosystem II (PSII) inhibitors group of the chemical class of triazinones, recommended for the control of broadleaf weeds in pre- or post-emergence (MENDES et al., 2022). It has high water solubility ($S_w = 10.700 \text{ mg L}^{-1}$ at 20°C), high mobility in the soil (sorption coefficient normalized by organic carbon content = K_{oc} of 38 mg L^{-1}) and high leaching potential (GUS index - *Groundwater Ubiquity Score*) = 2.96) (SARITHA et al., 2017; PPDB, 2023). Therefore, the high water solubility (S_w) and high leaching index make metribuzin considered a product with potential groundwater contamination. Residues of metribuzin were analyzed in water samples from the Samambaia River sub-basin in the Federal District and eastern Goiás (CORREIA et al., 2020). Metribuzin was detected at concentrations above the limit of quantification (LQ) of $2.37 \mu\text{g L}^{-1}$ in 73.2% of the water samples.

Natural sorbents (e.g., plant biomass) have become attractive for the immobilization of herbicides from water due to their high sorption capacity and low cost (MENDES et al., 2019b). Bone char (animal-based) is derived from the carbonization of animal bones, which involves heating them in a sealed iron retort at $500\text{-}800^\circ\text{C}$ for 4-6 hours (CHEN et al., 2008). Bonechar exhibited a high removal capacity for diuron, ametryn, sulfometuron-methyl, and hexazinone in water when 1 g was added to 1 L of water (MENDES et al., 2017). However, the use of granulated and/or powdered bone char makes it difficult to remove from the water, requiring a centrifugation step to extract it from the environment after herbicide removal from water. Additionally, direct application of carbonaceous material in water can increase the dissolved carbon content, affecting aquatic ecosystems by increasing turbidity and the toxicity of metals (LIPCZYNSKA-KOCHANY, 2018).

An alternative is the use of a composite material where fine bonechar particles are incorporated into solid particles through a biopolymer, which can facilitate the collection and/or reusability of the material after herbicide removal from water. Cellulose acetate is a thermoplastic and biodegradable natural polymer that is prepared by acetylating cellulose (PLUS et al., 2011). The processing of cellulose acetate influences the range of its applications, such as films, membranes, or fibers (FISCHER et al., 2008). Cellulose acetate, being biodegradable, natural, and abundant in the environment, is an environmentally viable alternative to be used as a support material for bonechar. A hybrid film of cellulose acetate with biochar was studied for its phosphorus adsorption capacity from water (PINTO et al., 2019). However, there are

no reports yet on the production of cellulose acetate and bone char films for herbicide removal in water, making it a technologically feasible alternative that is easy to handle.

The effects of biochars are dependent on the pyrolysis temperature, the feedstock used, and the application rates in soil or water. The objective of the study was to investigate the effects of soil modifications with different application rates of sugarcane straw biochar produced at different pyrolysis temperatures on the behavior of metribuzin and soil fertility. A second objective was the production of a cellulose acetate film with bonechar as a viable alternative for metribuzin removal from water. The results obtained in these studies provided insights into the dynamics of metribuzin in soils amended with sugarcane straw biochar and the use of cow bonechar as an alternative for producing an acetate film for herbicide removal from water.

2. REFERENCES

- AHMAD, M. et al. Biochar as a sorbent for contaminant management in soil and water: A review. **Chemosphere**, v. 99, p. 19–33, 2014.
- BIEDERMAN, L. A.; HARPOLE, W. S. Biochar and its effects on plant productivity and nutrient cycling: a meta-analysis. **GCB Bioenergy**, v. 5, n. 2, p. 202-214, 2013.
- CABRERA, A. et al. Influence of biochar amendments on the sorption-desorption of aminocyclopyrachlor, bentazone and pyraclostrobin pesticides to an agricultural soil. **Science of the Total Environment**, v. 470–471, p. 438–443, 2014.
- CORREIA, N. M.; CARBONARI, C. A.; VELINI, E. D. Detection of herbicides in water bodies of the Samambaia River sub-basin in the Federal District and eastern Goiás. **Journal Environmental Science Health Part B**, v. 55, n. 6, p. 574-582, 2020.
- CHEN, Y. N.; CHAI, L. Y.; SHU, Y. D. Study of arsenic (V) adsorption on bone char from aqueous solution. **Journal of Hazardous Materials**, v. 160, n. 1, p. 168-172, 2008.
- FISCHER, S., THÜMMLER, K., VOLKERT, B., HETTRICH, K., SCHMIDT, I., FISCHER, K. Properties and applications of cellulose acetate. **Macromolecular Symposia**, v. 262, n. 1, p. 89-96, 2008.
- GLASER, B. et al. Biochar organic fertilizers from natural resources as substitute for mineral fertilizers. **Agronomy for Sustainable Development**, v. 35, n. 2, p. 667-678, 2015.

- HUANG, H. et al. Effects of biochar amendment on the sorption and degradation of atrazine in different soils. **Soil and Sediment Contamination**, v. 27, n. 8, p. 643–657, 2018.
- HUSSAIN, M. et al. Biochar for crop production: potential benefits and risks. **Journal of Soils and Sediments**, v. 17, n. 3, p. 685-716, 2017.
- INOUE, M. H. et al. Critérios para avaliação do potencial de lixiviação dos herbicidas comercializados no Estado do Paraná. **Planta Daninha**, v. 21, n. 2, p. 313-323, 2003.
- KHORRAM, M. S. et al. Effects of aging process on adsorption–desorption and bioavailability of fomesafen in an agricultural soil amended with rice hull biochar. **Journal of Environmental Sciences**, v. 56, p. 180-191, 2016.
- LEHMANN, J.; JOSEPH, S. Biochar for environmental management: an introduction. *In*: LEHMANN, J. JOSEPH, S. **Biochar for environmental management: science, technology and implementation**. 2nd ed. London: Routledge, p. 1-1214, 2015.
- LIPCZYNSKA-KOCHANY, E. Effect of climate change on humic substances and associated impacts on the quality of surface water and groundwater: A review. **Science of the Total Environment**, v. 640, p. 1548-1565, 2018.
- MENG, L. et al. Soil-applied biochar increases microbial diversity and wheat plant performance under herbicide fomesafen stress. **Ecotoxicology and Environmental Safety**, v. 171, p. 75-83, 2019.
- MENDES, K. F. et al. Effect of Biochar Amendments on the Sorption and Desorption Herbicides in Agricultural Soil. *In*: EDEBALI, S. **Advanced Sorption Process Applications**. 1nd ed. London, UK: IntechOpen, v. 1, p. 1-25, 2019a.
- MENDES, K.F., RÉGO, A. P. J., TAKESHITA, V., TORNISIELO, V. L. Water resource pollution by herbicide residues. *In*: INCE, M., INCE, O. K., ONDRASEK, G. (eds). **Biochemical Toxicology - Heavy Metals and Nanomaterials**. London, UK: IntechOpen p. 1-16, 2019b.
- MENDES, K. F., FREGUGLIA, R. M. O., MARTINS, B. A. B., DIAS, R. C., PIMPINATO, R. F., TORNISIELO, V. L. Cow bonechar for pesticide removal from drinking water. **Scholars Journal of Agriculture and Veterinary Sciences**, v. 4, p. 504-512, 2017.
- MENDES, K. F.; SILVA, A. A.; MIELKE, K. C. Classificação, seletividade e mecanismos de ação de herbicidas. *In*: MENDES, K. F.; SILVA, A. A. (Eds.).

- Plantas daninhas: herbicidas.** São Paulo, SP:Oficina de Textos, p. 7-56, 2022.
- MIELKE, K. C., MENDES, K. F., GUIMARÃES, T. Biochars effects on sorption and desorption of herbicides in soil. In: MENDES, K. F. (ed.). **Interactions of Biochar and Herbicides in the Environment.** Boca Raton, USA: CRC Press, p. 131–157, 2022.
- PPDB – Pesticide Properties Database. **Footprint: creating tools for pesticide risk assessment and management in Europe.** Developed by the Agriculture & Environment Research Unit (AERU), University of Hertfordshire, funded by UK national sources and the EU-funded FOOTPRINT project (FP6-SSP-022704). Disponível em: <<https://sitem.herts.ac.uk/aeru/ppdb/en/Reports/469.htm>>. Acesso em: 10 de junho de 2023.
- PINTO, M. D. C. E., DA SILVA, D. D., GOMES, A. L. A., LEITE, V. D. S. A., E MORAES, A. R. F., DE NOVAIS, R. F., TRONTO, J., PINTO, F. G. Film based on magnesium impregnated biochar/cellulose acetate for phosphorus adsorption from aqueous solution. **RSC Advances**, v. 9, n. 10, p. 5620-5627, 2019.
- PULS, J., WILSON, S. A., HÖLTER, D. Degradation of cellulose acetate-based materials: a review. **Journal of Polymers and the Environment**, v. 19, n. 1, p. 152-165, 2011.
- RONSSSE, F. et al. Production and characterization of slow pyrolysis biochar: Influence of feedstock type and pyrolysis conditions. **GCB Bioenergy**, v. 5, n. 2, p. 104–115, 2013.
- SARITHA, J. D. Sorption Behaviour of Metribuzin in Tomato Growing Soils. **Chemical Science Review and Letters**, v. 6, n. 21, p. 143-148, 2017.
- SHAABAN, M. et al. A concise review of biochar application to agricultural soils to improve soil conditions and fight pollution. **Journal of Environmental Management**, v. 228, p. 429–440, 2018.
- SZMIGIELSKI, A. M.; HANGS, R. D.; SCHOENAU, J. J. Bioavailability of metsulfuron and sulfentrazone herbicides in soil as affected by amendment with two contrasting willow biochars. **Bulletin of Environmental Contamination and Toxicology**, v. 100, n. 2, p. 298–302, 2018.
- TATARKOVÁ, V.; HILLER, E.; VACULÍK, M. Impact of wheat straw biochar addition to soil on the sorption, leaching, dissipation of the herbicide (4-chloro-2-

methylphenoxy) acetic acid and the growth of sunflower (*Helianthus annuus* L.).

Ecotoxicology and Environmental Safety, v. 92, p. 215–221, 2013.

ZHAO, S. et al. Varying pyrolysis temperature impacts application effects of biochar on soil labile organic carbon and humic fractions. **Applied Soil Ecology**, v. 123, p. 484–493, 2018.

ZHANG, W. J., JIANG, F. B., OU, J. F. Global pesticide consumption and pollution: with China as a focus. **Proceedings of the International Academy of Ecology and Environmental Sciences**, v. 1, n. 2, p. 125, 2011.

Article

Pyrolysis Temperature and Application Rate of Sugarcane Straw Biochar Influence Sorption and Desorption of Metribuzin and Soil Chemical Properties

Kamila C. Mielke¹, Ana Flávia S. Laube², Tiago Guimarães², Maura Gabriela da S. Brochado¹, Bruna Aparecida de P. Medeiros¹ and Kassio F. Mendes¹ * 

¹ Department of Agronomy, Federal University of Viçosa, Viçosa 36.570-900, Brazil

² Department of Chemistry, Federal University of Viçosa, Viçosa 36.570-900, Brazil

* Correspondence: kfmendes@ufv.br

Abstract: Pyrolysis temperature and application rate of biochar to soil can influence herbicide behavior and soil fertility. The objective was to investigate the effect of soil amendments with application rates of sugarcane straw biochar, produced at different pyrolysis temperatures, on the sorption–desorption of metribuzin in soil. The analysis was performed using high-performance liquid chromatography (HPLC). The treatments were three pyrolysis temperatures (BC350, BC550 and BC750 °C) and seven application rates (0, 0.1, 0.5, 1, 1.5, 5 and 10% w w⁻¹). Amended soil with different application rates decreased H + Al and increased pH, OC, P, K, Ca, Mg, Fe, Mn, CEC and BS contents. K_f values of sorption and desorption of metribuzin were 1.42 and 0.78 mg^(1-1/n) L^{1/n} Kg⁻¹, respectively, in the unamended soil. Application rates < 1% of biochar sorbed ~23% and desorbed ~15% of metribuzin, similar to unamended soil, for all pyrolysis temperatures. Amended soil with 10% of BC350, BC550 and BC750 sorbed 63.8, 75.5 and 89.4% and desorbed 8.3, 5.8 and 3.7% of metribuzin, respectively. High pyrolysis temperature and application rates of sugarcane straw biochar show an ability to immobilize metribuzin and improve soil fertility, which may influence the effectiveness in weed control.

Keywords: carbonaceous material; soil fertility; herbicide behavior; residual in soil; environmental contamination



Citation: Mielke, K.C.; Laube, A.F.S.; Guimarães, T.; Brochado, M.G.d.S.; Medeiros, B.A.d.P.; Mendes, K.F. Pyrolysis Temperature and Application Rate of Sugarcane Straw Biochar Influence Sorption and Desorption of Metribuzin and Soil Chemical Properties. *Processes* **2022**, *10*, 1924. <https://doi.org/10.3390/pr10101924>

Academic Editor: Carmen Branca

Received: 25 August 2022

Accepted: 17 September 2022

Published: 23 September 2022

Publisher's Note: MDPI stays neutral with regard to jurisdictional claims in published maps and institutional affiliations.



Copyright: © 2022 by the authors. Licensee MDPI, Basel, Switzerland. This article is an open access article distributed under the terms and conditions of the Creative Commons Attribution (CC BY) license (<https://creativecommons.org/licenses/by/4.0/>).

1. Introduction

Biochar (BC) is defined as a carbon-rich product, produced by thermal conversion of organic material, with limited oxygen (O₂) supply and controlled temperatures, consisting mainly of carbon (C) and a variable proportion of oxygen (O) and hydrogen (H) [1]. BC has been used for many years as a corrective in general soil applications. BC has been shown to increase porosity, specific surface area (SSA), soil water holding capacity [2,3], availability of basic cations (Ca²⁺, Mg²⁺, K⁺) [4,5], increased pH and cation exchange capacity (CEC) [3], in addition to its significant content of recalcitrant C that offers the possibility of long-term C sequestration [6]. Corn residue BC produced at different pyrolysis temperatures was added to two different soils [7]. These authors observed that increasing the pyrolysis temperature of biochar added to sandy loam soil improved the pH (0.46 units), electrical conductivity (EC) (0.38 dS m⁻¹), N (120%) and K (41%), but decreased plant-available P (−86%), relative to unamended soil. Differently, a corn BC produced at a pyrolysis temperature of 200 °C and applied at a rate of 2% (w w⁻¹) in calcareous soil was more efficient in the availability of nutrients to the soil [8]. The effects on soil fertility and consequently on crop productivity are related to the physicochemical properties of soil, biochar, application rates and pyrolysis temperature of biochar production, which can provide different results in soil fertility [9].

Over the years, biochar has also proven to be a material capable of removing pollutants (herbicides, fungicides, insecticides, heavy metals, antibiotics, industrial chemicals, among

others) from soil and water through sorption–desorption and degradation processes [10]. The distinct characteristics of biochar related to surface chemistry (surface functional groups and cation exchange) and morphological structure (e.g., high SSA and microporosity) [11] enables biochar to have high sorptive capacity. The variability in the physical and chemical properties of biochar depends on the raw material and the conditions used during the pyrolysis process [1].

The potential to sorb herbicides in soil has been evidenced by different authors [12–16]. The high sorption of the herbicide in the biochar-amended soil generally decreases its bioavailability for uptake by plants, degradation by microorganisms and leaching into the soil profile [17]. As opposed to the sorption, there is usually a decrease in the desorption of the herbicide and, in some cases, it may become irreversible [18]. The increased sorption of herbicides by biochar decreases their loss through dissipation into the environment, decreasing the risk of human exposure and environmental pollution. However, it can have a high sorption capacity for residual herbicide-applied PRE emergence (directly to the soil), such as metribuzin and reduce the residual effect on weed control.

The metribuzin [4-amino-6-tert-butyl-4,5-dihydro-3-methylthio-1,2,4-triazin-5-one] belongs to the triazinone chemical group and acts in the inhibition of photosystem II (PSII), in the photochemical phase of photosynthesis [19]. The characteristics of high solubility ($S_w = 10,700 \text{ mg L}^{-1}$ at $20 \text{ }^\circ\text{C}$), high mobility in soil (sorption coefficient normalized by organic carbon content = K_{oc} of 38 mg L^{-1}), high leaching capacity (GUS index-Groundwater Ubiquity Score = 2.96) and low persistence (half-life degradation time, $DT_{50} = \sim 20 \text{ d}$) [20–22], make the herbicide a product with potential for environmental contamination. Metribuzin was frequently detected at a maximum concentration of $0.351 \text{ } \mu\text{g L}^{-1}$ in surface and groundwater in untreated human consumption sites in the region of Primavera do Leste, Mato Grosso (Midwestern Brazil) [23]. Metribuzin application contaminated groundwater with its metabolites when applied to sandy soil in Denmark [24]. The authors detected diketometribuzin and desaminodiketometribuzin in soil samples at concentrations exceeding the maximum residue limit set by the European Union ($0.1 \text{ } \mu\text{g L}^{-1}$).

The behavior of metribuzin in biochar-amended soils brought positive results for immobilization and decreased leaching [25–27]. However, the sorption–desorption results are distinct among authors and depend on the temperature in the pyrolysis process, soil application rate and feedstock used. Feedstocks with lower presence of lignin and cellulose (vegetable wastes) produce biochar with low bulk density, high pH and lower C stability than feedstocks with high lignin and cellulose content (wood) [28,29]. Higher pyrolysis temperatures, in general, increase the sorptive capacity of biochar [30]. The use of biochar in agriculture has usually been reported as a soil conditioner and can contribute to the lasting improvement in the chemical, physical, hydric and biological attributes of the soil. The addition of high application rates of biochar can directly interfere in the sorption and desorption of the herbicide-applied pre-emergence directly to the soil. The application of biochar must be carefully determined for its remediation and soil conditioning potential, since increased sorption can lead to decreased efficacy of PRE herbicides, decreasing their residual action.

The objective of this study was to investigate the effect of soil amendments with application rates of sugarcane straw biochar produced at different pyrolysis temperatures on the sorption–desorption processes of metribuzin in soil. The results of this study will determine the best pyrolysis temperature and application rate of sugarcane straw biochar to immobilize metribuzin, thus, reducing its leaching potential into the soil profile. It also seeks to determine, based on the sorptive capacity of biochar, the application rates that will positively influence the chemical attributes of the soil.

2. Materials and Methods

2.1 Sugarcane Straw Biochar

Sugarcane (*Saccharum officinarum*) straw waste was used as a source of raw material because it is a promising alternative for biochar production [31,32]. Straw is a residue from the mechanical harvesting of sugarcane, grown in abundance in Brazil. The sugarcane straw was crushed, sieved (mesh size 10 mesh, <2.0 mm) and dried in an oven with forced air circulation at 103 °C. The straw was placed in a sealed reactor to prevent the ingress of O₂. The reactor furnace was heated at a rate of 5 °C min⁻¹, in slow pyrolysis (4–6 h) at temperatures of 350°, 550° and 750 °C. The elemental composition and ash content of biochar was performed according to EPA 3051A [33]. The content of C, N and the C/N ratio was determined by combustion using an elemental analyzer (LECO CS-600, Shimadzu, Japan). The pH was determined according to the guidelines of the analytical methods guide for biochar [34], in which 5 g biochar samples were stirred with 50 mL deionized water (1:10 w v⁻¹) in a horizontal shaker for 1 h at 21 °C. The specific surface area (SSA) was obtained using the N₂-Brunauer–Emmett–Teller (BET) method [35] (Table 1).

Table 1. Selected properties of sugarcane straw biochar at different pyrolysis temperatures.

T °C	pH	C	N	C/N	Ash	SSA
	H ₂ O		%			m ² g ⁻¹
350	8.6	48.7	0.832	58.51	5.0	17
550	9.3	49.1	0.647	75.83	10.3	129
750	9.8	59.0	0.403	146.36	11.6	223

Temperature (T); Hydrogen Potential (pH), Carbon (C), Nitrogen (N), Carbon/Nitrogen Ratio (C/N), Specific Surface Area (SSA).

Surface morphology and elemental analysis of biochar were carried out by scanning electron microscopy (SEM) coupled with an X-ray energy dispersive spectrometer (EDS), in an SEM, brand JEOL (JSM-6010LA, Akishima, Tokyo, Japan). This microscope has a resolution of 4 nm (with beam at 20 kV), magnification from 8 to 300,000 and acceleration voltage from 500 V to 20 kV. Also used was an electron gun with pre-centered tungsten filament. Everhart–Thornley detector for secondary electron images and solid-state detector for retro-scattered electrons with contrast of topography, composition and variable shading. Silicon Drift detector for EDS analysis with 133 eV resolution was used. The biochar particles were attached to a metal stub by conductive carbon tape (PELCO Tabs™, Ted Pella, Inc., Redding, CA, USA) and sputter coated (Leica EM ACE 600, Buffalo Grove, IL, USA) with a 120 nm thick layer of gold.

Changes in biochar functional groups were analyzed by Fourier-transform infrared spectroscopy (FTIR), in a Bruker VERTEX 70 instrument (Bruker, Bremen, Germany), using the attenuated total reflectance (ATR) method in a range of 350–4000 cm⁻¹. Raman spectroscopy was carried out in a micro-Raman spectrometer (Renishaw InVia, Gloucestershire, England) equipped with an Nd-YAG laser (λ = 514 nm) and a 50× objective lens (Olympus B × 41) and the Raman spectrum acquisition time for each sample was defined as 10 s.

2.2 Soil Collection and Analysis

The agricultural soil samples were collected from the top layer (0–10 cm) in Viçosa, MG, Brazil (20°46′05″ S; 42°52′08″ W), being an area that has not been treated with herbicides for the last three years. The soil samples were air dried for 10 d, then sieved on 5.0 mm mesh and stored at room temperature. The soil was classified as Oxisol (*Latossolo Vermelho-Amarelo*).

The soil was amended with sugarcane straw biochar produced at different pyrolysis temperatures (BC350, BC550 and BC750 °C) in application rates of 0, 0.1, 0.5, 1, 1.5, 5 and 10% (w w⁻¹) representing 0, 1, 5, 10, 15, 50 and 100 Mg ha⁻¹, respectively, assuming a soil density of 1.2 g cm⁻³ and incorporation depth of 0.10 m. The analyses of P, Na, K, Fe, Zn, Mn and Cu were performed with the Mehlich 1 Extractor. For Ca, Mg and Al the KCl

extractor was used (1 mol L⁻¹). Potential acidity (H + Al) was extracted in calcium acetate (0.5 mol L⁻¹) at pH 7.0. For the determination of BS, hot water was used as an extractor and for S, monocalcium phosphate in acetic acid. Organic matter (OM) was quantified by the Walkley-Black titration method after wet oxidation. The conversion of OM into organic carbon (OC) was performed using the correction factor 1.72 (Table 2).

Table 2. Physicochemical attributes of the soil amended with sugarcane straw biochar and unamended soil used in this study.

Pyrolysis Temperature	Application Rate	Chemical Attributes													
		pH	OC	P	K	Ca	Mg	H + Al	Zn	Fe	Mn	Cu	B	CEC	BS
(°C)	(% w w ⁻¹)	H ₂ O	%	mg kg ⁻¹	mmolc kg ⁻¹					mg kg ⁻¹			mmolc kg ⁻¹	%	
-	unamended	5.5	1.2	1.3	77.0	15.9	5.4	33.0	3.0	129.8	91.0	3.9	0.1	23.3	99.8
350	0.1	5.5	1.2	1.5	97.0	16.0	5.7	33.3	2.9	129.6	99.1	3.8	0.1	24.2	99.8
	0.5	5.5	1.2	2.0	111.0	17.9	6.5	33.0	3.1	123.6	127.0	3.6	0.1	27.8	98.1
	1	5.8	1.2	3.3	125.0	17.5	6.8	26.4	2.8	148.1	130.0	3.7	0.1	29.3	93.8
	1.5	5.9	1.2	6.3	139.0	17.1	7.2	23.1	2.9	154.7	144.0	4.1	0.1	29.4	94.6
	5	6.8	1.2	10.0	240.0	17.7	8.3	13.3	2.9	234.4	155.0	3.8	0.1	36.7	87.6
	10	7.2	1.2	30.0	290.0	17.4	9.6	6.6	2.8	245.5	212.0	3.6	0.1	37.1	92.7
550	0.1	5.4	1.2	2.2	99.0	16.5	5.7	29.4	2.8	128.5	94.5	3.6	0.1	24.7	100.0
	0.5	5.6	1.2	2.7	132.0	16.2	5.8	29.7	3.1	157.4	97.9	4.1	0.1	24.8	100.0
	1	5.8	1.2	4.4	158.0	17.3	6.1	29.7	3.0	228.5	91.2	4.0	0.1	26.6	100.0
	1.5	5.9	1.2	8.7	161.0	17.8	5.8	19.8	2.8	266.5	157.0	3.4	0.1	25.2	100.0
	5	7.0	1.2	15.0	250.0	17.7	7.6	9.9	2.7	273.5	183.0	3.1	0.1	33.2	95.2
	10	7.3	1.3	33.0	340.0	18.1	8.4	3.3	2.9	297.5	202.0	3.6	0.1	38.5	91.4
750	0.1	5.4	1.2	2.9	108.0	16.8	5.6	33.0	2.7	135.0	96.6	3.6	0.1	25.2	99.8
	0.5	5.5	1.2	3.7	144.0	17.4	6.8	29.7	3.0	148.8	135.0	3.9	0.1	27.6	100.0
	1	5.8	1.2	7.8	178.0	17.8	7.0	29.7	2.8	147.6	122.0	4.0	0.1	29.4	99.8
	1.5	6.2	1.2	12.0	240.0	18.1	7.1	13.2	2.5	238.5	123.0	3.8	0.1	30.6	100.0
	5	7.2	1.3	55.0	500.0	19.7	9.8	3.3	2.9	267.5	177.0	3.7	0.1	39.3	100.0
	10	7.6	1.4	65.0	550.0	20.0	11.1	0.0	2.9	294.5	178.0	3.8	0.1	40.6	100.0
		Physical Attributes (g kg ⁻¹)													
Soil	unamended	Sand 500			Silt 120			Clay 380			Texture class sandy clay				

Source: Laboratory of Soil Analysis Viçosa LTDA, Viçosa, MG, Brazil. Hydrogen Potential (pH), Organic Carbon (OC), Phosphorus (P), Potassium (K), Calcium (Ca), Magnesium (Mg), Potential acidity (H + Al), Zinc (Zn), Iron (Fe), Manganese (Mn), Copper (Cu), Boron (B), Cation Exchange Capacity (effective) (CEC), Base Saturation (BS).

2.3 Sorption–Desorption Studies

The methodology for the sorption and desorption study was established according to the guidelines “106, Adsorption–Desorption Using a Batch Equilibrium Method” [36,37]. The stock solution was prepared at a concentration of 500 mg L⁻¹ of the standard Metribuzin-Pestanal™ (Analytical Standard, 98.8% purity Sigma-Aldrich, San Luis, MO, USA) and the working solution at a concentration of 100 mg L⁻¹, both in acetonitrile (99.9% purity). From the working solution, five concentrations of metribuzin were prepared in 0.01 mol L⁻¹ CaCl₂ solution. The concentrations were 0.5, 1, 2, 4 and 8 mg L⁻¹, where the concentration of 2 mg L⁻¹ corresponds to the highest recommended dose of the herbicide (1920 g a.i. ha⁻¹) for the sugarcane crop, assuming a soil density of 1.2 g cm⁻³ and incorporation depth of 0.10 m.

In Falcon tubes 2 g of soil from each treatment with biochar-amended and unamended soils were added and 10 mL of 0.01 mol L⁻¹ CaCl₂ solution was added, in triplicate for each treatment. The tubes were then subjected to rotary shaking, using an orbital shaker adapted to a motor (Fisatom 801, São Paulo, Brazil) at 45 rpm for 24 h until they reached the equilibrium concentration [25,26]. Subsequently, the tubes were added to a digital centrifuge (Kasvi, K14-0815P, Paraná, Brazil) at 3500 rpm for 7 min. A 2 mL aliquot was filtered on a Millipore filter (PRFE membrane 0.45 µm) and placed in a vial. Metribuzin was quantified in a high-performance liquid chromatograph (HPLC) (LC 20AT, Shimadzu, Japan), with photodiode array detector (SPD-M20A, Shimadzu, Japan) and stainless-steel C₁₈ column (Shimadzu VP-ODS Shim-pack 250 mm × 4.6 mm d.i., 5 µm of particle size).

The mobile phase was adapted from [25], composed of acetonitrile/water (acidified with 0.01% phosphoric acid) in a ratio 45/55 (v v⁻¹), injection volume of 30 µL, flow rate of 1.0 mL min⁻¹, wavelength of 254 nm and column oven temperature of 30 °C. The mobile phase showed good linearity in a range of 0.1 to 8 mg L⁻¹ of metribuzin. The analytical curve showed a coefficient of determination (R²) equal to 0.9993. The limit of detection (LoD) and quantification (LoQ) were 0.044 and 0.13 mg L⁻¹, respectively.

In the desorption study, the sorption supernatant was discarded from the Falcon tubes containing biochar-amended and unamended soils and then 10 mL of the new 0.01 mol L⁻¹ CaCl₂ solution without herbicide was added. The tubes were subjected to rotary shaking for 24 h until they reached the re-equilibrium concentration. Subsequently, the tubes were centrifuged at 3500 rpm for 7 min. A 2 mL aliquot was filtered and placed in a vial for HPLC analysis. The amount desorbed was calculated as the difference between the sorbed metribuzin in the soil and the amount remaining in the supernatant.

2.4 Freundlich Model for Sorption–Desorption and Apparent Coefficient

The sorption apparent coefficient (K_{d-app} , L kg⁻¹) was also calculated at $C_e = 2.0$ mg L⁻¹ (an intermediate value of the equilibrium concentrations studied in the sorption), using the following Equation (1):

$$K_{d-app} = C_s / C_e \quad (1)$$

where C_s is the amount of herbicide sorbed in the unamended and biochar-amended soil (mg kg⁻¹) (2):

$$C_s = (C_i - C_e) \times V / M \quad (2)$$

where C_i is the pesticide initial liquid concentration (mg L⁻¹), C_e is the equilibrium liquid concentration (mg L⁻¹), V is the volume of herbicide solution added (mL) and M is the mass of soil (g) [13].

The sorption coefficient (K_{d-app} , L kg⁻¹) normalized to the OC content of the biochar-amended and unamended soils (K_{oc} , L kg⁻¹) was calculated as follows (3):

$$K_{oc} = (K_{d-app} / \%OC) \times 100 \quad (3)$$

The desorption K_{d-app} value for desorption was also calculated for comparison to the sorption K_{d-app} .

The Freundlich model and its distribution coefficient were derived from Equation (4):

$$K_f = C_s / C_e^{1/n} \quad (4)$$

where n (dimensionless value) can range from 0 to 1, depending on the heterogeneity in the sorption sites.

The same sorption coefficient was also standardized, considering the soil OC content (K_{foc}). The hysteresis index (H) was calculated by Equation (5):

$$H = 1/n_{sorption} / 1/n_{desorption} \quad (5)$$

The thermodynamic parameter of Gibbs free energy (ΔG) to evaluate the degree of spontaneity of the sorption process was calculated by linear equation of van't Hoff (6). The average K_f (Freundlich coefficient) value of each treatment was used for the calculation.

$$\Delta G = - R \cdot T \cdot \ln K_f \quad (6)$$

where R is the gas constant (8314 J mol⁻¹ K⁻¹), T is the absolute temperature (298 K) and K_f is the Freundlich coefficient (mg^(1-1/n) L^{1/n} kg⁻¹).

3. Results and Discussion

3.1 Biochar Characterization

All biochar attributes varied as the pyrolysis temperature of the production system increased. The pH of BC350 was lower (8.6) than BC550 (9.3) and BC750 (9.8). BC750 increased the SSA 13-fold compared to BC350. Higher C/N ratio and ash content were observed for BC750 (Table 1). These results are in agreement with what has been observed in studies with different pyrolysis temperatures in sugarcane straw biochar [32,38,39]. The increase in pyrolysis temperature influences the SSA of biochar because there is a change in the carbon structure, with the formation of structures similar to graphene, which has a larger pore volume and, consequently, SSA [11]. The higher pH values of the biochar produced at high temperature (BC750) are positively correlated with carbonate formation, inorganic alkali content and increased ash content [40,41]. Ashes are mainly responsible for the generation of alkalinity in biochar, due to the presence of alkaline-reacting minerals, such as Na^+ , Ca^{2+} and Mg^{2+} [42]. The higher SSA of BC750 is probably related to the release of volatile substances present in the biomass and the change in the C structure, increasing the SSA and pore volume through degradation of OM [43,44]. The higher C/N ratio of BC750 may be related to N losses during the thermal production process. With increasing pyrolysis temperature, usually compounds with higher C content and lower N content are formed, because N is lost through volatilization at high temperatures [45]. Increases in C/N ratios may indicate the production of compounds that have higher levels of recalcitrant C [46].

The elemental composition of biochar is shown in Supplementary Material (Figure S1B), represented by the atomic percentage of elements located in EDS images (Figure S1A). C was predominant for the biochar produced at the three pyrolysis temperatures (BC350, BC550 and BC750) with values of ~90%. The O was 4.48, 8.04 and 12.6% for the BC350, BC550 and BC750, respectively. Higher percentages of the elements Mg, Ca, Al, P, K and Si were observed for BC550 and BC750. The increase in inorganic constituents in pyrolyzed biochar at high temperatures is related to the higher ash content that remains in the biochar after carbonization [47]. The characteristics of the biochar surface are presented in Figure S2. BC350 preserved the structural organization of the plant cell wall with a lamellar structure on the surface [48]. High pyrolysis temperatures showed deformation of the biochar surface, which was also observed by [49] when comparing biochars derived from wheat, corn, rape and rice straw at different pyrolysis temperatures.

The increase in pyrolysis temperature promoted a reduction in the amount of organic functional groups in the biochar (Figure 1A). The results of the FTIR spectrum showed variation in peaks and absorption intensity with variation in pyrolysis temperature. For BC350, a band is observed at 788 cm^{-1} that can be attributed to aromatic and alkali functional groups, such as C=C [50], a band at 1040 cm^{-1} that can be assigned to the C-O vibration [51], a band at 1580 cm^{-1} that can be attributed to aromatic groups elongating the C=C bond [52], a band at 2095 cm^{-1} , which is assigned to asymmetric aliphatic C-H stretches [53] and a band at 2100 cm^{-1} , assigned to C=C stretching [54]. The increase in pyrolysis temperature directly influenced the surface functional groups and may be attributed to the structural reorganization of biochar through depolymerization and volatilization due to ion losses of carbonaceous compounds (H^+ and O^-) [55,56]. The decrease in intensity of the aliphatic elongation (C-H) bands was also observed by [32] and is attributed to dehydration of the lignin and/or cellulose compounds, as well as structural changes in the aliphatic compounds.

The Raman spectra of all materials (Figure 1B) showed classical bands of carbonaceous materials, i.e., D and G located in the first-order region, 1100 to 1800 cm^{-1} . In the spectra, it was possible to observe that BC350 showed higher intensity for the G band compared to the D band when compared to BC550 and BC750. The analysis of the organizational structure of the biochars, analyzed by Raman spectrum, indicated that material synthesized at the minimum temperature (BC350) has a more organized structure and, although all biochars have well-defined D and G bands, their intensities are close. This indicates that

these materials have some degree of structural defects [57]. Raman spectra of samples of different biochars show a D-band at 1337–1361 cm^{-1} due to the A_{1g} symmetry breathing mode that is non-existent in perfect graphite and, thus, only becomes active in the presence of disturbances, often referred to as amorphous C [51]. The G band (1596–1604 cm^{-1}) is related to the presence of carbon with sp^2 hybridization, more specifically, the vibration of the double bonds (C=C) that form the graphitic planes of the materials [58]. The higher the value of the ratio between the intensities of the D and G bands (I_D/I_G), the lower the organization of the structure [59].

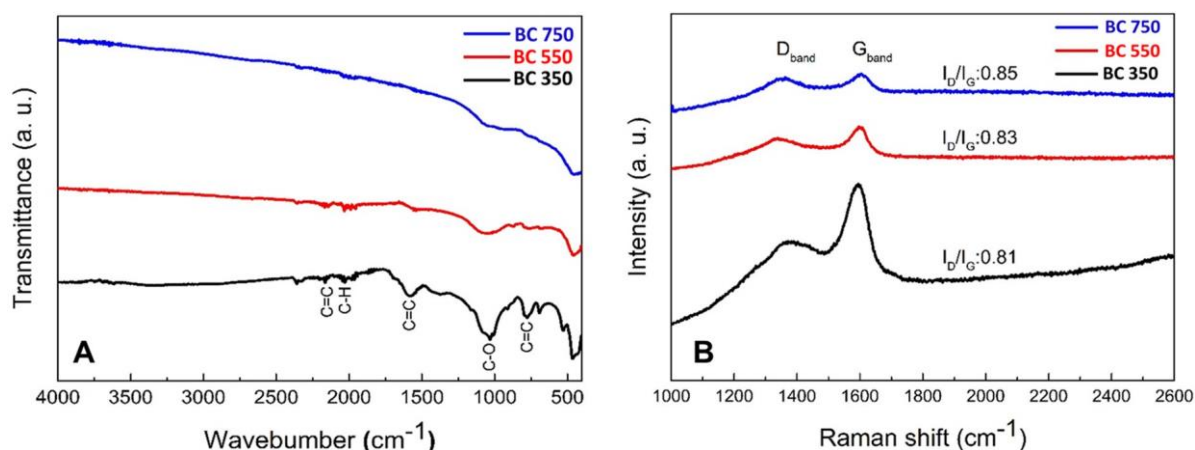


Figure 1. Fourier-transform infrared spectroscopy (FTIR) (A) and Raman spectra (B) of sugarcane straw biochar (BC) produced at pyrolysis temperatures of 350, 550 and 750 °C.

The physicochemical characteristics of biochar directly influence its sorptive capacity due to the distinct mechanisms of interaction between the herbicide molecule and the biochar. The nature of these interactions can be exclusively physical, chemical or both and result in the phenomenon of sorption [60]. The characteristics that directly influence the sorption of herbicides are related to porosity, SSA, aromatic structures, C contents, surface functional groups, pH and elemental composition [61]. Understanding the probable mechanisms for herbicide sorption by biochar ensures an understanding of the ability of each material to act as a potential soil remediator.

3.2 Characterization of Biochar-Amended and Unamended Soils

The chemical characteristics of the soils amended with BC350, BC550 and BC750 at different application rates are shown in Table 2. The pH of the amended soil with application rates 1.5%, regardless of pyrolysis temperature, increased the pH by ~0.5 units relative to the unamended soil. Higher pH values were observed for the soil amended with BC750, where the application rates of 5 and 10% increased pH by 1.7 and 2.1 units, respectively, relative to the unamended soil. The potential acidity ($H + Al$) in the biochar-amended soil, regardless of pyrolysis temperature, was similar to the unamended soil (33 mmolc kg^{-1}) for application rates $< 1.0\%$ (Table 2). Amended soil with 10% of BC350, BC550 and BC750 reduced potential acidity by 80, 90 and 100%, respectively. The increase in pH and reduction in potential acidity of the amended soil is possibly related to the amount of ash and basic cations in the biochar. Biochar can have a soil liming capacity due to the presence of basic cations (Ca, K, Mg and Si) that can form alkaline oxides or carbonates during the pyrolysis process and, once added to the soil, react with monomeric $H + Al$, increasing soil pH and, consequently, reducing exchangeable acidity [62]. One study, analyzing a 3% application rate of rice straw biochar to a soil with a pH of 5.24, reported increased soil pH by 4.5 units compared to the control [63].

The OC content of the unamended soil was 1.2% and increased to 1.3 and 1.4 in the amended soils, with application rates of 5 and 10% of BC750, respectively. The 10% application rate of BC550 increased the OC content to 1.3%. Regardless of the application

rate, no changes in OC were observed for the soil amended with BC350 (Table 2). The OC was also analyzed in a soil amended with six biochars [64]. These authors observed that OC content increased from 4.9% of the unamended soil to 5.4 and 5.2% in the amended soil with peanut shell and cassava bagasse biochar, respectively, and it was attributed to the higher OC content in the feedstocks, which is indicative that biochar applications to soils can increase C accumulation and sequestration.

Amended soil with BC350, BC550 and BC750 increased P for all application rates (Table 2). The rates application < 1.0% of biochar, regardless of pyrolysis temperature, increased the P concentration ~2-fold relative to unamended soil. The soil amended with 10% of BC350, BC550 and BC750 increased P by ~23-, 25- and 5-fold, respectively, relative to the unamended soil. Increases in P availability in amended soil with different biochars have been reported by different authors [65–67]. This result is directly related to the increase in pH and the change in the sorption site of P by the biochar-amended soil. P in more acidic soils is prone to complexing with Al or Fe and increasing soil pH above 7 may result in precipitation of free Al and Fe and, thus, decrease active P sorption sites [68]. The increased availability of P to the soil amended with BC750 is possibly related to characteristics of the biochar produced at high temperature, such as surface area and changes in soil exchange sites, preventing the fixation of P [69]. A study analyzed the potential of corn stover biochar produced at a pyrolysis temperature of 500 °C on the availability of P in soil [8]. The authors observed that P increased by 2.6-fold for 2% application rate, relative to the control soil. K content in the amended soils increased for all application rates (Table 2). The 0.1% application rate of biochar, independent of pyrolysis temperature, increased the K in the amended soil by ~1.3-fold compared to the unamended soil. The 10% application rate of BC350, BC550 and BC750 increased the K by 3.7-, 4.4- and 7-fold, respectively, over unamended soil. Biochar typically contains a large proportion of K, which is dependent on pyrolysis temperature and feedstock [70]. For mild pyrolysis temperatures < 500 °C, the C and N contents are volatile; however, K starts to volatilize at higher temperatures > 700 °C, which provides an increase in K concentration in the biochar produced at high temperature [71]. Amended soil with 0.3% application rate of cassava stem biochar and rice husk were analyzed for K [72]. The authors reported release of ~148 mg kg⁻¹ of K after 7 d of incubation of amended soil with cassava stem biochar and ~188 mg kg⁻¹ of K after 1 d of incubation for rice husk biochar, being two biochars with high potential for K accumulation in soil.

Ca and Mg contents increased with soil modification with biochar; however, small variations were observed between application rates and pyrolysis temperature (Table 2). Application rate of 10% biochar, regardless of pyrolysis temperature, increased Ca and Mg by ~1.2- and 1.9-fold, respectively, relative to unamended soil. The increase in Ca was also observed in a study with six different biochars [64]. The authors observed that compared to the unamended soil, the Ca content increased by 1.2–5.9%.

The contents of the micronutrients Zn, Cu and B showed no variations in relation to the unamended soil, for all pyrolysis temperatures and application rates (Table 2). Fe and Mn contents increased ~2-fold, relative to unamended soil, for the 10% application rate, regardless of pyrolysis temperature (Table 2). In more alkaline soils (pH > 7.0), Zn and Cu can form associations with Fe oxides and their availability in the soil solution is decreased. The application of different rates of hardwood biochar (*Quercus* spp. and *Carya* spp.) to alkaline soils was analyzed in terms of soil chemical modifications [73]. The authors observed that increasing the application rate of biochar provided higher Fe and Mn content but showed no effect for Zn and Cu in the amended soil.

The CEC was similar to unamended soil (23.3 mmol c kg⁻¹) for application rates < 1.0%, regardless of pyrolysis temperature. Amended soil with 10% of BC350, BC550 and BC750 increased CEC by 1.6-, 1.65- and 1.7-fold, respectively, compared to unamended soil. The mechanisms that increase the SSA of the amended soil are probably mediated by the higher SSA, negative surface charge and charge density in the biochar [74], and the increase in soil pH, as presented in this study. Increased pH after biochar addition may

result in deprotonation of functional groups of minerals, such as kaolinite, resulting in the development of negative charges that increase the CEC of the amended soil [75].

The BS of the soil amended with BC350, BC550 and BC750 increased to 85, 90 and 100% at 10% application rate. Similar results were observed in the application of poultry litter biochar produced at 350 °C [76]. The authors reported increased soil BS of 33.58% and 43.28% for the two highest application rates (0.4 and 0.5%, respectively) when compared to unamended soil.

Overall, the sugarcane straw biochar produced at different pyrolysis temperatures directly influenced soil fertility when applied at high rates (5 and 10%). However, application rates of 1 and 1.5% have potential in reducing potential acidity, increasing pH, high P and K contents, maintaining Ca and Mg values and the micronutrients Fe and Mn and improving soil CEC. Improvements in soil chemical attributes are provided by adding application rates of 1 to 1.5% of BC350, BC550 and BC750 of sugarcane straw and may be an alternative for soil fertility.

3.3 Sorption–Desorption Metribuzin in Biochar-Amended and Unamended Soils

The sorption–desorption isotherms were adequately fitted using the Freundlich model to describe the sorption–desorption of metribuzin in amended soil at different biochar application rates and pyrolysis temperature, as indicated by the high coefficients of determination (R^2 0.98) of the equations (Figures 2 and 3). The degree of linearity ($1/n$) ranged from 0.34 to 0.89 for sorption and 0.41 to 1.05 for desorption, indicating that the sorption and desorption isotherm is classified as type L (Tables 3 and 4). This type of isotherm is indicative that the sorbent (biochar-amended soil) showed lower sorption capacity at high concentrations of the sorbate (herbicide) [77]. Thus, at low concentrations, metribuzin showed higher affinity for biochar-amended soil, due to the high availability of sorption sites at higher application rates (>1.5%), independent of pyrolysis temperature. As the concentration of metribuzin increased, the number of binding sites decreased and the concentration in the soil solution increased, consequently reducing its sorption by the biochar-amended soil. This behavior was also observed for the sorption of metribuzin on biochar from grapevine pruning residues and bonechar (cow bone) [26,27].

According to the sorption coefficients (Table 3), for both the Freundlich model (K_f) and the median concentration (K_{d-app}), metribuzin showed increasing sorption as the biochar application rate to the soil increased. The K_f value was low for unamended soil ($1.42 \text{ mg}^{(1-1/n)} \text{ L}^{1/n} \text{ kg}^{-1}$). Studies analyzing the sorption and desorption of metribuzin in different soils have reported sorption K_f values between 0.18 and $2.5 \text{ mg}^{(1-1/n)} \text{ L}^{1/n} \text{ kg}^{-1}$, being dependent on clay content, OM and soil pH [27,78–80].

BC750-amended soil improved the sorption of metribuzin between 1 and 10-fold over unamended soil as application rates increased from 0.1 to 10%. BC350- and BC550-amended soils showed similar sorption with ~1.3- and 6-fold increases in sorption at application rates of 1.5 and 10%, respectively, compared to unamended soil. The K_f and K_{d-app} of the sorption of metribuzin were normalized by the OC content in the soil, showing that the overall sorption trends were not altered by the OC (Table 3). The K_{foc} values for the sorption of metribuzin on the amended soil increased proportionally to the application rate and pyrolysis temperature. The K_{foc} for the 10% application rate was 504, 726 and $1236 \text{ mg}^{(1-1/n)} \text{ L}^{1/n} \text{ kg}^{-1}$ for the amended soil with BC350, BC550 and BC750, respectively (Table 3). The higher sorption of metribuzin in the soil amended with BC750 can be attributed to the higher SSA compared to BC350 and BC550. The increased sorption capacity of biochar is directly related to higher SSA, because the number of pores increases proportionally with SSA, providing a greater number of herbicide binding sites [81]. The K_f value of metribuzin sorption was evaluated in a study with sugarcane bagasse biochar, produced at different pyrolysis temperatures [82]. These authors observed that the biochar produced at 700 °C presented K_f of $47.2 \text{ mg}^{(1-1/n)} \text{ L}^{1/n} \text{ kg}^{-1}$ and SSA of $82 \text{ m}^2 \text{ g}^{-1}$, while for the biochar produced at 350 °C, the K_f was $9.77 \text{ mg}^{(1-1/n)} \text{ L}^{1/n} \text{ kg}^{-1}$ and SSA was $2.6 \text{ m}^2 \text{ g}^{-1}$.

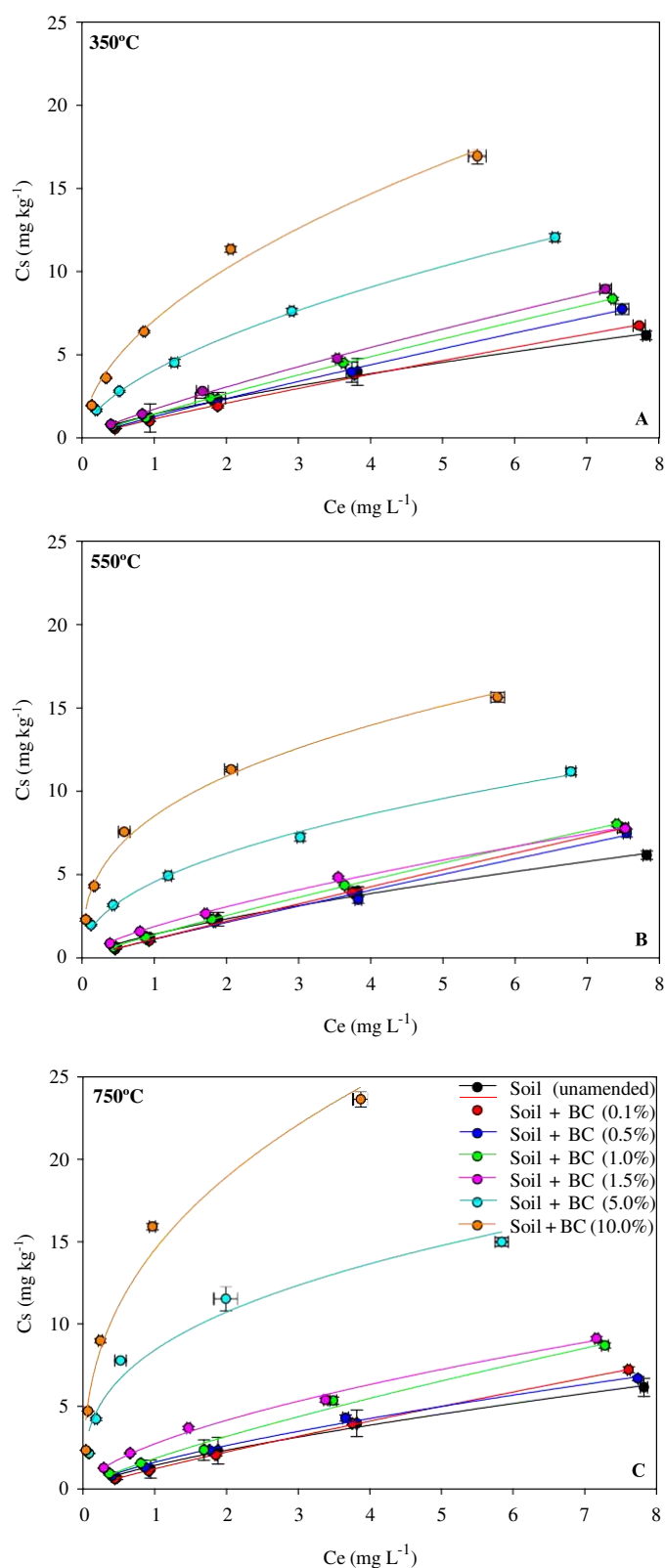


Figure 2. Sorption isotherms of the Freundlich model of metribuzin applied in soil amended and unamended (control) with sugarcane straw biochar (BC) produced at pyrolysis temperatures of 350 °C (A), 550 °C (B) and 750 °C (C). The vertical and horizontal bars represent standard error ($n = 3$) of C_e (equilibrium concentration) and C_s (soil concentration). Symbols can cover the bars.

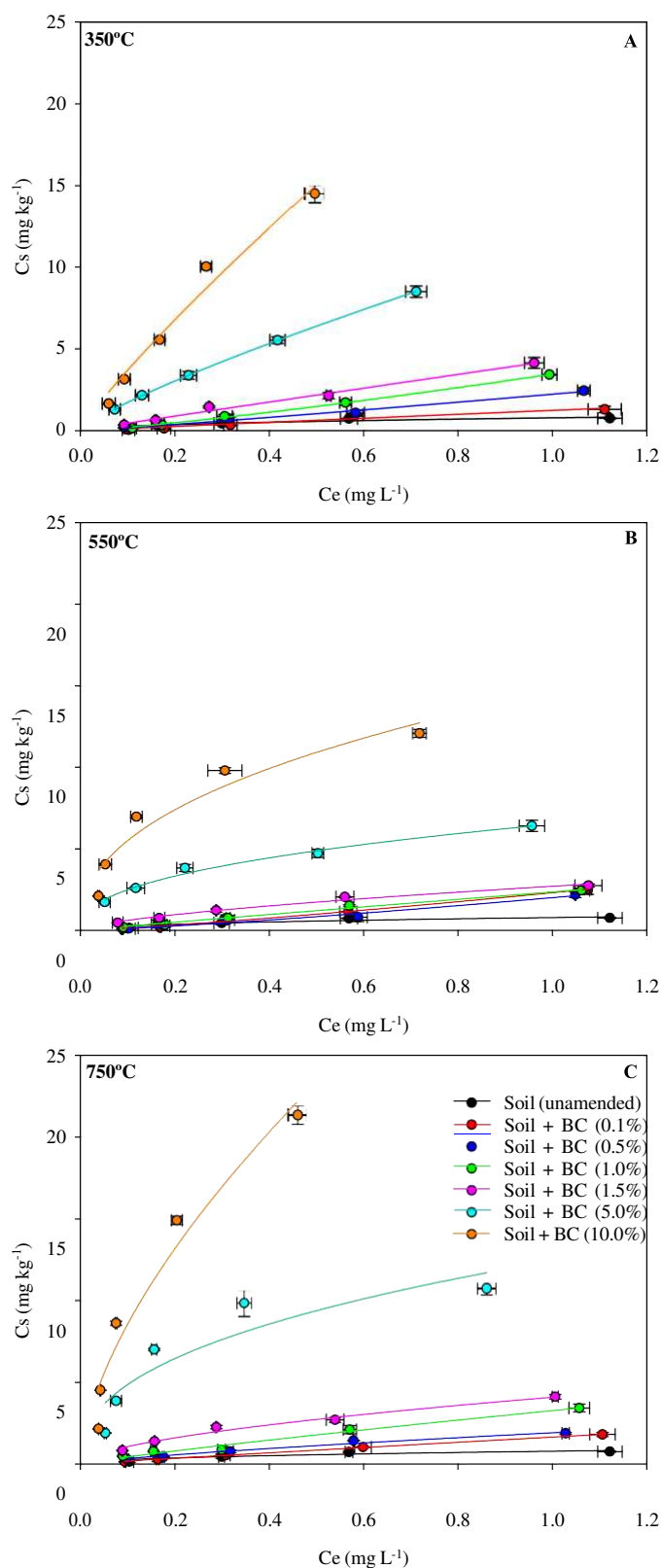


Figure 3. Desorption isotherms of the Freundlich model of metribuzin applied in soil amended and unamended (control) with sugarcane straw biochar (BC) produced at pyrolysis temperatures of 350 °C (A), 550 °C (B) and 750 °C (C). The vertical and horizontal bars represent standard error ($n = 3$) of C_e (equilibrium concentration) and C_s (soil concentration). Symbols can cover the bars.

Table 3. Sorption isotherm parameters of Freundlich model. Sorption coefficient (K_{d-app}) of 2 mg L⁻¹ and Gibbs free energy (ΔG) concentration for metribuzin applied to soil amended with sugarcane straw biochar and unamended soil.

Pyrolysis Temperature	Application Rate	Freundlich					K_{d-app}	K_{oc}	ΔG
		K_f	K_{foc}	$1/n$	R^2				
(°C)	(%) w w ⁻¹	(mg ^(1-1/n) L ^{1/n} kg ⁻¹)				L kg ⁻¹	Sorbed (%)	kJ mol ⁻¹	
-	unamended	1.42 ± 0.26 ^a	114.5	0.721 ± 0.04	0.99	1.66 ± 0.71	133	23.17 ± 2.80	-868.77
	0.1	1.13 ± 0.05	96	0.875 ± 0.05	0.99	0.96 ± 0.07	82	18.9 ± 0.28	-302.80
	0.5	1.27 ± 0.14	116	0.894 ± 0.03	0.99	1.39 ± 0.14	127	22.8 ± 0.76	-592.18
	1	1.33 ± 0.05	122	0.885 ± 0.03	0.99	1.37 ± 0.04	117	23.8 ± 0.48	-706.55
	1.5	1.71 ± 0.10	137	0.830 ± 0.01	0.99	1.60 ± 0.10	129	28.0 ± 0.61	-1329.20
350	5	4.05 ± 0.15	311	0.579 ± 0.02	0.99	3.04 ± 0.34	233	45.2 ± 1.56	-3465.42
	10	7.06 ± 0.16	504	0.527 ± 0.01	0.99	6.99 ± 0.11	499	63.8 ± 0.98	-4842.27
	0.1	1.21 ± 0.08	105	0.807 ± 0.02	0.99	1.22 ± 0.15	104	20.4 ± 0.62	-472.27
	0.5	1.38 ± 0.10	117	0.877 ± 0.03	0.99	1.23 ± 0.05	105	21.9 ± 0.72	-797.98
	1	1.13 ± 0.08	91	0.854 ± 0.01	0.99	1.33 ± 0.23	107	22.0 ± 0.82	-302.80
550	1.5	1.87 ± 0.04	159	0.708 ± 0.02	0.99	1.58 ± 0.16	134	26.4 ± 0.39	-1550.80
	5	4.55 ± 0.15	417	0.460 ± 0.02	0.99	4.77 ± 0.32	437	49.2 ± 1.38	-3753.83
	10	8.50 ± 0.10	726	0.358 ± 0.02	0.99	14.0 ± 0.14	1196	75.5 ± 0.74	-5302.16
	0.1	1.54 ± 0.07	107	0.881 ± 0.01	0.99	1.03 ± 0.09	83	23.6 ± 0.56	-532.95
	0.5	1.60 ± 0.09	136	0.704 ± 0.03	0.99	1.35 ± 0.18	115	23.4 ± 0.75	-1164.46
750	1	1.84 ± 0.21	157	0.788 ± 0.06	0.99	1.09 ± 1.0	93	23.5 ± 1.90	-1510.73
	1.5	2.73 ± 0.08	220	0.606 ± 0.03	0.99	2.58 ± 0.17	208	39.9 ± 0.79	-2488.22
	5	8.41 ± 0.22	718	0.349 ± 0.04	0.98	14.2 ± 0.18	1210	77.8 ± 1.31	-5275.79
	10	14.51 ± 0.15	1239	0.383 ± 0.06	0.98	45.0 ± 0.21	3846	89.4 ± 0.70	-6627.10

^a Average of the value of each parameter ± standard deviation of the mean (n = 3).

Table 4. Desorption isotherm parameters of Freundlich model. Sorption coefficient (K_{d-app}) of 2 mg L⁻¹. Hysteresis coefficient (H) and Gibbs free energy (ΔG) for metribuzin applied to soil amended with sugarcane straw biochar and unamended soil.

Biochar		Freundlich					K_{d-app}	K_{oc}	ΔG	
Pyrolysis Temperature	Application Rate	K_f	K_{foc}	$1/n$	H	R^2				
(°C)	(%) w w ⁻¹	(mg ^(1-1/n) L ^{1/n} kg ⁻¹)					L kg ⁻¹	Desorbed (%)	kJ mol ⁻¹	
-	unamended	0.78 ± 0.09 ^a	62	0.468 ± 0.13	0.65	0.91	1.49 ± 0.09	117	15.8 ± 0.54	-615.58
	0.1	1.23 ± 0.08	105	0.974 ± 0.30	1.11	0.96	1.07 ± 0.04	91	15.5 ± 0.25	-512.89
	0.5	2.22 ± 0.18	203	1.006 ± 0.10	1.24	0.99	2.27 ± 0.10	208	15.7 ± 0.45	-1975.88
	1	3.45 ± 0.06	294	1.029 ± 0.04	1.39	0.99	2.86 ± 0.10	244	15.1 ± 0.72	-3068.16
	1.5	3.27 ± 0.12	344	0.976 ± 0.08	1.18	0.99	5.33 ± 0.06	429	13.5 ± 0.15	-2935.40
350	5	6.51 ± 0.18	597	0.418 ± 0.03	0.91	0.99	14.76 ± 0.07	1135	11.0 ± 0.32	-5985.60
	10	14.64 ± 0.11	1251	0.425 ± 0.07	1.19	0.96	33.10 ± 0.07	2364	5.8 ± 0.19	-8218.33
	0.1	2.30 ± 0.09	196	1.023 ± 0.06	1.52	0.99	2.03 ± 0.07	173	15.2 ± 0.13	-2062.59
	0.5	2.00 ± 0.08	170	1.059 ± 0.20	1.44	0.97	2.21 ± 0.03	188	15.1 ± 0.30	-1717.32
	1	2.35 ± 0.09	189	0.970 ± 0.08	1.02	0.99	2.40 ± 0.14	193	15.5 ± 0.23	-2116.87
550	1.5	2.69 ± 0.05	229	0.645 ± 0.05	0.91	0.99	4.23 ± 0.10	361	14.3 ± 0.18	-2451.65
	5	11.28 ± 0.17	961	0.818 ± 0.03	0.91	0.99	17.26 ± 0.22	1583	11.4 ± 0.44	-4641.33
	10	27.58 ± 0.18	1970	0.815 ± 0.07	1.19	0.96	58.86 ± 0.09	5030	8.3 ± 0.32	-6649.20
	0.1	1.64 ± 0.06	132	0.960 ± 0.02	1.09	0.99	1.72 ± 0.09	138	15.1 ± 0.37	-1225.61
	0.5	1.90 ± 0.18	162	0.766 ± 0.09	1.09	0.98	2.40 ± 0.07	205	15.7 ± 0.26	-1590.23
750	1	3.26 ± 0.12	281	0.877 ± 0.09	1.11	0.99	7.02 ± 0.03	600	14.9 ± 0.33	-2927.80
	1.5	4.08 ± 0.09	329	0.583 ± 0.05	0.96	0.99	7.85 ± 0.11	566	14.3 ± 0.18	-3483.70
	5	12.44 ± 0.27	1063	0.468 ± 0.10	1.34	0.91	44.9 ± 0.06	3837	11.8 ± 0.31	-6245.75
	10	35.91 ± 0.19	3069	0.623 ± 0.09	1.62	0.97	114.5 ± 0.13	9786	3.7 ± 0.17	-8872.22

^a Average of the value of each parameter ± standard deviation of the mean (n = 3).

FTIR analysis showed that with increasing pyrolysis temperature, losses of surface functional groups occurred, which may increase the sorptive capacity of BC750. Low-temperature biochar (350 °C) has more polar, aliphatic surface groups that are amorphous in character [83], while high-temperature biochar has surface groups that resemble graphitic aromatic C, rich in π electrons [84]. The increased sorption capacity on BC750 could also occur due to π - π -type binding between metribuzin and BC750. Triazine herbicides, such as metribuzin, can behave as a π -electron donor while the polyaromatic surfaces of biochar act as an electron acceptor, indicating a combination of a π - π force between metribuzin and the biochar surface [85]. Wheat straw biochar produced at a pyrolysis temperature of 800 °C was analyzed for the sorption potential of metribuzin for environmental remediation [86]. These authors observed that the predominant sorption process was linked to chemical sorption via π - π interactions.

The pH has an influence on the sorption and desorption of metribuzin in the amended soil. Metribuzin is a strong acid ($pK_a = 1.3$) and shows low sorption due to its ionic form (negatively charged) that provides repulsion with the negative charges of the soil under conditions of high pH values [78,87]. However, even as the pH of the biochar-amended soil increased, the sorption of metribuzin was higher than in the unamended soil. Although the herbicide is mostly in ionic form, the mechanisms related to porous structure, SSA and surface groups provide high capacity to sorb the herbicides that are in the soil solution [88]. Similar results were observed by [89], analyzing pH and biochar addition on the sorption of two acidic herbicides (2,4-D and imazethapyr). The authors observed that in unamended soil, sorption decreased as soil pH increased, providing injury to the rice crop. As 2 and 8% biochar were added to the soil, pH increased; however, sorption increased proportionally, decreasing crop injury.

The application rates of biochar produced at different pyrolysis temperatures influenced the percentage sorbed (relative to the total initially applied) of metribuzin in the soil (Table 3). Application rates of 0.1, 0.5 and 1% biochar had similar percentages of metribuzin sorbed to unamended soil (~23%) for all pyrolysis temperatures. The 5% application rate of BC750 to soil increased the sorption of metribuzin by 70%, while amended soil with BC350 and BC550 sorbed 45 and 49%, respectively. At the highest application rate, the percentage of metribuzin sorbed was 63.8, 75.5 and 89.4% relative to the total applied, for the amended soil with BC350, BC550 and BC750, respectively (Table 3). The presence of 5% biochar can directly influence the effectiveness of metribuzin in the soil for weed control. Sugarcane straw biochar with a high sorptive capacity, such as BC750, applied at high rates may result in a scenario where even higher doses will be required to control weeds after the addition of this material to the area. However, the application of biochar to soil for agronomic purposes is considered undesirable [61]. In a remediation scenario for soils contaminated with metribuzin, sugarcane straw biochar presented itself as a viable alternative for immobilization of the herbicide at application rates above 5%.

Increased sorption of metribuzin at higher application rates was observed using different biochars [25,90,91]. Application rates of olive mill waste biochar were analyzed for the sorption potential of metribuzin in the soil [25]. These authors observed that the application of 2.5 and 5% biochar increased the sorption of metribuzin by 1.5- and 2.5-fold, respectively, relative to unamended soil. The effectiveness of metribuzin was reduced when sugarcane bagasse biochar was applied (350 and 700 °C) at rates of 1 to 4% in clayey soil [82]. The authors observed that the application rate of 8% biochar reduced the residual effect of metribuzin and provided increased germination of Palmer amaranth (*Amaranthus palmeri*), being larger than the unamended soil. The reduction in herbicide residual effect was also observed by [92], in which an application rate of only 1.6% of bonechar in the soil was sufficient to reduce the level of weed injury by 50%.

The desorption coefficients (Table 4) for the Freundlich model (K_f) and at the median concentration (K_{d-app}) showed that desorption was reduced as the application rate of biochar to the soil increased. The K_f value of the unamended soil desorption was $0.78 \text{ mg}^{(1-1/n)} \text{ L}^{1/n} \text{ kg}^{-1}$. The desorption of metribuzin decreased between 2- and 46-times for the application rate of 0.1 to 10% for the BC750-amended soil compared to the unamended soil. Soil amended with BC350 and BC550 decreased desorption by up to 18- and 35-fold, respectively, for the 10% application rate, relative to unamended soil. The higher K_f (desorption) value for metribuzin in the amended soils, relative to the unamended soil,

regardless of pyrolysis temperature, indicated that the presence of carbonaceous material decreased the desorption of metribuzin. Lipophilic herbicides, such as metribuzin ($\text{Log } K_{ow} = 1.75$), can establish chemical interactions between non-polar groups in the biochar and increase stability, reducing desorption. Both the C content and the aromatic structure are important factors affecting the low desorption capacity of biochar for lipophilic herbicides [13,93].

The percent of metribuzin desorbed in the soil with application rates of 0.1, 0.5 and 1% biochar was similar to the unamended soil (~15%) at all pyrolysis temperatures (Table 4). The 10% application rate of biochar to soil provided the least desorption of metribuzin, being desorbed 8.3, 5.8 and 3.7% for BC350, BC550 and BC750, respectively. The desorption K_{foc} values for the 10% application rate were 1970, 1251 and 3069 $\text{mg}^{(1-1/n)} \text{L}^{1/n} \text{kg}^{-1}$ in the BC350-, BC550- and BC750-amended soils, respectively. The hysteresis (H) of the isotherms of metribuzin in the unamended soil was 0.65 and when biochar was added, the H was greater than 1, which is classified as negative hysteresis ($H > 1$) (Table 4). When H is negative, it indicates that desorption is greater than the sorption rate [94]. With increasing application rates of BC750 biochar, the H values increased, showing that the application of this biochar can decrease the bioavailability of metribuzin in the soil solution. Metribuzin also showed negative H in soils amended with fly ashes [95]. The results of the lower desorption of metribuzin presented in this study showed that, in addition to the high sorption capacity, the sugarcane straw biochar presented available pores for herbicide diffusion. The porous structures of biochar can lead to herbicide immobilization [96]. The lowest desorption of atrazine was also observed when applied directly to the amended soil with biochar from cassava waste obtained at 750 °C [97]. The authors reported that the lower desorption could be related to the irreversibility of chemical bonding or sequestration of atrazine in meso- or micro-pores of the biochar.

In general, the Gibbs free energy value (ΔG) of the sorption and desorption reaction of metribuzin in the biochar-amended soils decreased with increasing pyrolysis temperature and application rates (Tables 3 and 4). This indicates that as pyrolysis temperature and application rates increased, the molecules of this herbicide remained sorbed onto the biochar, indicating that sorption increased while desorption decreased. The change in Gibbs free energy (ΔG) indicates the degree of spontaneity in a sorption process and a larger negative value reflects more energetically favorable sorption [98]. The more negative ΔG value for the BC750-amended soil (Table 3) indicated that sorption of metribuzin was not exclusively governed by chemical reactions, since an absolute ΔG value of less than 40 kJ/mol indicates mainly physical sorption [99]. However, both physical and chemical sorption are processes that can occur concomitantly [100]. Sorption is a thermodynamic process, i.e., physical sorption (related to surface interaction, pore filling, Coulomb forces, van der Waals and hydrogen bonds) and chemical sorption (valence forces, electron donor-acceptor (EDA) mechanisms, π -interactions) involve the conversion of heat and other forms of energy [60].

Overall, soil modification with higher application rates (1.5, 5 and 10%) of BC750 had a high influence on the sorption and desorption of metribuzin from the soil and may reduce the potential of the herbicide to control weeds. However, lower rates (<1.5%) of BC350 and 550 provided less impact on sorption and desorption of metribuzin and improved the chemical attributes in the amended soils. This information is important for determining the application of these biochars to the soil, either as fertilizer or to reduce the risk of environmental contamination of the herbicide. The sorption and desorption study showed that the successful use of biochar will depend on the relationship between pyrolysis temperature and application rate.

4. Conclusions

Pyrolysis temperature altered the physicochemical attributes of sugarcane straw biochar. BC750C showed higher SSA, C/N ratio, pH and decreased presence of surface functional groups, which may be directly linked to higher sorption and lower desorption of metribuzin in the amended soil. The physicochemical characterization allows the analysis of the biochar composition and the main positive aspects related to herbicide immobilization.

Using application rates of 1 and 1.5% of BC350, BC550 and BC750 can improve soil fertility by making P, K, Mg, Fe and Mn available, reducing potential acidity (H + Al) and increasing soil pH. The lower rates of BC350 and 550 provided less impact on the sorption and desorption of metribuzin and may be an alternative for the use of sugarcane straw biochar produced at low pyrolysis temperatures as a source of fertilizer. However, it is important to note that the sorption and desorption behavior takes into account the physicochemical attributes of the herbicide; in this case, the same biochar evaluated in this study may present lower or higher sorption capacity when analyzed with another herbicide. Soil amended with BC750, from an environmental remediation perspective, has a high potential to decrease the mobility and risks of metribuzin in environmental contamination. However, sorption of metribuzin increased and desorption decreased with increasing rates of biochar application, which may negatively affect the bioavailability of metribuzin in the soil solution and, in an agronomic approach, may influence the residual effect of metribuzin in the soil and decrease its activity in weed control efficacy.

Supplementary Materials: The following supporting information can be downloaded at: <https://www.mdpi.com/article/10.3390/pr10101924/s1>, Figure S1. Surficial elemental composition C (red), O (yellow), Si (green), Ca, K, P, Al, P and Na (undetected) by energy dispersive X-ray spectrometry (EDS) analysis of biochar (BC) (A) and EDS spectrogram (B) in different pyrolysis temperatures (350, 550 and 750 °C); Figure S2. Images of the biochar (BC) derived from sugar cane straw at different pyrolysis temperatures (350, 550 and 750 °C) by scanning electron microscopy (SEM) at 500- and 3000-times magnification.

Author Contributions: Conceptualization, K.C.M.; Data curation, K.C.M., A.F.S.L., M.G.d.S.B. and B.A.d.P.M.; Investigation, Methodology, Validation, A.F.S.L., T.G., K.C.M. and K.F.M.; Writing—review and editing, K.C.M. and K.F.M.; Project administration, Formal analysis, Funding acquisition, K.F.M. All authors have read and agreed to the published version of the manuscript.

Funding: This research was funded by Coordination for the Improvement of Higher Education Personnel (CAPES-88887.479265/2020-00), Foundation for Research Support of the State of Minas Gerais (FAPEMIG-2070.01.0004768/2021-84).

Data Availability Statement: Not applicable.

Acknowledgments: The authors thanks the Federal University of Viçosa and the Matheus Bortolanza Soares from the “Luiz de Queiroz” College of Agriculture, University of São Paulo for kindly donating the biochar.

Conflicts of Interest: The authors declare no conflict of interest.

5. References

1. Lehmann, J.; Joseph, S. *Biochar for environmental management: An introduction*, In *Biochar for Environmental Management: Science, Technology and Implementation*; Lehmann, J., Joseph, S., Eds.; Routledge: New York, NY, USA, 2015; pp. 1–13.
2. Gul, S.; Whalen, J.K.; Thomas, B.W.; Sachdeva, V.; Deng, H. Physico-chemical properties and microbial responses in biochar-amended soils: Mechanisms and future directions. *Agric. Ecosyst. Environ.* **2015**, *206*, 46–59. [[CrossRef](#)]
3. Zhang, Y.; Wang, J.; Feng, Y. The effects of biochar addition on soil physicochemical properties: A review. *Catena* **2021**, *202*, 105284. [[CrossRef](#)]
4. Liang, B.; Lehmann, J.; Solomon, D.; Kinyangi, J.; Grossman, J.; O'Neill, B.; Skjemstad, J.O.; Thies, J.; Luizão, F.J.; Petersen, J.; et al. Black carbon increases cation exchange capacity in soils. *Soil Sci. Soc. Am. J.* **2006**, *70*, 1719–1730. [[CrossRef](#)]
5. Mosley, L.M.; Willson, P.; Hamilton, B.; Butler, G.; Seaman, R. The capacity of biochar made from common reeds to neutralise pH and remove dissolved metals in acid drainage. *Environ. Sci. Pollut. Res.* **2015**, *22*, 15113–15122. [[CrossRef](#)] [[PubMed](#)]
6. Woolf, D.; Amonette, J.E.; Street-Perrott, F.A.; Lehmann, J.; Joseph, S. Sustainable biochar to mitigate global climate change. *Nat. Commun.* **2010**, *1*, 1–9. [[CrossRef](#)]
7. Khadem, A.; Raiesi, F.; Besharati, H.; Khalaj, M.A. The effects of biochar on soil nutrients status, microbial activity and carbon sequestration potential in two calcareous soils. *Biochar* **2021**, *3*, 105–116. [[CrossRef](#)]
8. Karimi, A.; Moezzi, A.; Chorom, M.; Enayatizamir, N. Application of biochar changed the status of nutrients and biological activity in a calcareous soil. *J. Soil Sci. Plant Nutr.* **2020**, *20*, 450–459. [[CrossRef](#)]
9. Hussain, M.; Farooq, M.; Nawaz, A.; Al-Sadi, A.M.; Solaiman, Z.M.; Alghamdi, S.S.; Ammara, U.; Ok, Y.S.; Siddique, K.H. Biochar for crop production: Potential benefits and risks. *J. Soils Sediments* **2017**, *17*, 685–716. [[CrossRef](#)]

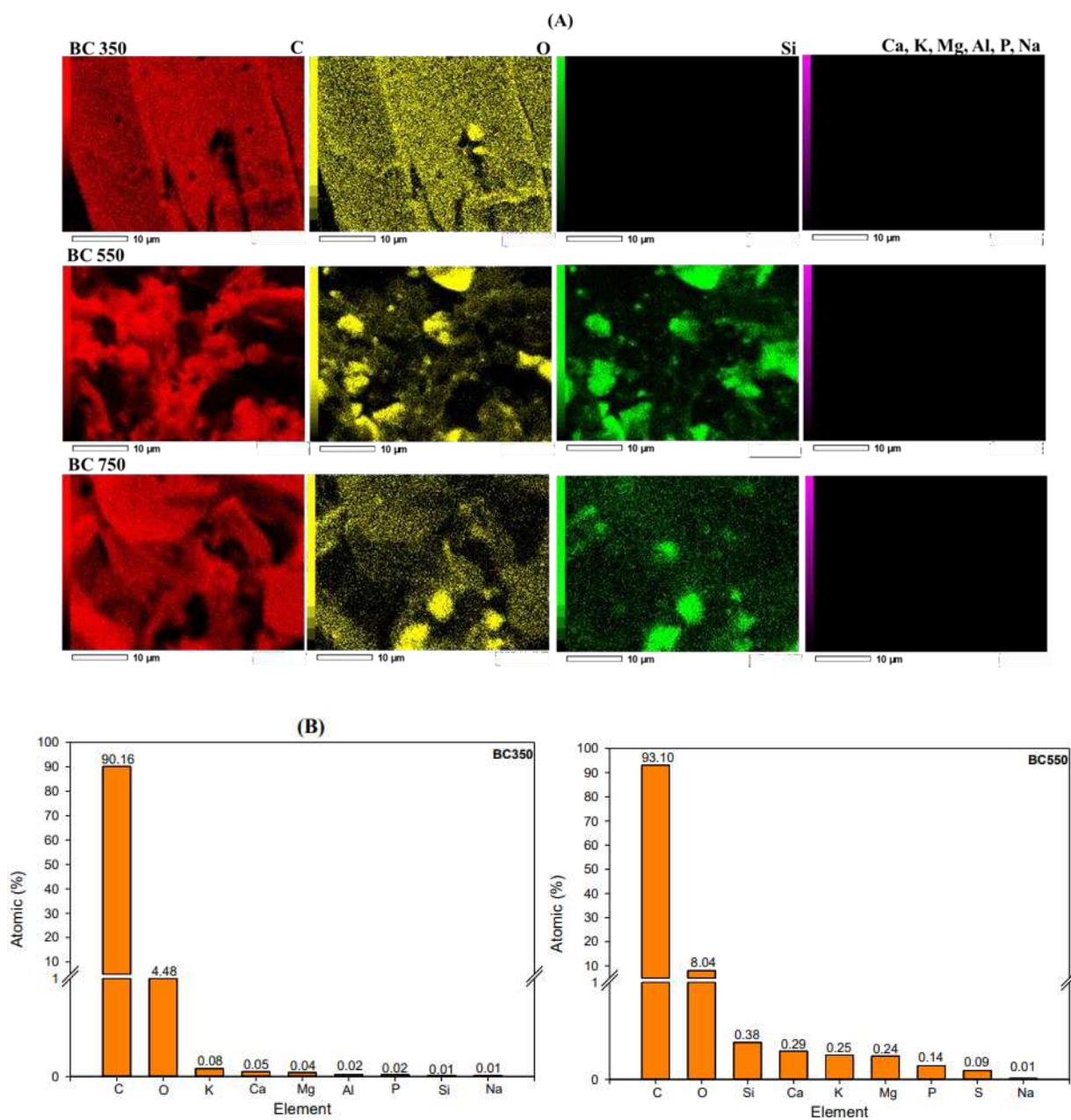
10. Bartoli, M.; Giorcelli, M.; Jagdale, P.; Rovere, M.; Tagliaferro, A. A review of non-soil biochar applications. *Materials* **2020**, *13*, 261. [[CrossRef](#)]
11. Ahmad, M.; Rajapaksha, A.U.; Lim, J.E.; Zhang, M.; Bolan, N.; Mohan, D.; Vithanage, M.; Lee, S.S.; Ok, Y.S. Biochar as a sorbent for contaminant management in soil and water: A review. *Chemosphere* **2014**, *99*, 19–33. [[CrossRef](#)]
12. Yu, X.Y.; Mu, C.L.; Gu, C.; Liu, C.; Liu, X.J. Impact of woodchip biochar amendment on the sorption and dissipation of pesticide acetamiprid in agricultural soils. *Chemosphere* **2011**, *85*, 1284–1289. [[CrossRef](#)] [[PubMed](#)]
13. Cabrera, A.; Cox, L.; Spokas, K.U.R.T.; Hermosín, M.C.; Cornejo, J.; Koskinen, W.C. Influence of biochar amendments on the sorption-desorption of aminocyclopyrachlor, bentazone and pyraclostrobin pesticides to an agricultural soil. *Sci. Total Environ.* **2014**, *470*, 438–443. [[CrossRef](#)] [[PubMed](#)]
14. Huang, H.; Zhang, C.; Zhang, P.; Cao, M.; Xu, G.; Wu, H.; Zhang, J.; Li, C.; Rong, Q. Effects of biochar amendment on the sorption and degradation of atrazine in different soils. *Soil Sediment Contam.* **2018**, *27*, 643–657. [[CrossRef](#)]
15. Szmigielski, A.M.; Hangs, R.D.; Schoenau, J.J. Bioavailability of metsulfuron and sulfentrazone herbicides in soil as affected by amendment with two contrasting willow biochars. *Bull. Environ. Contam. Toxicol.* **2018**, *100*, 298–302. [[CrossRef](#)]
16. Mendes, K.F.; Júnior, A.F.D.; Takeshita, V.; Régo, A.P.J.; Tornisielo, V.L. Effect of biochar amendments on the sorption and desorption herbicides in agricultural soil. In *Advanced Sorption Process Applications*; Edebali, S., Ed.; IntechOpen: London, UK, 2019; pp. 1–25.
17. Jensen, L.C.; Becerra, J.R.; Escudey, M. Impact of physical/chemical properties of volcanic ash-derived soils on mechanisms involved during sorption of ionisable and non-ionisable herbicides. In *Advanced Sorption Process Applications*; Edebali, S., Ed.; IntechOpen: London, UK, 2018; pp. 1–23.
18. Mielke, K.C.; Mendes, K.F.; Guimarães, T. Biochars effects on sorption and desorption of herbicides in soil. In *Interactions of Biochar and Herbicides in the Environment*; Mendes, K.F., Ed.; CRC Press: Boca Raton, FL, USA, 2022; pp. 131–157.
19. Trebst, A.; Wietoska, H. Mode of action and structure-activity-relationships of the aminotriazinone herbicide Metribuzin. Inhibition of photosynthetic electron transport in chloroplasts by Metribuzin. *Z. fur Nat. Sect. C Biosci.* **1975**, *30*, 499–504.
20. Saritha, J.D.; Ramprakash, T.; Rao, P.C.; Madhavi, M. Persistence of metribuzin in tomato growing soils and tomato fruits. *Nat. Environ. Pollut. Technol.* **2017**, *16*, 505.
21. Guimarães, A.C.D.; Mendes, K.F.; Campion, T.F.; Christoffoleti, P.J.; Tornisielo, V.L. Leaching of herbicides commonly applied to sugarcane in five agricultural soils. *Planta Daninha.* **2019**, *37*, e019181505. [[CrossRef](#)]
22. PPDB—Pesticide Properties Database. Footprint: Creating Tools for Pesticide Risk Assessment and Management in Europe. Developed by the Agriculture & Environment Research Unit (AERU), University of Hertfordshire, Funded by UK National Sources and the EU-funded FOOTPRINT Project (FP6-SSP-022704). Available online: <https://sitem.herts.ac.uk/aeru/ppdb/en/Reports/469.htm> (accessed on 10 March 2022).
23. Dores, E.F.G.C.; Navickiene, S.; Cunha, M.L.; Carbo, L.; Ribeiro, M.L.; De-Lamonica-Freire, E.M. Multiresidue determination of herbicides in environmental waters from Primavera do Leste Region (Middle West of Brazil) by SPE-GC-NPD. *J. Braz. Chem. Soc.* **2006**, *17*, 866–873. [[CrossRef](#)]
24. Kjær, J.; Olsen, P.; Henriksen, T.; Ullum, M. Leaching of metribuzin metabolites and the associated contamination of a sandy Danish aquifer. *Environ. Sci. Technol.* **2005**, *39*, 8374–8381. [[CrossRef](#)]
25. López-Piñeiro, A.; Peña, D.; Albarrán, A.; Becerra, D.; Sánchez-Llerena, J. Sorption, leaching and persistence of metribuzin in Mediterranean soils amended with olive mill waste of different degrees of organic matter maturity. *J. Environ. Manag.* **2013**, *122*, 76–84. [[CrossRef](#)] [[PubMed](#)]
26. Loffredo, E.; Parlavecchia, M.; Perri, G.; Gattullo, R. Comparative assessment of metribuzin sorption efficiency of biochar, hydrochar and vermicompost. *J. Environ. Sci. Health Part B* **2019**, *54*, 728–735. [[CrossRef](#)] [[PubMed](#)]
27. Mendes, K.F.; de Sousa, R.N.; Takeshita, V.; Alonso, F.G.; Régo, A.P.J.; Tornisielo, V.L. Cow bone char as a sorbent to increase sorption and decrease mobility of hexazinone, metribuzin, and quinclorac in soil. *Geoderma* **2019**, *343*, 40–49. [[CrossRef](#)]
28. Sigua, G.C.; Stone, K.C.; Hunt, P.G.; Cantrell, K.B.; Novak, J.M. Increasing biomass of winter wheat using sorghum biochars. *Agron. Sustain. Dev.* **2015**, *35*, 739–748. [[CrossRef](#)]
29. Jafri, N.; Wong, W.Y.; Doshi, V.; Yoon, L.W.; Cheah, K.H. A review on production and characterization of biochars for application in direct carbon fuel cells. *Process Saf. Environ. Prot.* **2018**, *118*, 152–166. [[CrossRef](#)]
30. Shaaban, M.; Van Zwieten, L.; Bashir, S.; Younas, A.; Núñez-Delgado, A.; Chhajro, M.A.; Kubar, K.A.; Ali, U.; Rana, M.S.; Mehmood, M.A.; et al. A concise review of biochar application to agricultural soils to improve soil conditions and fight pollution. *J. Environ. Manag.* **2018**, *228*, 429–440. [[CrossRef](#)]
31. Soares, M.B.; dos Santos, F.H.; Alleoni, L.R.F. Iron-modified biochar from sugarcane straw to remove arsenic and lead from contaminated water. *Water Air Soil Pollut.* **2021**, *232*, 1–13. [[CrossRef](#)]
32. Soares, M.B.; Milori, D.M.B.P.; Alleoni, L.R.F. How does the biochar of sugarcane straw pyrolysis temperature change arsenic and lead availabilities and the activity of the microorganisms in a contaminated sediment? *J. Soils Sediments* **2021**, *21*, 3185–3200. [[CrossRef](#)]
33. USEPA. *Method 3051A: Microwave Assisted Acid Digestion of Sediments, Sludges, Soils and Oils*; EPA: Washington, DC, USA, 2007.
34. Singh, B.; Camps-Arbestain, M.; Lehmann, J. *Biochar: A Guide to Analytical Methods*; CRC Press: Boca Raton, FL, USA, 2017.
35. Song, W.; Guo, M. Quality variations of poultry litter biochar generated at different pyrolysis temperatures. *J. Anal. Appl. Pyrolysis.* **2012**, *94*, 138–145. [[CrossRef](#)]

36. OECD—Organisation for Economic Co-Operation and Development. *Adsorption—Desorption Using a Batch Equilibrium Method*; OECD: Paris, France, 2000; 44p.
37. Mendes, K.F.; Sousa, R.N.; Soares, M.B.; Viana, D.G.; Souza, A.J. Sorption and desorption studies of herbicides in the soil by batch equilibrium and stirred flow methods. In *Radioisotopes in Weed Research*; Mendes, K.F., Ed.; CRC Press: Boca Raton, FL, USA, 2021; Volume 1, pp. 17–61.
38. Melo, L.C.; Coscione, A.R.; Abreu, C.A.; Puga, A.P.; Camargo, O.A. Influence of pyrolysis temperature on cadmium and zinc sorption capacity of sugar cane straw-derived biochar. *BioResources* **2013**, *8*, 4992–5004. [[CrossRef](#)]
39. Riaz, M.; Khan, M.; Ali, S.; Khan, M.D.; Ahmad, R.; Khan, M.J.; Rizwan, M. Sugarcane waste straw biochar and its effects on calcareous soil and agronomic traits of okra. *Arab. J. Geosci.* **2018**, *11*, 1–7. [[CrossRef](#)]
40. Ding, Y.; Liu, Y.; Liu, S.; Li, Z.; Tan, X.; Huang, X.; Zeng, G.; Zhou, L.; Zheng, B. Biochar to improve soil fertility. A review. *Agron. Sustain. Dev.* **2016**, *36*, 1–18. [[CrossRef](#)]
41. Tomczyk, A.; Sokołowska, Z.; Boguta, P. Biochar physicochemical properties: Pyrolysis temperature and feedstock kind effects. *Rev. Environ. Sci. Biotechnol.* **2020**, *19*, 191–215. [[CrossRef](#)]
42. Fidel, R.B.; Laird, D.A.; Thompson, M.L.; Lawrinenko, M. Characterization and quantification of biochar alkalinity. *Chemosphere* **2017**, *167*, 367–373. [[CrossRef](#)] [[PubMed](#)]
43. Novotny, E.H.; Maia, C.M.B.F.; Carvalho, M.T.M.; Madari, B.E. Biochar—Pyrogenic carbon for agricultural use—A critical review. *Rev. Bras. Cienc. Solo.* **2015**, *39*, 321–344. [[CrossRef](#)]
44. Zhao, S.X.; Ta, N.; Wang, X.D. Effect of temperature on the structural and physicochemical properties of biochar with apple tree branches as feedstock material. *Energies* **2017**, *10*, 1293. [[CrossRef](#)]
45. Farid, I.M.; Siam, H.S.; Abbas, M.H.; Mohamed, I.; Mahmoud, S.A.; Tolba, M.; Abbas, H.H.; Yang, X.; Antoniadis, V.; Rinklebe, J.; et al. Co-composted biochar derived from rice straw and sugarcane bagasse improved soil properties, carbon balance, and zucchini growth in a sandy soil: A trial for enhancing the health of low fertile arid soils. *Chemosphere* **2022**, *292*, e133389. [[CrossRef](#)]
46. Figueiredo, C.; Lopes, H.; Coser, T.; Vale, A.; Busato, J.; Aguiar, N.; Novotny, E.; Canellas, L. Influence of pyrolysis temperature on chemical and physical properties of biochar from sewage sludge. *Arch. Agron. Soil Sci.* **2018**, *64*, 881–889. [[CrossRef](#)]
47. Domingues, R.R.; Trugilho, P.F.; Silva, C.A.; Melo, I.C.N.D.; Melo, L.C.; Magriotis, Z.M.; Sanchez-Monedero, M.A. Properties of biochar derived from wood and high-nutrient biomasses with the aim of agronomic and environmental benefits. *PLoS ONE* **2017**, *12*, e0176884. [[CrossRef](#)]
48. Liu, Q.; Li, Y.; Chen, H.; Lu, J.; Yu, G.; Möslang, M.; Zhou, Y. Superior adsorption capacity of functionalised straw adsorbent for dyes and heavy-metal ions. *J. Hazard. Mater.* **2020**, *382*, 121040. [[CrossRef](#)]
49. Zhang, X.; Zhang, P.; Yuan, X.; Li, Y.; Han, L. Effect of pyrolysis temperature and correlation analysis on the yield and physicochemical properties of crop residue biochar. *Bioresour. Technol.* **2020**, *296*, 122318. [[CrossRef](#)]
50. Huang, F.; Zhang, S.M.; Wu, R.R.; Zhang, L.; Wang, P.; Xiao, R.B. Magnetic biochars have lower adsorption but higher separation effectiveness for Cd²⁺ from aqueous solution compared to nonmagnetic biochars. *Environ. Pollut.* **2021**, *275*, 116485. [[CrossRef](#)]
51. Lopes, R.P.; Astruc, D. Biochar as a support for nanocatalysts and other reagents: Recent advances and applications. *Coord. Chem. Rev.* **2021**, *426*, 213585. [[CrossRef](#)]
52. Trivedi, M.; Branton, A.; Trivedi, D.; Nayak, G.; Singh, R.; Jana, S. Characterization of physical, spectral and thermal properties of biofield treated 1, 2, 4-Triazole. *Curr. Org. Chem.* **2015**, *3*, 1000128. [[CrossRef](#)]
53. Kamran, U.; Park, S.J. MnO₂-decorated biochar composites of coconut shell and rice husk: An efficient lithium ions adsorption-desorption performance in aqueous media. *Chemosphere* **2020**, *260*, 127500. [[CrossRef](#)] [[PubMed](#)]
54. Chandra, S.; Bhattacharya, J. Influence of temperature and duration of pyrolysis on the property heterogeneity of rice straw biochar and optimization of pyrolysis conditions for its application in soils. *J. Clean. Prod.* **2019**, *215*, 1123–1139. [[CrossRef](#)]
55. Collard, F.X.; Blin, J. A review on pyrolysis of biomass constituents: Mechanisms and composition of the products obtained from the conversion of cellulose, hemicelluloses and lignin. *Renew. Sustain. Energy Rev.* **2014**, *38*, 594–608. [[CrossRef](#)]
56. Hassan, M.; Liu, Y.; Naidu, R.; Parikh, S.J.; Du, J.; Qi, F.; Willett, I.R. Influences of feedstock sources and pyrolysis temperature on the properties of biochar and functionality as adsorbents: A meta-analysis. *Sci. Total Environ.* **2020**, *744*, 140714. [[CrossRef](#)]
57. Wang, Y.; Jiang, B.; Wang, L.; Feng, Z.; Fan, H.; Sun, T. Hierarchically structured two-dimensional magnetic microporous biochar derived from hazelnut shell toward effective removal of p-arsanilic acid. *Appl. Surf. Sci.* **2021**, *540*, 148372. [[CrossRef](#)]
58. Silva, R.C.F.; Ardisson, J.D.; Cotta, A.A.C.; Araujo, M.H.; Carvalho, A.P.T. Use of iron mining tailings from dams for carbon nanotubes synthesis in fluidized bed for 17 α -ethinylestradiol removal. *Environ. Pollut.* **2020**, *260*, 114099. [[CrossRef](#)]
59. Huang, H.; Guo, T.; Wang, K.; Li, Y.; Zhang, G. Efficient activation of persulfate by a magnetic recyclable rape straw biochar catalyst for the degradation of tetracycline hydrochloride in water. *Sci. Total Environ.* **2021**, *758*, 143957. [[CrossRef](#)]
60. Sousa, R.N.; Soares, M.B.; Santos, F.H.; Leite, C.N.; Mendes, K.F. Interaction mechanisms between biochar and herbicides. In *Interactions of Biochar and Herbicides in the Environment*; Mendes, K.F., Ed.; CRC Press: Boca Raton, FL, USA, 2022; pp. 80–105.
61. Khalid, S.; Shahid, M.; Murtaza, B.; Bibi, I.; Naeem, M.A.; Niazi, N.K. A critical review of different factors governing the fate of pesticides in soil under biochar application. *Sci. Total Environ.* **2020**, *711*, 134645. [[CrossRef](#)]
62. Novak, J.M.; Busscher, W.J.; Laird, D.L.; Ahmedna, M.; Watts, D.W.; Niandou, M.A. Impact of biochar amendment on fertility of a southeastern coastal plain soil. *Soil Sci.* **2009**, *174*, 105–112. [[CrossRef](#)]

63. El-Naggar, A.; Lee, S.S.; Awad, Y.M.; Yang, X.; Ryu, C.; Rizwan, M.; Rinklebe, J.; Tsang, D.C.W.; Ok, Y.S. Influence of soil properties and feedstocks on biochar potential for carbon mineralization and improvement of infertile soils. *Geoderma* **2018**, *332*, 100–108. [[CrossRef](#)]
64. Oliveira, F.S.; Takeshita, V.; Mendes, K.F.; Tornisielo, V.L.; Alonso, F.G.; Junqueira, L.V.; Neto, M.B.; Lins, H.A.; Silva, D.V. Addition of raw feedstocks and biochars to the soil on the sorption–desorption and biodegradation of ¹⁴C-saflufenacil. *Int. J. Environ. Sci. Technol.* **2022**, *1*, 1–18. [[CrossRef](#)]
65. Chintala, R.; Schumacher, T.E.; McDonald, L.M.; Clay, D.E.; Malo, D.D.; Papiernik, S.K.; Clay, S.A.; Julson, J.L. Phosphorus sorption and availability from biochars and soil/Biochar mixtures. *Clean—Soil Air Water* **2014**, *42*, 626–634. [[CrossRef](#)]
66. Glaser, B.; Lehr, V.I. Biochar effects on phosphorus availability in agricultural soils: A meta-analysis. *Sci. Rep.* **2019**, *9*, 1–9. [[CrossRef](#)]
67. Fernandes, J.D.; Chaves, L.H.G.; Dantas, E.R.B.; Tito, G.A.; Guerra, H.O.C. Phosphorus availability in soil incubated with biochar: Adsorption study. *Rev. Caatinga* **2022**, *35*, 206–215. [[CrossRef](#)]
68. Hong, C.; Lu, S. Does biochar affect the availability and chemical fractionation of phosphate in soils? *Environ. Sci. Pollut. Res.* **2018**, *25*, 8725–8734. [[CrossRef](#)]
69. Naeem, M.A.; Khalid, M.; Aon, M.; Abbas, G.; Tahir, M.; Amjad, M.; Murtaza, B.; Yan, A.; Akhtar, S.S. Effect of wheat and rice straw biochar produced at different temperatures on maize growth and nutrient dynamics of a calcareous soil. *Arch. Agron. SoilSci.* **2017**, *63*, 2048–2061. [[CrossRef](#)]
70. Jindo, K.; Audette, Y.; Higashikawa, F.S.; Silva, C.A.; Akashi, K.; Mastrolonardo, G.; Sánchez-Monedero, M.A.; Mondini, C. Role of biochar in promoting circular economy in the agriculture sector. Part 1: A review of the biochar roles in soil N, P and K cycles. *Chem. Biol. Technol. Agric.* **2020**, *7*, 1–12. [[CrossRef](#)]
71. Ippolito, J.A.; Spokas, K.A.; Novak, J.M.; Lentz, R.D.; Cantrell, K.B. Biochar elemental composition and factors influencing nutrient retention. In *Biochar for Environmental Management: Science, Technology and Implementation*; Lehmann, J., Stephen, J., Eds.; Routledge: New York, NY, USA, 2015; pp. 137–161.
72. Kongthod, T.; Thanachit, S.; Anusontpornperm, S.; Wiriyakitnateekul, W. Effects of biochars and other organic soil amendments on plant nutrient availability in an ustoxic quartzipsamment. *Pedosphere* **2015**, *25*, 790–798. [[CrossRef](#)]
73. Ippolito, J.A.; Stromberger, M.E.; Lentz, R.D.; Dungan, R.S. Hardwood biochar influences calcareous soil physicochemical and microbiological status. *J. Environ. Manag.* **2014**, *43*, 681–689. [[CrossRef](#)]
74. Li, S.; Barreto, V.; Li, R.; Chen, G.; Hsieh, Y.P. Nitrogen retention of biochar derived from different feedstocks at variable pyrolysis temperatures. *J. Anal. Appl. Pyrolysis.* **2018**, *133*, 136–146. [[CrossRef](#)]
75. Hailegnaw, N.S.; Mercl, F.; Pračke, K.; Száková, J.; Tlustoš, P. Mutual relationships of biochar and soil pH, CEC, and exchangeable base cations in a model laboratory experiment. *J. Soils Sediments* **2019**, *19*, 2405–2416. [[CrossRef](#)]
76. Da Silva Mendes, J.; Fernandes, J.D.; Chaves, L.H.G.; Guerra, H.O.C.; Tito, G.A.; de Brito Chaves, I. Chemical and physical changes of soil amended with biochar. *Water Air Soil Pollut.* **2021**, *232*, 1–13. [[CrossRef](#)]
77. Limousin, G.; Gaudet, J.P.; Charlet, L.; Szenknect, S.; Barthes, V.; Krimissa, M. Sorption isotherms: A review on physical bases, modeling and measurement. *Appl. Geochem.* **2007**, *22*, 249–275. [[CrossRef](#)]
78. Rigi, M.R.; Farahbakhsh, M.; Rezaei, K. Adsorption and desorption behavior of herbicide metribuzin in different soils of Iran. *J. Agric. Sci. Technol.* **2015**, *17*, 777–787.
79. Peña, D.; López-Piñeiro, A.; Albarrán, Á.; Rato-Nunes, J.M.; Sánchez-Llerena, J.; Becerra, D.; Ramírez, M. De-oiled two-phase olive mill waste may reduce water contamination by metribuzin. *Sci. Total Environ.* **2016**, *541*, 638–645. [[CrossRef](#)] [[PubMed](#)]
80. Saritha, J.D.; Prakash, T.R.; Madhavi, M.; Rao, P.C. Adsorption of metribuzin in tomato growing soils. *Int. J. Chem. Stud.* **2017**, *5*, 740–746.
81. Downie, A.; Crosky, A.; Munroe, P. Physical properties of Biochar. In *Biochar for Environmental Management, Science and Technology*; Lehmann, J.L., Joseph, S., Eds.; Earthscan: London, UK, 2009; pp. 13–32.
82. White, P.M., Jr.; Potter, T.L.; Lima, I.M. Sugarcane and pinewood biochar effects on activity and aerobic soil dissipation of metribuzin and pendimethalin. *Ind. Crops Prod.* **2015**, *74*, 737–744. [[CrossRef](#)]
83. Gámiz, B.; Hall, K.; Spokas, K.A.; Cox, L. Understanding activation effects on low-temperature biochar for optimization of herbicide sorption. *Agronomy* **2019**, *9*, 588. [[CrossRef](#)]
84. Keiluweit, M.; Nico, P.S.; Johnson, M.G.; Kleber, M. Dynamic molecular structure of plant biomass-derived black carbon (biochar). *Environ. Sci. Technol.* **2010**, *44*, 1247–1253. [[CrossRef](#)]
85. Xiao, F.; Pignatello, J.J. π^+ – π Interactions between (Hetero) aromatic Amine cations and the graphitic surfaces of pyrogenic carbonaceous materials. *Environ. Sci. Technol.* **2015**, *49*, 906–914. [[CrossRef](#)] [[PubMed](#)]
86. Cara, I.G.; Filip, M.; Bulgariu, L.; Raus, L.; Topa, D.; Jitareanu, G. Environmental remediation of metribuzin herbicide by mesoporous carbon-rich from wheat straw. *Appl. Sci.* **2021**, *11*, 4935. [[CrossRef](#)]
87. Kah, M.; Sigmund, G.; Xiao, F.; Hofmann, T. Sorption of ionizable and ionic organic compounds to biochar, activated carbon and other carbonaceous materials. *Water Res.* **2017**, *124*, 673–692. [[CrossRef](#)]
88. Wei, L.; Huang, Y.; Li, Y.; Huang, L.; Mar, N.N.; Huang, Q.; Liu, Z. Biochar characteristics produced from rice husks and their sorption properties for the acetanilide herbicide metolachlor. *Environ. Sci. Pollut. Res.* **2017**, *24*, 4552–4561. [[CrossRef](#)]
89. Liu, K.; He, Y.; Xu, S.; Hu, L.; Luo, K.; Liu, X.; Liu, M.; Zhou, X.; Bai, L. Mechanism of the effect of pH and biochar on the phytotoxicity of the weak acid herbicides imazethapyr and 2,4-D in soil to rice (*Oryza sativa*) and estimation by chemical methods. *Ecotoxicol. Environ. Saf.* **2018**, *161*, 602–609. [[CrossRef](#)]
90. Delgado-Moreno, L.; Almendros, G.; Peña, A. Raw or incubated olive-mill wastes and its biotransformed products as agricultural soil amendments e effect on sorption e desorption of triazine herbicides. *J. Agric. Food Chem.* **2007**, *55*, 836e843. [[CrossRef](#)]

91. Majumdar, K.; Singh, N. Effect of soil amendments on sorption and mobility of metribuzin in soils. *Chemosphere* **2007**, *66*, 630e637. [[CrossRef](#)]
92. Mendes, K.F.; Furtado, I.F.; Sousa, R.N.D.; Lima, A.D.C.; Mielke, K.C.; Brochado, M.G.D.S. Cow bonechar decreases indaziflam pre-emergence herbicidal activity in tropical soil. *J. Environ. Sci. Health Part B* **2021**, *56*, 532–539. [[CrossRef](#)]
93. Lian, F.; Xing, B. Black carbon (biochar) in water/soil environments: Molecular structure, sorption, stability, and potential risk. *Environ. Sci. Technol.* **2017**, *51*, 13517–13532. [[CrossRef](#)]
94. Barriuso, E.; Laird, D.A.; Koskinen, W.C.; Dowdy, R.H. Atrazine desorption from smectites. *Soil Sci. Soc. Am. J.* **1994**, *58*, 1632–1638. [[CrossRef](#)]
95. Singh, N.; Raunaq; Singh, S.B. Effect of fly ash on sorption behavior of metribuzin in agricultural soils. *J. Environ. Sci. Health Part B* **2012**, *47*, 89–98. [[CrossRef](#)]
96. Yu, X.Y.; Ying, G.G.; Kookana, R.S. Sorption and desorption behaviors of diuron in soils amended with charcoal. *J. Agric. Food Chem.* **2006**, *54*, 8545–8550. [[CrossRef](#)]
97. Deng, H.; Feng, D.; He, J.X.; Li, F.Z.; Yu, H.M.; Ge, C.J. Influence of biochar amendments to soil on the mobility of atrazine using sorption-desorption and soil thin-layer chromatography. *Ecol. Eng.* **2017**, *99*, 381–390. [[CrossRef](#)]
98. Liu, Y. Is the free energy change of adsorption correctly calculated? *J. Chem. Eng. Data* **2009**, *54*, 1981–1985. [[CrossRef](#)]
99. Carter, M.C.; Kilduff, J.E.; Weber, W.J. Site energy distribution analysis of preloaded adsorbents. *Environ. Sci. Technol.* **1995**, *29*, 1773–1780. [[CrossRef](#)]
100. Gisi, S.; Lofrano, G.; Grassi, M.; Notarnicola, M. Characteristics and adsorption capacities of low-cost sorbents for wastewater treatment: A review. *Sustain. Mater. Technol.* **2016**, *9*, 10–40. [[CrossRef](#)]

6. Attachment



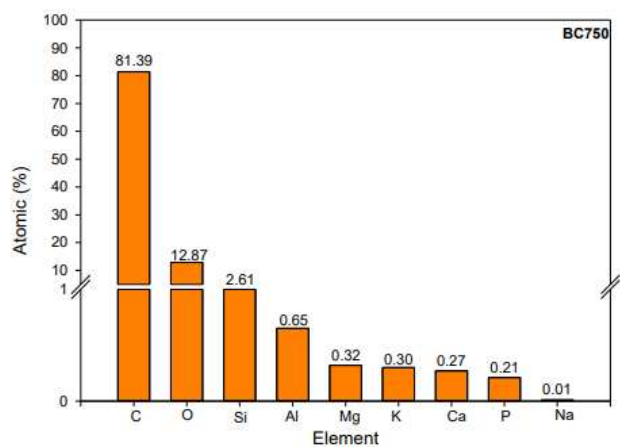


Figure. S1. Surficial elemental composition C (red), O (yellow), Si (green), Ca, K, P, Al, P, and Na (undetected) by energy dispersive X-ray spectrometry (EDS) analysis of biochar (BC) (A) and EDS spectrogram (B) in different pyrolysis temperatures (350, 550, and 750°C).

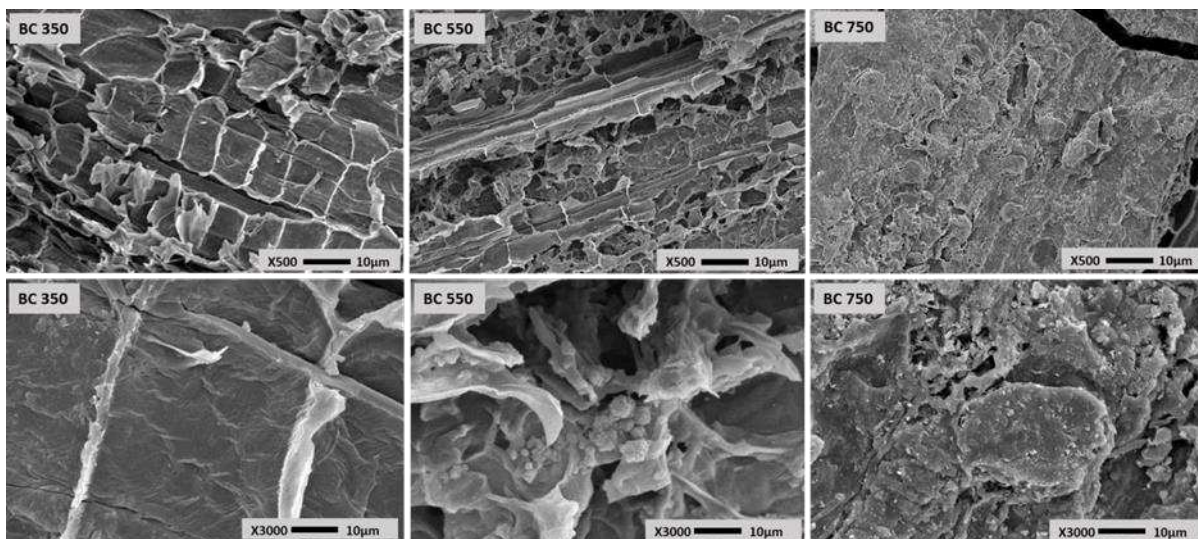


Figure. S2. Images of the biochar (BC) derived from sugar cane straw at different pyrolysis temperatures (350, 550, and 750°C) by Scanning Electron Microscopy (SEM) at 500- and 3000-times magnification.



Article

Pyrolysis Temperature vs. Application Rate of Biochar Amendments: Impacts on Soil Microbiota and Metribuzin Degradation

Kamila Cabral Mielke¹, Maura Gabriela da Silva Brochado¹, Ana Flávia Souza Laube², Tiago Guimarães², Bruna Aparecida de Paula Medeiros¹ and Kassio Ferreira Mendes^{1,*}

¹ Department of Agronomy, Federal University of Viçosa, Viçosa 36570-900, MG, Brazil; kamila.mielke@ufv.br (K.C.M.); maura.brochado@ufv.br (M.G.d.S.B.); bruna.medeiros@ufv.br (B.A.d.P.M.)

² Department of Chemistry, Federal University of Viçosa, Viçosa 36570-900, MG, Brazil; anaf.laube@gmail.com (A.F.S.L.); tguimaraes.quimica@gmail.com (T.G.)

* Correspondence: kfmendes@ufv.br

Abstract: Biochar-amended soils influence the degradation of herbicides depending on the pyrolysis temperature, application rate, and feedstock used. The objective of this study was to evaluate the influence of sugarcane straw biochar (BC) produced at different pyrolysis temperatures (350 °C, 550 °C, and 750 °C) and application rates in soil (0, 0.1, 0.5, 1, 1.5, 5, and 10% *w/w*) on metribuzin degradation and soil microbiota. Detection analysis of metribuzin in the soil to find time for 50% and 90% metribuzin degradation (DT₅₀ and DT₉₀) was performed using high-performance liquid chromatography (HPLC). Soil microbiota was analyzed by respiration rate (C-CO₂), microbial biomass carbon (MBC), and metabolic quotient (*q*CO₂). BC350 °C-amended soil at 10% increased the DT₅₀ of metribuzin from 7.35 days to 17.32 days compared to the unamended soil. Lower application rates (0.1% to 1.5%) of BC550 °C and BC750 °C decreased the DT₅₀ of metribuzin to ~4.05 and ~5.41 days, respectively. BC350 °C-amended soil at high application rates (5% and 10%) provided high C-CO₂, low MBC fixation, and high *q*CO₂. The addition of low application rates (0.1% to 1.5%) of sugarcane straw biochar produced at high temperatures (BC550 °C and BC750 °C) resulted in increased metribuzin degradation and may influence the residual effect of the herbicide and weed control efficiency.

Keywords: application rate; carbonaceous material; degradation time; herbicide residual; pyrolysis temperature



Citation: Mielke, K.C.; Brochado, M.G.d.S.; Laube, A.F.S.; Guimarães, T.; Medeiros, B.A.d.P.; Mendes, K.F. Pyrolysis Temperature vs. Application Rate of Biochar Amendments: Impacts on Soil Microbiota and Metribuzin Degradation. *Int. J. Mol. Sci.* **2023**, *24*, 11154. <https://doi.org/10.3390/ijms241311154>

Academic Editor: Dalibor Broznic[†]

Received: 5 May 2023

Revised: 29 June 2023

Accepted: 4 July 2023

Published: 6 July 2023



Copyright: © 2023 by the authors. Licensee MDPI, Basel, Switzerland. This article is an open access article distributed under the terms and conditions of the Creative Commons Attribution (CC BY) license (<https://creativecommons.org/licenses/by/4.0/>).

1. Introduction

Herbicides are used for weed control in pre- or post-emergence, and regardless of the mode of application, they can reach the soil and persist with a residual effect for weed control and cause carryover problems in succeeding crops or contaminate non-target organisms and the environment [1]. The negative impacts of herbicide residues can be categorized based on the chemical structure of the herbicides, crop species, environmental conditions, and soil properties. These impacts include plant phytotoxicity, reduction in biomass with or without recovery, and significant impairment of crop development [2]. Contamination of potable and groundwater, soil resources, and microbial activities are considered critical aspects regarding the environmental risks associated with herbicide use [3]. Furthermore, the effects of herbicides on human health, particularly due to the bioaccumulation of these substances' molecules in the body, represent a significant concern in terms of herbicide-related biosafety [4].

The soil is the main site where physical, chemical, and biological interactions of herbicides occur [5]. Herbicide degradation into secondary compounds (metabolites) can occur through biotic processes (microbial degradation) or abiotic processes (hydrolysis,

photolysis, and oxidation) [6,7]. Hydrolysis is characterized by the breakdown of the herbicide molecule through hydrolysis reactions involving ether, amide, cyano group, and acyl chloride bonds. In the photolysis reaction, the herbicide absorbs light radiation and generates hydroxyl radicals, superoxide, and ozone, which induce a molecular reaction, breaking the bonds and degrading the herbicide [8]. The rate of herbicide degradation depends on the type of soil, pH, organic carbon (OC) content, moisture, and soil colloid nature [9].

Biochar is a carbonaceous material produced during the thermochemical decomposition (pyrolysis) of biomass under a limited O₂ supply [10]. The pyrolyzed feedstocks and pyrolysis conditions determine the physicochemical characteristics of biochar, such as nutrient content, OC, porosity, and specific surface area (SSA), among others, which are determinants for herbicide sorption and degradation [11]. The application of biochar generally stimulates the establishment of local microbial communities, such as arbuscular mycorrhizal fungi and bacteria, due to the increased availability of OC and nutrients in the soil [12,13].

Biochar-amended soils can directly influence the degradation half-life time (DT₅₀) of herbicide depending on the molecule, pyrolysis temperature, application rate, and feedstock used [1]. For example, the total amount of hexazinone (mineralized residue + non-extracted or bound residue) in soils amended with biochar from eucalyptus wood waste produced at pyrolysis temperatures of BC850 °C (46%) and BC950 °C (49%) was higher compared to biochar produced at BC650 °C (33%) and BC750 °C (42%) [14]. In contrast, the degradation of the non-ionizable herbicide oxyfluorfen applied in pre-emergence was faster (DT₅₀ of 2 days and 23 days) with the addition of rice husk biochar produced at 500 °C, at an application rate of 2%, than in unamended soil [15]. Different application rates of hardwood biochar showed positive effects on the mineralization of ¹⁴C-atrazine in Brazilian soil, representing increases of 50% (0.1% *w/w*), 48% (1.0% *w/w*), and 46% (5.0% *w/w*) compared to unamended soil [16]. The high persistence of herbicides in soils amended with biochar, due to the unavailability of the molecules in the soil solution for microorganisms, can significantly alter biodegradation processes; however, degradation responses are dependent on the physicochemical characteristics of the herbicide, biochar production, and soil type [1,17].

The relationship between the addition of biochar to soil and the degradation of metribuzin is reported in the scientific literature; however, the results are distinct. Metribuzin is a pre- and post-emergent herbicide, a selective residual of the triazinone group, with the ability to effectively control a wide spectrum of eudicot weeds [18]. The herbicide blocks photosynthetic processes by inhibiting electron transport in photosystem II (PSII), causing physiological and morphological changes in leaf structures that undergo necrosis and death [19]. Metribuzin [4-amino-6-tert-butyl-3-methylsulfanyl-1,2,4-triazin-5-one] is a strong acid herbicide with high water solubility ($S_w = 10.700 \text{ mg L}^{-1}$ at 20 °C), high mobility in soil (coefficient of sorption normalized by OC, $K_{oc} = 38 \text{ mg L}^{-1}$), high leaching index (groundwater ubiquity score = 2.96), and low persistence in soil (DT₅₀ = ~20 days) [20–22]. This herbicide showed high sorption in carbonaceous materials produced at different pyrolysis temperatures [13,23,24]. The addition of biochar and organic compost decreased the DT₅₀ of metribuzin by 4 days when compared to the unamended soil (DT₅₀ = 34 days) [25]. The degradation and mobility of metribuzin under simulated light and dark conditions decreased with the addition of 1% biochar [26]. The authors reported that can be attributed to the enhanced sorption properties of biochar.

To understand the impact of biochar on the fate of metribuzin in soil, it is necessary to detail the effects of different types of biochar, pyrolysis temperature, and application rate on metribuzin degradation in soil, which is important to assess the risk and fate of this herbicide in the environment. Therefore, the objective of this study was to evaluate the influence of biochar from sugarcane straw produced at different pyrolysis temperatures and application rates in soil on metribuzin degradation and soil microbiota.

2. Results

2.1. Metribuzin Degradation

The sugarcane straw biochar (BC) samples produced at different pyrolysis temperatures (350 °C, 550 °C and 750 °C) were denominated BC350 °C, BC550 °C and BC750 °C. The interaction between pyrolysis temperature, application rate of biochar in the soil, and degradation time was significant ($F = 2.738$ and $p \leq 0.002$). The regression curves of metribuzin over time in amended and unamended soils with different application rates of biochar (0, 0.1, 0.5, 1, 1.5, 5, and 10% w/w) produced at different pyrolysis temperatures (BC350 °C, BC550 °C, and BC750 °C) are presented in Figure 1. The first-order kinetic model provided a suitable fit with metribuzin degradation with a coefficient of determination (R^2) greater than 0.940 (Table 1). The degradation time values of 50% (DT_{50}) and 90% (DT_{90}) of metribuzin applied in the unamended soil were 7.37 days and 24.49 days, respectively (Table 1). The temperature and rainfall during the study varied from 25 °C to 35 °C and from 0 mm to 4 mm, respectively (Figure 2). At 150 days after application (DAA), the degradation of metribuzin in the unamended soil was approximately 100% of the initially applied amount.

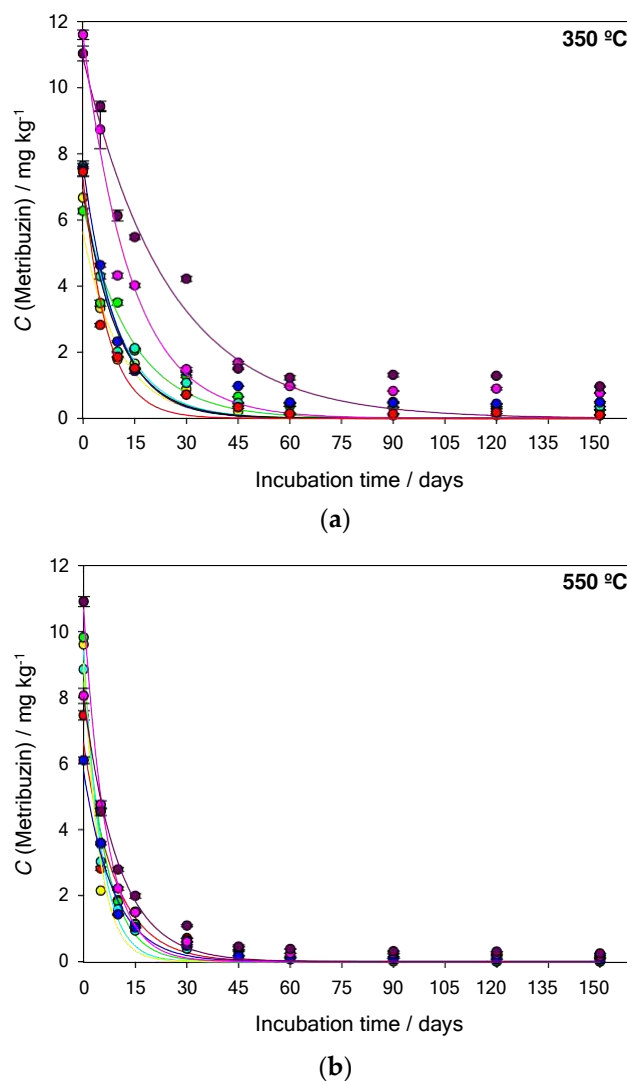


Figure 1. Cont.

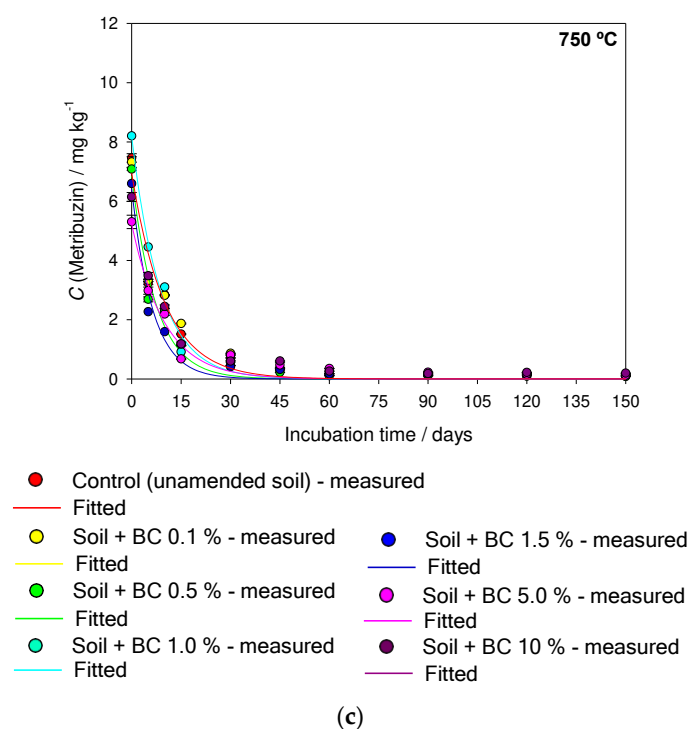


Figure 1. Concentration (C) of metribuzin in unamended soil and amended with different application rates of sugarcane straw biochar (BC) produced at different pyrolysis temperatures (a) 350 °C, (b) 550 °C, and (c) 750 °C. Degradation data were fitted to the kinetic model $C_t = C_0 \times e^{-kx^t}$. Vertical bars represent the standard deviation of the means ($n = 3$).

Table 1. Degradation parameters of metribuzin in unamended soil and amended with different application rates of sugarcane straw biochar (BC) produced at three different temperatures (350 °C, 550 °C, and 750 °C).

Pyrolysis Temperature/°C	Biochar Application Rate % (w/w)	C_0	k	DT_{50}	DT_{90}	p -Value	R^2
		mg kg ⁻¹	Days ⁻¹	Days	Days		
350	Unamended	7.22 ± 0.01 ^a	0.094	7.37	24.49	<0.0001	0.989
	0.1	5.61 ± 0.02	0.094	7.35	24.41	<0.0001	0.976
	0.5	6.39 ± 0.03	0.090	7.70	25.58	<0.0001	0.948
	1.0	6.91 ± 0.05	0.093	7.45	24.75	<0.0001	0.955
	1.5	7.64 ± 0.01	0.103	6.72	22.35	<0.0001	0.940
	5.0	11.55 ± 0.03	0.072	9.62	31.98	<0.0001	0.962
	10.0	10.89 ± 0.02	0.040	17.32	57.56	<0.0001	0.947
550	0.1	9.02 ± 0.05	0.220	3.14	10.46	<0.0001	0.966
	0.5	8.45 ± 0.08	0.156	4.44	14.76	<0.0001	0.991
	1.0	9.40 ± 0.07	0.199	3.46	15.57	<0.0001	0.991
	1.5	5.75 ± 0.01	0.134	5.17	17.18	<0.0001	0.987
	5.0	8.07 ± 0.01	0.138	5.02	16.68	<0.0001	0.991
	10.0	8.63 ± 0.02	0.114	6.08	20.19	<0.0001	0.983
750	0.1	5.22 ± 0.07	0.110	6.30	20.93	<0.0001	0.970
	0.5	6.85 ± 0.05	0.135	5.13	17.05	<0.0001	0.972
	1.0	8.18 ± 0.06	0.157	4.15	14.66	<0.0001	0.986
	1.5	6.41 ± 0.02	0.114	6.08	20.19	<0.0001	0.967
	5.0	7.15 ± 0.03	0.101	6.86	22.79	<0.0001	0.960
	10.0	6.04 ± 0.02	0.097	7.14	23.73	<0.0001	0.980

^a Average of the value of each parameter ± standard deviation of the mean ($n = 3$).

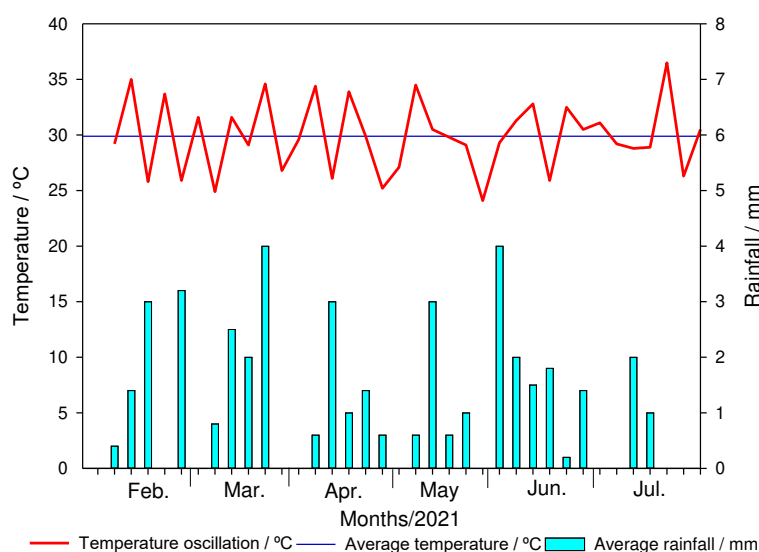


Figure 2. Temperature (°C) and precipitation (mm) recorded in the greenhouse in Viçosa, MG, Brazil, during the experimental period.

The intensity of metribuzin degradation was dependent on the pyrolysis temperature and application rate of biochar in the soil (Figure 1 and Table 1). At 150 DAA, metribuzin degradation in amended soil with BC350 °C, BC550 °C, and BC750 °C was approximately 100% of the initially applied concentration. The initial concentration (C_0) of metribuzin in amended soil with BC350 °C, BC550 °C, and BC750 °C varied among the application rates (Figure 1 and Table 1).

BC350 °C-amended soil increased the DT_{50} of metribuzin from 7.35 days to 17.32 days and the DT_{90} from 24.41 days to 57.56 days compared to unamended soil, when application rates when the application rates were 0.5%, 1, 5% and 10%. BC550 °C-amended soil increased the DT_{50} of metribuzin from 3.14 days to 6.08 days as the application rate increased from 0.1% to 10%. The DT_{50} of metribuzin for BC750 °C was similar among the application rates ~6.59 days, except for the 0.5% and 1% rates, which were below this value (Table 1).

The application rates of biochar produced at different pyrolysis temperatures influenced the DT_{50} of metribuzin in soil (Table 1). Application rates of 0.1%, 0.5%, and 1.0% of BC350 °C demonstrated metribuzin DT_{50} similar to unamended soil (7.37 days). Metribuzin DT_{50} increased from 7.37 days in unamended soil to 9.62 days and 17.32 days when rates of 5% and 10% of BC350 °C were added, respectively. Regardless of the application rate of BC550 °C and BC750 °C, the DT_{50} of metribuzin was lower than in unamended soil. However, it was observed that with an increase in the application rate from 0.1% to 10% of BC350 °C and BC550 °C, the DT_{50} increased on average by 3 days. Lower application rates of biochar produced at different pyrolysis temperatures decreased the DT_{50} and DT_{90} of metribuzin, aligned mainly with the higher pyrolysis temperatures (BC550 °C and BC750 °C).

2.2. Respiration Rate of the Microbial Rhizosphere

The timing of metribuzin application in biochar-amended soil produced at different pyrolysis temperatures and application rates showed different responses in soil microbiological parameters (Figures 3 and 4, Table 2). The maximum respiration rate of unamended soil was at 9 days after incubation (DAI), with values of 600 and 800 $\mu\text{g CO}_2 \text{ g soil}^{-1} \text{ day}^{-1}$, respectively, at 0 DAA and 150 DAA of metribuzin, respectively. The maximum respiration rate at 0 DAA was at 9 DAI, with respiration ranging from 600 $\mu\text{g CO}_2 \text{ g soil}^{-1} \text{ day}^{-1}$ to 900 $\mu\text{g CO}_2 \text{ g soil}^{-1} \text{ day}^{-1}$, depending on the application rate and pyrolysis temperature. At 150 DAA, the maximum respiration was between 9 and 13 DAI, with respiration rates

between 400 $\mu\text{g CO}_2 \text{ g soil}^{-1} \text{ day}^{-1}$ and 900 $\mu\text{g CO}_2 \text{ g soil}^{-1} \text{ day}^{-1}$, depending on the application rate of BC350 °C, BC550 °C, and BC750 °C (Figure 3).

The interaction between pyrolysis temperature and biochar soil application rate for total respiration was significant for 0 DAA ($F = 2.796$ and $p \leq 0.03$) and for 150 DAA ($F = 3.140$ and $p \leq 0.01$). The unamended soil presented a total respiration (C-CO₂) of 3066 $\mu\text{g CO}_2 \text{ g soil}^{-1}$ and 2503 $\mu\text{g CO}_2 \text{ g soil}^{-1}$ at 0 DAA and 150 DAA, respectively (Figure 4). At 0 DAA, C-CO₂ was influenced by the pyrolysis temperature only for the highest application rates (5% and 10%) of BC350 °C, BC550 °C, and BC750 °C. In BC350 °C-amended soil, higher C-CO₂ was observed by 20.7% (average of rates 5% and 10%) compared to BC550 °C and BC750 °C-amended soil. There was no significant effect between application rates of BC550 °C and BC750 °C in the soil. The application rates of 5% and 10% of BC350 °C provided greater C-CO₂ from the soil microbiota, 4424 $\mu\text{g CO}_2 \text{ g soil}^{-1}$ and 4644 $\mu\text{g CO}_2 \text{ g soil}^{-1}$, respectively, when compared to unamended soil (3066 $\mu\text{g CO}_2 \text{ g soil}^{-1}$) (Figure 4). There were no differences in C-CO₂ for different application rates when BC750 °C was used at 150 DAA (Figure 4). Rates of 5% and 10% showed C-CO₂ of 2933 $\mu\text{g CO}_2 \text{ g soil}^{-1}$ and 3072 $\mu\text{g CO}_2 \text{ g soil}^{-1}$, respectively, when BC350 °C was added. Rates between 1% and 10% of BC550 °C increased C-CO₂, on average, by 13% compared to rates of 0.1% and 0.5% (Figure 4).

The interaction between factors for MBC was significant at 0 DAA ($F = 8.565$ and $p \leq 0.001$) and for 150 DAA ($F = 5.549$ and $p \leq 0.004$). Unamended soil presented an average MBC of 40 $\mu\text{g MBC g soil}^{-1}$ and 60 $\mu\text{g MBC g soil}^{-1}$ at 0 DAA and 150 DAA, respectively (Figure 4). At 0 DAA, BC350 °C and BC550 °C-amended soil increased MBC by > 100% when compared to BC750 °C at a 1.0% application rate. Application rates of 0.5%, 1.0%, and 1.5% provided higher MBC, averaging 152 $\mu\text{g MBC g soil}^{-1}$, for BC350 °C compared to other application rates. Rates of 0.1%, 0.5%, and 1.0% increased MBC by an average of 67.0% compared to rates of 0%, 1.5%, 5.0%, and 10% for BC550 °C. The 0.5% rate of BC750 °C-amended soil increased MBC by 65% when compared to unamended soil and rates of 0.1%, 1.0%, 1.5%, 5.0%, and 10% (Figure 4). At 150 DAA, BC750 °C and BC550 °C-amended soil reported higher MBC, averaging 31.7%, when compared to BC350 °C at a 10% rate (Figure 4). The 5% rate of BC350 °C showed higher MBC (225 $\mu\text{g MBC g soil}^{-1}$) when compared to unamended soil and rates of 0.1%, 0.5%, 1.0%, 1.5%, and 10% (averaging 131.87 $\mu\text{g MBC g soil}^{-1}$). Rates of 5% and 10% of BC550 °C-amended soil increased MBC by 42.2%, on average, when compared to unamended soil, and rates of 0.1%, 0.5%, 1.0%, and 1.5% (Figure 4).

The interaction between factors for metabolic quotient ($q\text{CO}_2$) was significant at 0 DAA ($F = 7.727$ and $p \leq 0.001$) and for 150 DAA ($F = 6.914$ and $p \leq 0.003$). The metabolic quotient ($q\text{CO}_2$) of unamended soil at 0 DAA and 150 DAA was 63.7 $\mu\text{g CO}_2/\mu\text{g MBC}$ and 39.1 $\mu\text{g CO}_2/\mu\text{g MBC}$, respectively (Figure 4). At 0 DAA, BC750 °C-amended soil showed high $q\text{CO}_2$ (73.9 $\mu\text{g CO}_2/\mu\text{g MBC}$) when compared to BC550 °C and BC350 °C-amended soil (average of 21.49 $\mu\text{g CO}_2/\mu\text{g MBC}$) at a rate of 1.0%. Rates of up to 5.0% application of BC350 °C showed low $q\text{CO}_2$ (average of 23.77 $\mu\text{g CO}_2/\mu\text{g MBC}$) when compared to unamended soil and a rate of 10% (average of 63.7 $\mu\text{g CO}_2/\mu\text{g MBC}$). The highest rates (1.5%, 5.0%, and 10%) of BC550 °C and BC750 °C provided $q\text{CO}_2 \sim 58.4 \mu\text{g CO}_2/\mu\text{g MBC}$, a value lower than unamended soil (63.7 $\mu\text{g CO}_2/\mu\text{g MBC}$) (Figure 4). At 150 DAA, BC750 °C-amended soil showed, on average, higher $q\text{CO}_2$ (11.1 $\mu\text{g CO}_2/\mu\text{g MBC}$) when compared to BC550 °C and BC350 °C-amended soil (Figure 4). Application rates of BC350 °C, BC550 °C, and BC750 °C showed significant results only in relation to unamended soil. The application rates provided an average $q\text{CO}_2$ of 17.6, 16.4, and 19.3 $\mu\text{g CO}_2/\mu\text{g MBC}$ for BC350 °C, BC550 °C, and BC750 °C-amended soil, respectively (Figure 4).

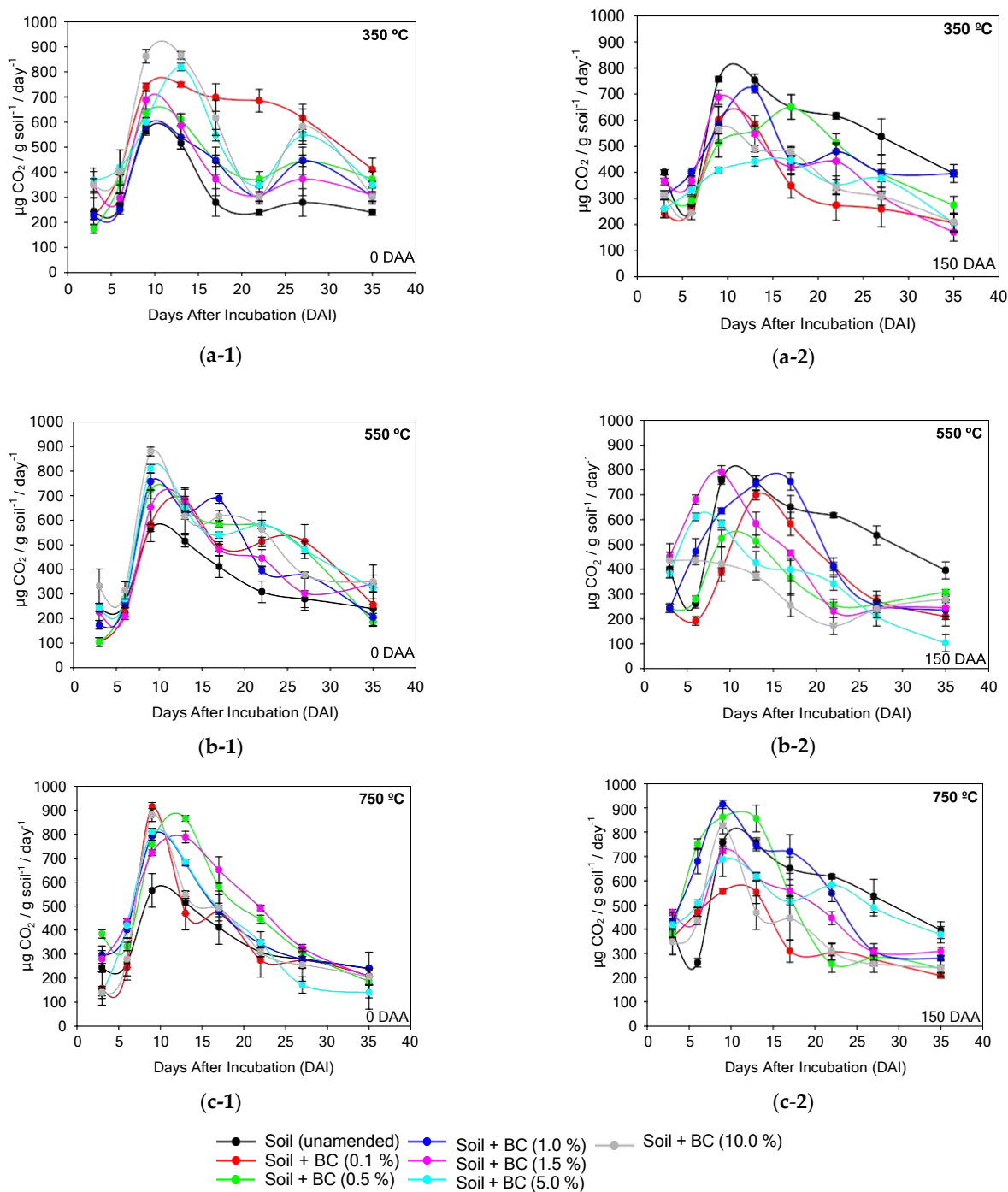


Figure 3. Microbiota respiration rate (C-CO₂) at different incubation periods of soil amended and unamended with different application rates of sugarcane straw biochar produced at different pyrolysis temperatures (a) BC350 °C, (b) BC550 °C, (c), and BC750 °C, at 0 (1) and 150 (2) days after application (DAA) of metribuzin. The solid line represents the union of the dots that are the days after incubation (DAI) (3, 6, 9, 13, 17, 22, 27, and 35 days). Vertical bars at the symbols represent the standard deviation of the means ($n = 4$).

Table 2. Physicochemical attributes of the soil amended with sugarcane straw biochar and unamended soil.

Pyrolysis Temperature/°C	Application Rate % (w/w)	Chemical Attributes													
		pH	OC	P	K	Ca	Mg	H + Al	Zn	Fe	Mn	Cu	B	CEC	BS
		H ₂ O	%	mg kg ⁻¹		mmol _c kg ⁻¹				mmol _c kg ⁻¹		mg kg ⁻¹		mmol _c kg ⁻¹	%
-	Unamended	5.5	1.2	1.3	77.0	15.9	5.4	33.0	3.0	129.8	91.0	3.9	0.1	23.3	41.0
350	0.1	5.5	1.2	1.5	97.0	16.0	5.7	33.3	2.9	129.6	99.1	3.8	0.1	24.2	40.0
	0.5	5.5	1.2	2.0	111.0	17.9	6.5	33.0	3.1	123.6	127.0	3.6	0.1	27.8	46.0
	±	5.8	1.2	3.3	125.0	17.5	6.8	26.4	2.8	148.1	130.0	3.7	0.1	29.3	52.0
	1.5	5.9	1.2	6.3	139.0	17.1	7.2	23.1	2.9	154.7	144.0	4.1	0.1	29.4	56.0
	5	6.8	1.2	10.0	240.0	17.7	8.3	13.3	2.9	234.4	155.0	3.8	0.1	36.7	73.0
	10	7.2	1.2	30.0	290.0	17.4	9.6	6.6	2.8	245.5	212.0	3.6	0.1	37.1	85.0
550	0.1	5.4	1.2	2.2	99.0	16.5	5.7	29.4	2.8	128.5	94.5	3.6	0.1	24.7	48.0
	0.5	5.6	1.2	2.7	132.0	16.2	5.8	29.7	3.1	157.4	97.9	4.1	0.1	24.8	45.0
	±	5.8	1.2	4.4	158.0	17.3	6.1	29.7	3.0	228.5	91.2	4.0	0.1	26.6	47.0
	1.5	5.9	1.2	8.7	161.0	17.8	5.8	19.8	2.8	266.5	157.0	3.4	0.1	25.2	56.0
	5	7.0	1.2	15.0	250.0	17.7	7.6	9.9	2.7	273.5	183.0	3.1	0.1	33.2	77.0
	10	7.3	1.3	33.0	340.0	18.1	8.4	3.3	2.9	297.5	202.0	3.6	0.1	38.5	90.0
750	0.1	5.4	1.2	2.9	108.0	16.8	5.6	33.0	2.7	135.0	96.6	3.6	0.1	25.2	43.0
	0.5	5.5	1.2	3.7	144.0	17.4	6.8	29.7	3.0	148.8	135.0	3.9	0.1	27.6	48.0
	±	5.8	1.2	7.8	178.0	17.8	7.0	29.7	2.8	147.6	122.0	4.0	0.1	29.4	49.0
	1.5	6.2	1.2	12.0	240.0	18.1	7.1	13.2	2.5	238.5	123.0	3.8	0.1	30.6	70.0
	5	7.2	1.3	55.0	500.0	19.7	9.8	3.3	2.9	267.5	177.0	3.7	0.1	39.3	92.0
	10	7.6	1.4	65.0	550.0	20.0	11.1	0.0	2.9	294.5	178.0	3.8	0.1	40.6	100.0
Physical attributes (g kg ⁻¹)															
Soil	Unamended	Sand			Silt			Clay			Texture class				
		500			120			380			Sandy clay				

Source: from Mielke et al. [24] and Lab. Soil Analysis, Viçosa LTDA. Hydrogen potential (pH), organic carbon (OC), phosphorus (P), potassium (K), calcium (Ca), magnesium (Mg), potential acidity (H + Al), zinc (Zn), iron (Fe), manganese (Mn), copper (Cu), boron (B), cation exchange capacity (effective) (CEC), base saturation (BS).

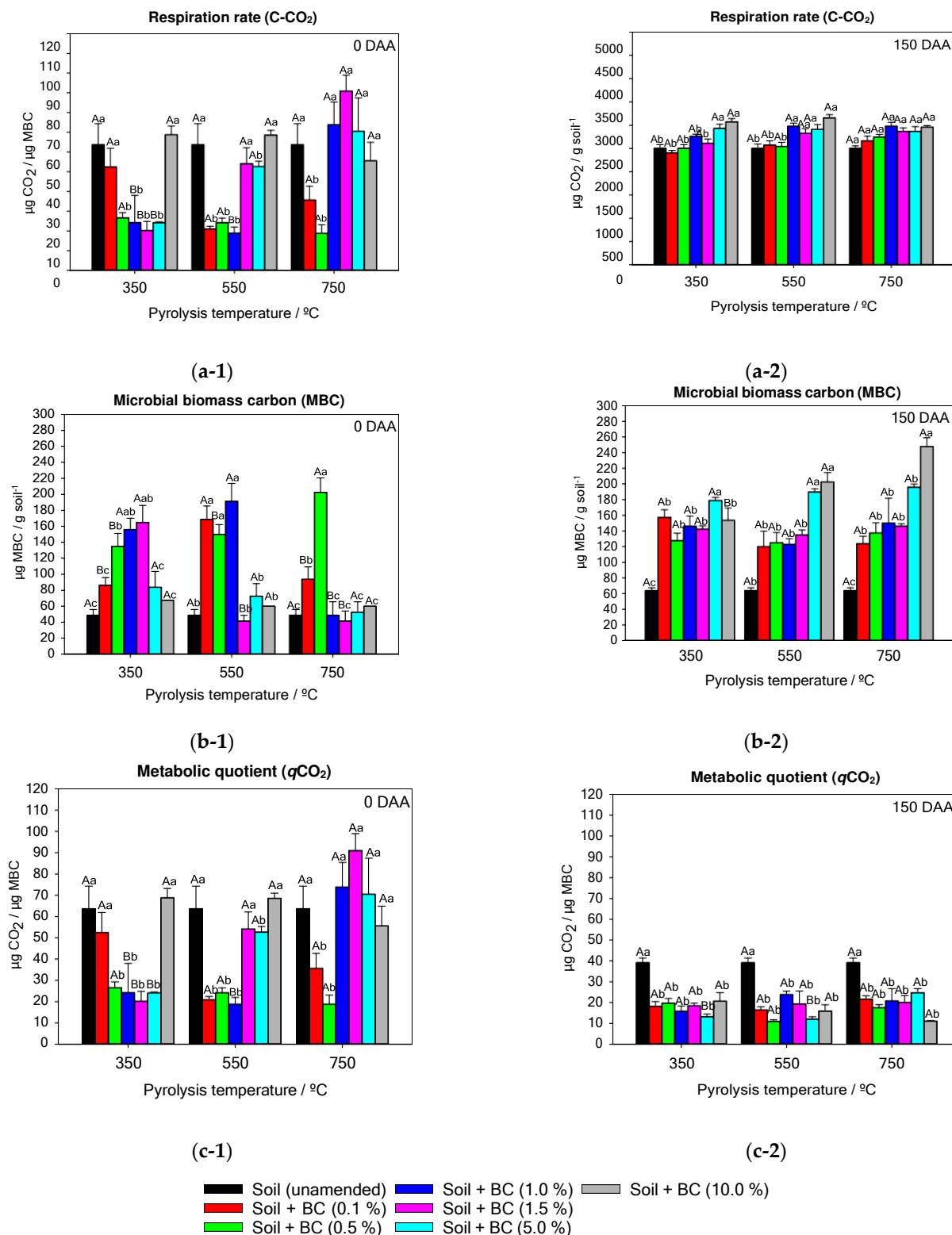


Figure 4. Respiration rate (C-CO₂) (a), microbial biomass carbon (MBC) (b), and metabolic quotient (qCO₂) (c) of soil microbiota amended and unamended with different application rates of sugarcane straw biochar produced at different pyrolysis temperatures BC350 °C, BC550 °C, and BC750 °C, at 0 (1) and 150 (2) days after application (DAA) of metribuzin. Same lowercase letters between application rates and same uppercase letters between pyrolysis temperatures do not differ by Tukey's test ($p < 0.05$). Vertical bars at the symbols represent the standard deviation of the means ($n = 4$).

3. Discussion

The values of metribuzin DT₅₀ range from 7.03 days to 138 days, depending on climate, soil, and field and laboratory conditions [7,22,27–29]. Generally, its degradation occurs

more rapidly in the first month after application. In the conditions of this study, temperature and humidity were tropical, with high temperatures and well-distributed rainfall, using soil with an OC content of 1.2% and a sandy loam texture. These characteristics may have favored the rapid degradation of metribuzin during the study, as the DT_{50} values of metribuzin were dependent on temperature, humidity, and soil physicochemical characteristics, such as OC content [21,30,31]. Metribuzin degradation showed a strong dependence on soil type (sandy or silty) and temperature (5 °C, 15 °C, and 28 °C) [30]. The authors reported that an increase in temperature from 5 °C to 15 °C reduced the concentration of metribuzin in the soil by 25%, decreasing the DT_{50} from ~385 days to 105 days for soil with a higher sand content (~60%) and lower OC content (0.15%). Metribuzin has high S_w , low sorption, and persistence, suggesting a high potential for movement and ready availability for microbial degradation in the soil. This is particularly true for soils with high OC content [32,33]. The impact of abiotic factors such as soil type, application rate, soil pH, microorganisms, and sunlight on metribuzin persistence has been evaluated [34]. The authors observed that DT_{50} values varied significantly with the metribuzin application rate and the physical–chemical characteristics of the soil, with values ranging from 15.17 days to 46.59 days.

The variation in C_0 may have occurred due to the initial sorption process of metribuzin in soils with different application rates, which directly reflects the amount of bioavailable herbicide in the soil solution for degradation. Mielke et al. [18] reported that high doses of metribuzin in soil ($>2 \text{ mg L}^{-1}$) were less sorbed (60%) in soils amended with BC350 °C, especially for lower application rates (0.1% to 1.5%). The authors reported that the amended soil with BC550 °C and BC750 °C showed sorption percentages greater than 80% of metribuzin in the soil. Biochars have different physical and chemical characteristics as the pyrolysis temperature changes during production. Herbicide sorption is directly influenced by characteristics such as porosity, SSA, aromatic structures, carbon contents, surface functional groups, pH, and the elemental composition of the soil [35]. The biochar produced at 750 °C (BC750 °C) showed a higher C/N ratio, ash content, lower number of surface functional groups, and a 13-fold higher surface area than the biochar produced at 350 °C (BC350 °C), which increases the sorption capacity of BC750 °C [24].

The results showed that biochar produced at low temperatures (BC350 °C) negatively influenced the degradation of metribuzin in the soil. The greater degradation of metribuzin in soils amended with BC550 °C and BC750 °C may be related to the physicochemical characteristics of the biochar, as high pyrolysis temperatures produced a material with high pH (9.7), ash content (11%), OC (1.4%), and high nutrient content [24]. These factors can favor chemical degradation through increased pH, active groups, and generation of free radicals [36], and the level of C and ash content can affect soil microbial activities due to the presence of nutrient-rich materials (N, S, P, among others). Soil modifications with BC300 °C from maize straw promoted the biological degradation of triclopyr, increasing the abundance of microorganisms and improving the activity of nitrile hydratase (NHase) [36]. The authors reported that modifications with BC500 °C and BC700 °C inhibited biodegradation by reducing the availability of triclopyr; however, chemical degradation occurred mainly through high pH, active groups on the mineral surface, and generation of hydroxyls and other free radicals.

The effect of biochar on the degradation behavior of herbicides in the soil is a complex process that involves the interaction between soil, herbicide, and the physicochemical characteristics of biochar. When an adequate amount of biochar was added to the soil (0.1% to 1.5%), better degradation of metribuzin was observed, which may be related to the inhibition of microbial activity by excess biochar, influencing the richness and abundance of the microbial community and the higher sorption capacity of the herbicide at high rates of application of sugarcane straw biochar produced at high pyrolysis temperatures ($>500 \text{ °C}$) [24,26,37,38]. Therefore, as the sorption rate increased, the DT_{50} of metribuzin also increased. In most cases, degradation decreases with increasing biochar application rates, associated with greater herbicide sorption [39–41]. Similar results were observed in

the degradation of flumioxazin in soils with different biochar contents [42]. The authors found that soil amended with cornstalk biochar with application rates of 0, 0.5, 2.0, 5.0, and 10.0% provided a DT₅₀ of flumioxazin of 11.1, 9.0, 11.1, 13.2, and 15.4 days, respectively.

Metribuzin is a strong acid (acid dissociation constant, pK_a = 1.3), and under conditions of high pH, it is more in the ionic form, negatively charged, increasing the repulsion of soil colloids, mainly the predominance of negative charges in the organic matter [43,44]. The soil pH with BC350 °C addition was lower (8.6) than BC550 °C (9.3) and BC750 °C (9.8), and higher pH values were observed for soil corrected with BC750 °C, where doses of 5% and 10% increased pH by 1.7 and 2.1 units, respectively, compared to uncorrected soil [24]. Therefore, under these conditions, a greater amount of metribuzin was available for microbial degradation in the soil, which may explain why the DT₅₀ value of metribuzin was lower than in unamended soil, regardless of the application rate of BC550 °C and BC750 °C. Although Mielke et al. [24] reported greater sorption at higher application rates of BC550 °C and BC750 °C, these materials showed greater potential for microbial colonization and, consequently, greater degradation of metribuzin.

Biological degradation and mineralization are the main pathways of herbicide dissipation in the soil [45]. When herbicides are sorbed onto biochar, their availability for degradation by microorganisms is reduced. However, sorption can be reversed by the process of desorption, and any subsequent remobilization of the herbicide, if bound as a residue to biochar, can create availability for further degradation in the soil solution. The addition of BC550 °C and BC750 °C at low application rates in the soil (0.1% to 1%) increased metribuzin sorption [24] compared to unamended soil and resulted in greater metribuzin degradation, potentially acting initially as a remediation technique to immobilize herbicides via sorption, and eventually desorbing the molecules from soil colloids. Consequently, the combination of increased sorption and increased biological degradation has the potential to effectively reduce metribuzin in the soil. However, this positive effect on the remediation of contaminated soils may negatively influence the agronomic efficacy of metribuzin in the soil, reducing the control of weed seed banks. The fact that biochar can reduce herbicide efficacy is not a desired effect, as it may require an increased herbicide dose to achieve similar levels of control as in soil not altered by biochar, increasing production costs and potential environmental risk [46]. Therefore, it is important to understand the physicochemical characteristics of biochar, soil, and herbicides, as well as the possible interactions between these factors, in order to achieve satisfactory recommendations and functionality of biochars as fertilizer sources and herbicide sorbents without posing an environmental risk.

The pyrolysis temperature and application rate of biochar influenced the soil microbiota. In general, structural and compositional differences in soil microbiota can be related to biochar (feedstock, pyrolysis condition, application rate), soil (pH, OC, temperature, moisture, aeration), environmental factors (vegetation, land use, management intensity, herbicide action), and physicochemical characteristics of herbicides [47,48]. In the present study, biochar mitigated the negative impact of metribuzin on soil microbial community, and these effects may be related to increased microbiota through interaction mechanisms with biochar, such as physical-chemical structure (macro and micropores, surface area, nutrient content, organic substances, and enzymatic activity) and increased sorption, reducing bioavailability and toxicity to soil microbiota [24,49–52]. In the study by Mielke et al. [24], it was reported that the use of application rates of 1% and 1.5% of BC350 °C, BC550 °C, and BC750 °C improved soil fertility, making P, K, Mg, Fe, and Mn available, reducing potential acidity (H + Al), and increasing soil pH with less impact on metribuzin sorption and desorption. These soil modifications possibly had a positive impact on the increased degradation of metribuzin in soil amended with BC550 °C and BC750 °C, as observed in this study.

Microorganisms can use hydrocarbons on the surface of biochar as a carbon source [53]. Organic-mineral complexes can form on the surface and in the pores of biochar, modifying its sorption properties and providing habitats for microbial colonization [44,54]. Biochar can

provide habitats for different microorganisms through its pores of different sizes (macro-, meso-, and micropores), which potentially protect these microorganisms from desiccation and predation [55]. Furthermore, biochar application can increase the availability of mineral elements and microbiological activity, which may be related to cation exchange capacity (CEC) and soil pH increase [44]. The increase in soil pH with biochar addition can reduce aluminum toxicity and increase nutrient availability, generating positive effects on microbial colonization [56].

Higher basal respiration found in treatments with higher pyrolysis temperatures and biochar application rates may be an indication of increased biological activity in these treatments. However, the increase in microbial basal respiration must be aligned with the increase in MBC since a high respiration rate and low MBC indicate negative changes in soil microbiota [57]. High $q\text{CO}_2$ values suggest unfavorable conditions for soil microbiota, and low values indicate greater MBC efficiency [58,59]. BC350 °C-amended soil at high application rates provided a microbial imbalance in the soil, as it showed high respiration, low microbial carbon fixation, and high metabolic quotients, unlike BC550 °C and BC750 °C-amended soil (Figure 4). These results are consistent with those observed in the study of metribuzin degradation in soil, where a higher DT₅₀ value of metribuzin was observed in BC350 °C-amended soil when compared to BC550 °C and BC750 °C (Table 1).

The addition of a large amount of carbon can stimulate enhanced microbial action in the soil and therefore cause greater microbial degradation. In addition, the addition of biochar produced at high pyrolysis temperatures increased soil nutrient levels, especially P, K, and SSA (223 m² g⁻¹) [24], which can stimulate microbial activity and consequently improve biological degradation. The increase in MBC can also be attributed to the addition of biochar produced at high temperatures, which constituted the most readily available source of energy for soil microorganisms. Microbial biomass is considered the living fraction of soil organic matter (OM) and a significant nutrient reservoir [60]. The application of hardwood-derived biochar increased the mineralization of atrazine by stimulating atrazine-adapted microflora compared to unamended soil [16].

At 150 DAA, it was possible to observe that the $q\text{CO}_2$ of soils, regardless of pyrolysis temperature and application rate, were lower than the unamended soil. Possibly, the addition of biochar in the soil boosted the microbiota, reducing the energy expenditure used in maintaining the microbial community and directing resources to cell synthesis, improving microbial growth [61].

Biochar has a high capacity for sorbing and retaining soluble organic matter, gases, nutrients, and water and can therefore provide soil microorganisms with various energy resources, nutrients, moisture, and the formation of macroaggregates [37,62–64]. Although biochar is highly recalcitrant, it can be degraded by microorganisms co-metabolically [65]. The labile part of biochar is biologically degradable in a few months after application, while the stable fraction consists of recalcitrant compounds that remain years after biochar application [66]. Increases in nutrients and labile C can be provided by biochar application to soil, and the effect of herbicide mineralization will depend on the proportion of labile C and nutrient content in the applied biochar. Therefore, the impact of biochar application on soil is dependent on the physicochemical characteristics of biochar, which may differ when the amount applied or the raw material source is altered. Two biochars produced from different feedstocks (cocoa husk and rice husk) applied at a rate of 0.3% were analyzed for the degradation of atrazine and paraquat in soil [67]. The authors reported that cocoa husk biochar increased MBC by an average of 72% for atrazine and paraquat compared to rice husk biochar. This was due to the higher level of the nutrient composition of total N and available P in cocoa husk biochar compared to rice husk. The higher degradation of oxyfluorfen was observed in soils amended with different rates of rice husk biochar application, decreasing DT₅₀ between 2 days and 23 days compared to unamended soil [68].

In addition, sugarcane straw biochar produced at high pyrolysis temperatures (>550 °C) and at moderate application rates (between 0.5% and 1.5%) boosted the soil microbiota and improved metribuzin degradation. This result reinforces the idea that materials with high

sorptive capacity, such as biochar produced at high pyrolysis temperatures, can be used as soil amendments to improve soil microbiota as long as the application rate is controlled. However, it is important to note that this result may differ in other soil types, biochar feedstocks, application rates, and pyrolysis temperatures, and specific studies are necessary for each utilization scenario.

4. Materials and Methods

4.1. Soil Collection and Analysis

The agricultural soil samples were collected from the top layer (0–10 cm) in Viçosa, MG, Brazil (20°46′05″ S; 42°52′08″ W), an area that has not been treated with herbicides for the last three years. The soil samples were air-dried for 10 days, then sieved on 5.0 mm mesh and stored at room temperature. The soil was classified as Oxisol (*Latossolo Vermelho-Amarelo*).

The sugarcane straw biochar (BC) samples produced at different pyrolysis temperatures (350 °C, 550 °C, and 750 °C) were denominated BC350 °C, BC550 °C and BC750 °C. The soil was amended with sugarcane straw biochar produced at different pyrolysis temperatures (BC350 °C, BC550 °C, and BC750 °C) in the application rates of 0, 0.1, 0.5, 1, 1.5, 5, and 10% (*w/w*) representing 0, 1, 5, 10, 15, 50, and 100 Mg ha⁻¹, respectively, assuming a soil density of 1 g cm⁻³ and incorporation depth of 0.10 m. The physicochemical attributes of unamended and biochar-amended soil produced at different pyrolysis temperatures were reported by Mielke et al. [24], shown in Table 2.

4.2. Sugarcane Straw Biochar

The sugarcane straw was crushed, sieved (10 mesh, <2.0 mm), and dried in an oven with forced air circulation at 103 ±2 °C for 72 h. The straw was placed in a sealed reactor to prevent the ingress of O₂. The reactor oven was heated at a rate of 5 °C min⁻¹, and the pyrolysis temperatures were 350 °C, 550 °C, and 750 °C. The physicochemical characterization of sugarcane straw biochar was described by Mielke et al. [24], shown in Table 3.

Table 3. Selected properties of sugarcane straw biochar (BC) at different pyrolysis temperatures.

Pyrolysis Temperature/ °C	pH	C	N	Ash	C/N	SSA
	H ₂ O		%		-	m ² g ⁻¹
350	8.6	48.7	0.832	5.0	58.51	17
550	9.3	49.1	0.647	10.3	75.83	129
750	9.8	59.0	0.403	11.6	146.36	223

Source: Mielke et al. [24]. Temperature (T); hydrogen potential (pH); carbon (C); nitrogen (N); carbon/nitrogen ratio (C/N); specific surface area (SSA).

4.3. Soil Preparation and Application of Metribuzin

The experimental design was a completely randomized triple factorial scheme 3 × 3 × 10 with 3 replications. The first factor was three pyrolysis temperatures (350 °C, 550 °C, and 750 °C), the second factor was the application rates of biochar in the soil (0, 0.1, 0.5, 1.0, 1.5, 5.0, and 10% (*w/w*)), and the third factor was the evaluation time (0, 5, 10, 15, 30, 45, 60, 90, 120, and 150 days). The soil amended with sugarcane straw biochar was added to pots with a capacity of 0.5 kg. The application of metribuzin (Sencor®480, Bayer CropScience LP, Kansas City, MO, USA) was carried out at the maximum recommended dose (1920 g a.i. ha⁻¹) for sugarcane crop, with a control treatment without herbicide application. In this procedure, a CO₂-pressurized sprayer equipped with two TT110.02 nozzles spaced 0.5 m apart was used, maintained at a pressure of 1.96 bar and a spray volume of 170 L ha⁻¹. The pots were kept in a greenhouse, and soil samples were collected at 0, 5, 10, 15, 30, 45, 60, 90, 120, and 150 days after herbicide application (DAA). The temperature inside the greenhouse was recorded during the experiment. Soil moisture was adjusted by irrigation of the pots according to the rainfall distribution in 2021 for Viçosa, MG, Brazil [69] (Figure 2).

At the time of collection, the soil amended with biochar was homogenized, and the samples were stored in previously identified jars and taken to freezing at 18 °C in a freezer for later chromatographic analysis.

4.4. Extraction of Metribuzin

The stock solution was prepared at a concentration of 500 mg L⁻¹ of the analytical standard Metribuzin-Pestanal™ (98.8% purity Sigma-Aldrich, San Luis, MO, USA) and the working solution at a concentration of 100 mg L⁻¹, both in acetonitrile (99.9% purity grade). From the working solution, three concentrations of metribuzin (2.45, 3.45, and 4.45 mg L⁻¹) were prepared. The extraction of the herbicide in the soil was performed as described by Mehdizadeh et al. [70]. The method consisted of adding 20 mL of the extraction solution (methanol) to Falcon tubes containing 5 g of soil. Then, the tubes were subjected to rotary shaking for 24 h [13] and centrifuged (Kasvi, K14-0815P, Curitiba, Paraná, Brazil) at 1372 g for 7 min. The supernatant was collected and filtered through a Millipore filter (PRFE membrane, 0.45 µm). An aliquot of 1.50 mL was placed in a vial to be analyzed in high-performance liquid chromatography (HPLC, LC 20AT, Shimadzu, Kyoto, Japan). The recovery level of metribuzin in fortified soil samples was, on average, 100.2%.

4.5. Chromatographic Conditions

Validation of the chromatographic method was according to the criteria of AN-VISA [71]. The linearity of the extraction method was determined by preparing analytical curves where soil samples were fortified with different concentrations of metribuzin (0.01, 0.05, 1.00, 1.50, 2.45, 3.45, 4.45, 5.00, and 5.45 mg kg⁻¹). After chromatographic analysis and obtaining the analytical curves, linearity was evaluated by linear regression of the area as a function of metribuzin concentrations and the coefficient of determination (R^2). The analytical curve presented an R^2 equal to 0.9999 (Figure 5). The limit of detection (LoD) and quantification (LoQ) were 0.01369 and 0.04150 mg L⁻¹, respectively.

The quantification of metribuzin was carried out on an HPLC, with a photodiode array detector (SPD-M20A, Shimadzu, Kyoto, Japan), stainless steel C18 column (Shimadzu VP-ODS Shim-pack 250 mm × 4.6 mm i.d., 5 µm particle size, Shimadzu, Kyoto, Japan). The mobile phase was adapted from López-Piñeiro et al. [13,24], composed of acetonitrile/water (acidified with 0.01% phosphoric acid) in a ratio of 45/55 (v/v), an injection volume of 30 µL, flow rate of 1.0 mL min⁻¹, wavelength of 254 nm, and column oven temperature of 30 °C. Under these conditions, the retention time was 8.2 min.

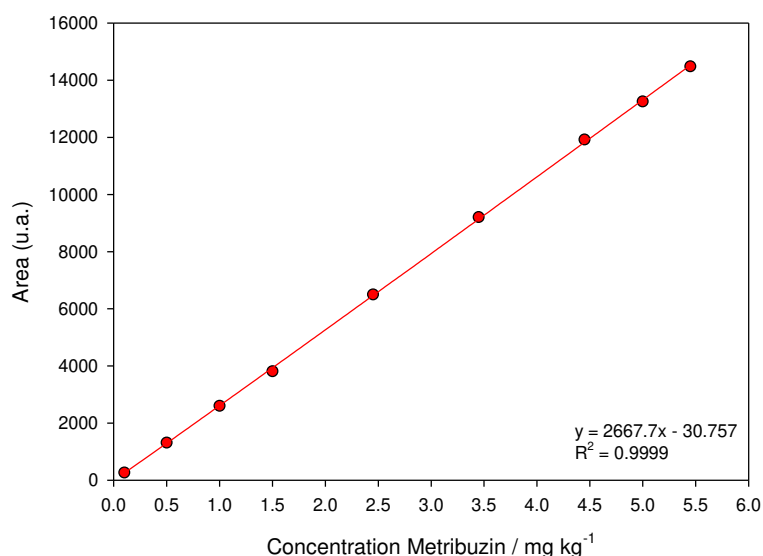


Figure 5. Linear chromatographic calibration curve of metribuzin. The points correspond to the mean ($n = 3$) of metribuzin concentrations (0.10, 0.50, 1.0, 1.50, 2.45, 3.45, 4.45, 5.0, and 5.45 mg kg⁻¹). The line represents first-order linear model fit.

4.6. Degradation Kinetics of Metribuzin in Soil

The degradation data of metribuzin in the unamended soil and biochar-amended soil were fitted to a first-order kinetics model according to Equation (1).

$$C_t = C_0 \times e^{-kxt} \quad (1)$$

where C_t is the total concentration (mg kg^{-1}) of herbicide remaining in the soil at time t ; C_0 is the initial concentration of herbicide at time zero; k is the degradation rate constant (days^{-1}), and t is incubation time in days.

From the k values, the time required for 50% and 90% of the initial amount of metribuzin to be degraded (DT_{50} and DT_{90}) was determined (Equations (2) and (3)).

$$DT_{50} = \frac{\ln 2}{k} \quad (2)$$

$$DT_{90} = \frac{\ln 10}{k} \quad (3)$$

4.7. Respiration Rate of the Microbial Rhizosphere

After completion of the collections of the unamended and biochar-amended soil for analysis of metribuzin degradation at 150 DAA and 0 DAA (at the same time as herbicide application), the carbon content in soil microbial biomass by induced respiration was based on the measurement of the initial maximum emission of CO_2 over a period of time [72]. In this study, an entirely randomized design was performed in a 3×7 double factorial scheme with 4 repetitions. The first factor represented the pyrolysis temperatures (BC350 °C, BC550 °C, and BC750 °C), and the second factor was the biochar soil application rates (0, 0.1, 0.5, 1.0, 1.5, 5.0, and 10% w/w).

The soil collected from the rhizosphere of each experimental unit was homogenized, and 50 g was taken for analysis. Soil samples were sieved (2 mm mesh), moistened (70% field capacity), and incubated in hermetically sealed vials in a Biochemical Oxygen Demand chamber (BOD ElectroLab, São Paulo, Brazil) at 25 °C without light. The respiratory frequency of the soil microbiota was evaluated with the respirometric method of C- CO_2 release at 3, 6, 9, 13, 17, 22, 27, and 35 days after the start of incubation (DAI). The C- CO_2 released from the soil was transported by a continuous air flow (CO_2 -free) to a vial containing 10 mL of 0.5 mol L^{-1} NaOH solution. Precipitation of the carbonate formed was carried out with the addition of 10 mL of BaCl_2 0.05 mol L^{-1} and titrated with 0.25 mol L^{-1} HCl plus three drops of the 1% phenolphthalein indicator [73]. After 40 days, 10 g soil samples from each vial were taken to determine the microbial biomass carbon (MBC) [74]. The metabolic quotient ($q\text{CO}_2$) was determined as follows in Equation (4) [75].

$$q\text{CO}_2 = \frac{C - \text{CO}_2}{\text{MBC}} \quad (4)$$

4.8. Statistical Analysis

The data were subjected to analysis of variance (ANOVA) to evaluate the interaction between factors in each study. The analyses were performed using Sisvar software (version 5.6, Lavras, Minas Gerais, Brazil). When the interaction between factors was significant ($p \leq 0.05$), the degradation curves of metribuzin in soil were plotted in Sigma Plot® (version 14.0 for Windows, Systat Software Inc., Point Richmond, VA, USA), and the parameter data were presented as means and standard deviation ($n = 3$). For C- CO_2 , MBC, and $q\text{CO}_2$, when significant ($p \leq 0.05$) among factors, the means were separated by Tukey's test and presented as means and standard deviation ($n = 4$), and the figures were also plotted in Sigma Plot®.

5. Conclusions

The degradation values of metribuzin (DT₅₀ and DT₉₀) in unamended soil were 7.37 days and 24.94 days, respectively, reflecting the low residual effect capacity of this herbicide in the studied soil.

The intensity of metribuzin degradation was dependent on the pyrolysis temperature and biochar application rate in the soil. The highest degradation of metribuzin was observed in soils amended with BC550 °C and BC750 °C when added at lower application rates (0.1% to 1.5%). The highest values of DT₅₀ and DT₉₀ for metribuzin were observed in BC350 °C-amended soil applied at rates of 5% (9.62 days) and 10% (17.32 days).

The degradation process of metribuzin in BC350 °C, BC550 °C, and BC750 °C was shown to be related to the negative impact of these carbonaceous materials on the soil microbiota since in BC350 °C-amended soil at high application rates, a higher microbial imbalance was observed, presenting high respiration, low microbial carbon fixation, and high metabolic quotients, unlike BC550 °C and BC750 °C-amended soil. Even though providing greater sorption of metribuzin in the soil, the addition of low application rates of BC550 °C and BC750 °C to the soil may lead to an increase in metribuzin degradation.

This material can also become an alternative for environmental remediation and reduce problems related to crop carryover. However, it may negatively influence the residual effect of the herbicide in the soil and consequently reduce the efficacy of the product in controlling weeds in the seed bank and increase the application of post-emergent herbicides.

Author Contributions: Conceptualization, K.C.M.; Data curation, K.C.M., A.F.S.L., M.G.d.S.B. and B.A.d.P.M.; Investigation, Methodology, Validation, A.F.S.L., T.G., K.C.M. and K.F.M.; Writing—review and editing, K.C.M. and K.F.M.; Project administration, Formal analysis, Funding acquisition, K.F.M. All authors have read and agreed to the published version of the manuscript.

Funding: This research was funded by the Coordination for the Improvement of Higher Education Personnel (CAPES—88887.479265/2020-00), the National Council for Scientific and Technological Development (CNPq—404240/2021-6), and the Foundation for Research Support of the State of Minas Gerais (FAPEMIG—2070.01.0004768/2021-84).

Informed Consent Statement: Not applicable.

Data Availability Statement: Not applicable.

Acknowledgments: The authors thank the Federal University of Viçosa and the Matheus Bortolanza Soares from the Luiz de Queiroz College of Agriculture—University of São Paulo for kindly donating the biochar.

Conflicts of Interest: The authors declare no conflict of interest.

6. References

- Mielke, K.C.; Mendes, K.F.; Sousa, R.N.; Medeiros, B.A.P. Degradation Process of Herbicides in Biochar-Amended Soils: Impact on Persistence and Remediation. In *Biodegradation Technology of Organic and Inorganic Pollutants*; Mendes, K.F., Sousa, R.N., Mielke, K.C., Eds.; IntechOpen: Rijeka, Croatia, 2022; pp. 1–23.
- Mehdizadeh, M.; Mushtaq, W.; Siddiqui, S.A.; Ayadi, S.; Kaur, P.; Yeboah, S.; Mazraedoost, S.; AL-Taey, D.K.A.; Tampubolon, K. Herbicide residues in agroecosystems: Fate, detection, and effect on non-target plants. *Rev. Agric. Sci.* **2021**, *9*, 157–167. [[CrossRef](#)]
- Tudararo-Aherobo, L.E.; Ataikiru, T.L. Effects of chronic use of herbicides on soil physicochemical and microbiological characteristics. *Microbiol. Res. J. Int.* **2020**, *30*, 9–19. [[CrossRef](#)]
- Pathak, V.M.; Verma, V.K.; Rawat, B.S.; Kaur, B.; Babu, N.; Sharma, A.; Cunill, J.M. Current status of pesticide effects on environment, human health and its eco-friendly management as bioremediation: A comprehensive review. *Front. Microbiol.* **2022**, *13*, 2833. [[CrossRef](#)] [[PubMed](#)]
- Pateiro-Moure, M.; Arias-Estévez, M.; Simal-Gándara, J. Critical review on the environmental fate of quaternary ammonium herbicides in soils devoted to vineyards. *Environ. Sci. Technol.* **2013**, *47*, 4984–4998. [[CrossRef](#)]
- Mendes, K.F.; Mielke, K.C.; Júnior, L.H.B.; de la Cruz, R.A.; Sousa, R.N. Anaerobic and aerobic degradation studies of herbicides and radiorespirometry of microbial activity in soil. In *Radioisotopes in Weed Research*; Mendes, K.F., Ed.; CRC Press: Boca Raton, FL, USA, 2021; pp. 95–125.

7. Guimarães, A.C.D.; Inoue, M.H.; Mendes, K.F.; Santos, A.W.; Oliveira, A.M. Processo de Degradação Biológica (Biodegradação) dos Herbicidas no Solo. In *Herbicidas no Ambiente: Comportamento e Destino*; Mendes, K.F., Inoue, M.H., Tornisielo, V.L., Eds.; Editora UFV: Viçosa, Brazil, 2022; pp. 9–35.
8. Meng, X.; Guo, Y.; Wang, Y.; Fan, S.; Wang, K.; Han, W. A Systematic Review of Photolysis and Hydrolysis Degradation Modes, Degradation Mechanisms, and Identification Methods of Pesticides. *J. Chem.* **2022**, *2022*, 9552466. [CrossRef]
9. Łozowicka, B.; Wołejko, E.; Kaczyński, P.; Konecki, R.; Iwaniuk, P.; Dragowski, W.; Jabłońska-Trypuć, A. Effect of microorganism on behaviour of two commonly used herbicides in wheat/soil system. *Appl. Soil Ecol.* **2021**, *162*, 103879. [CrossRef]
10. Lehmann, J.; Joseph, S. Biochar for environmental management: An introduction. In *Biochar for Environmental Management: Science*; Lehmann, J., Joseph, S., Eds.; Technology e Implementation; Routledge: New York, NY, USA, 2015; pp. 1–13.
11. Liu, Y.; Lonappan, L.; Brar, S.K.; Yang, S. Impact of biochar amendment in agricultural soils on the sorption, desorption, and degradation of pesticides: A review. *Sci. Total Environ.* **2018**, *645*, 60–70. [CrossRef]
12. Ameloot, N.; Graber, E.R.; Verheijen, F.G.; De Neve, S. Interactions between biochar stability and soil organisms: Review and research needs. *Eur. J. Soil Sci.* **2013**, *64*, 379–390. [CrossRef]
13. López-Piñeiro, A.; Peña, D.; Albarrán, A.; Becerra, D.; Sánchez-Llerena, J. Sorption, leaching and persistence of metribuzin in Mediterranean soils amended with olive mill waste of different degrees of organic matter maturity. *J. Environ. Manag.* **2013**, *122*, 76–84. [CrossRef] [PubMed]
14. Fernandes, B.C.C.; Mendes, K.F.; Tornisielo, V.L.; Teófilo, T.M.S.; Takeshita, V.; das Chagas, P.S.F.; Silva, D.V. Effect of pyrolysis temperature on eucalyptus wood residues biochar on availability and transport of hexazinone in soil. *Int. J. Environ. Sci. Technol.* **2021**, *19*, 499–514. [CrossRef]
15. Wu, C.; Liu, X.; Wu, X.; Dong, F.; Xu, J.; Zheng, Y. Sorption, degradation and bioavailability of oxyfluorfen in biochar-amended soils. *Sci. Total Environ.* **2019**, *658*, 87–94. [CrossRef]
16. Jablonowski, N.D.; Borchard, N.; Zajkoska, P.; Fernández-Bayo, J.D.; Martinazzo, R.; Berns, A.E.; Burauel, P. Biochar-mediated [¹⁴C] atrazine mineralization in atrazine-adapted soils from Belgium and Brazil. *J. Agric. Food Chem.* **2013**, *61*, 512–516. [CrossRef] [PubMed]
17. Takeshita, V.; de Oliveira, F.S.; Munhoz-Garcia, G.V.; Fernandes, B.C.C.; da Silva Teófilo, T.M.; Mendes, K.F.; Tornisielo, V.L. Effects of Biochar on Degradation Herbicides in the Soil. In *Interactions of Biochar and Herbicides in the Environment*; Mendes, K.F., Ed.; CRC Press: Boca Raton, FL, USA, 2022; pp. 189–218.
18. Hashem, A.; Collins, R.M.; Bowran, D.G. Efficacy of interrow weed control techniques in wide row narrow-leaf lupin. *Weed Technol.* **2011**, *25*, 135–140. [CrossRef]
19. Karimmojeni, H.; Rezaei, M.; Tseng, T.M.; Mastinu, A. Effects of metribuzin herbicide on some morpho-physiological characteristics of two Echinacea species. *Horticulturae* **2022**, *8*, 169. [CrossRef]
20. Saritha, J.D.; Ramprakash, T.; Rao, P.C.; Madhavi, M. Persistence of metribuzin in tomato growing soils and tomato fruits. *Nat. Environm. Pollut. Technol.* **2017**, *16*, 505.
21. Guimarães, A.C.D.; Mendes, K.F.; dos Reis, F.C.; Campion, T.F.; Christoffoleti, P.J.; Tornisielo, V.L. Role of Soil Physicochemical Properties in Quantifying the Fate of Diuron, Hexazinone, and Metribuzin. *Environ. Sci. Pollut. Res.* **2018**, *25*, 12419–12433. [CrossRef] [PubMed]
22. PPDB—Pesticide Properties Database. Footprint: Creating Tools for Pesticide Risk Assessment and Management in Europe. Metribuzin. Developed by the Agriculture & Environment Research Unit (AERU), University of Hertfordshire, Funded by UK National Sources and the EU-Funded FOOTPRINT Project (FP6-SSP-022704). Available online: <https://sitem.herts.ac.uk/aeru/ppdb/en/Reports/469.htm> (accessed on 18 April 2023).
23. Loffredo, E.; Parlavecchia, M.; Perri, G.; Gattullo, R. Comparative assessment of metribuzin sorption efficiency of biochar, hydrochar e vermicompost. *J. Environ. Sci. Health Part B* **2019**, *54*, 728–735. [CrossRef] [PubMed]
24. Mielke, K.C.; Laube, A.F.S.; Guimarães, T.; Brochado, M.G.D.S.; Medeiros, B.A.D.P.; Mendes, K.F. Pyrolysis temperature and application rate of sugarcane straw biochar influence sorption and desorption of metribuzin and soil chemical properties. *Processes* **2022**, *10*, 1924. [CrossRef]
25. Abdollahi, K.; Naeini, S.A.M.; Motlagh, M.B.; Ebrahimi, P.; Roshani, G. Evaluation the effect of organic amendments (manure and biochar) on metribuzin herbicide persistence in soil. *Appl. Soil Res.* **2020**, *8*, 149–161.
26. Haskis, P.; Mantzos, N.; Hela, D.; Patakioutas, G.; Konstantinou, I. Effect of biochar on the mobility and photodegradation of metribuzin and metabolites in soil-biochar thin-layer chromatography plates. *Int. J. Environ. Anal. Chem.* **2019**, *99*, 310–327. [CrossRef]
27. Mutua, G.K.; Ngigi, A.N.; Getenga, Z.M. Degradation Characteristics of Metribuzin in Soils within the Nzoia River Drainage Basin, Kenya. *Toxicol. Environ. Chem.* **2016**, *98*, 800–813.
28. Mahanta, K.; Sarma, A.; Deka, J. Metribuzin dissipation pattern in soil and its residue in soil and chilli. *Indian J. Weed Sci.* **2018**, *50*, 405–407. [CrossRef]
29. Takeshita, V.; Carvalho, L.B.; Galhardi, J.A.; Munhoz-Garcia, G.V.; Pimpinato, R.F.; Oliveira, H.C.; Fraceto, L.F. Development of a preemergent nanoherbicide: From efficiency evaluation to the assessment of environmental fate and risks to soil microorganisms. *ACS Nanosci. Au* **2022**, *2*, 307–323. [CrossRef]
30. Benoit, P.; Perceval, J.; Stenrød, M.; Moni, C.; Eklo, O.M.; Barriuso, E.; Kværner, J. Availability and biodegradation of metribuzin in alluvial soils as affected by temperature and soil properties. *Weed Res.* **2007**, *47*, 517–526. [CrossRef]

31. Juhler, R.K.; Henriksen, T.H.; Ernstsens, V.; Vinther, F.P.; Rosenberg, P. Impact of basic soil parameters on pesticide disappearance investigated by multivariate partial least square regression and statistics. *J. Environ. Qual.* **2008**, *37*, 1719–1732. [[CrossRef](#)] [[PubMed](#)]
32. Khoury, R.; Coste, C.M.; Kwar, N.S. Degradation of metribuzin in two soil types of Lebanon. *J. Environ. Sci. Health B* **2006**, *41*, 795–806. [[CrossRef](#)] [[PubMed](#)]
33. Wahla, A.Q.; Iqbal, S.; Anwar, S.; Firdous, S.; Mueller, J.A. Optimizing the metribuzin degrading potential of a novel bacterial consortium based on Taguchi design of experiment. *J. Hazard. Mater.* **2018**, *15*, 1–9. [[CrossRef](#)] [[PubMed](#)]
34. Kaur, P.; Rani, G.; Bhullar, M.S. Persistence of metribuzin in aridisols as affected by various abiotic factors and its effect on soil enzymes. *Int. J. Environ. Anal. Chem.* **2022**, *1*, 20. [[CrossRef](#)]
35. Khalid, S.; Shahid, M.; Murtaza, B.; Bibi, I.; Naeem, M.A.; Niazi, N.K. A critical review of different factors governing the fate of pesticides in soil under biochar application. *Sci. Total Environ.* **2020**, *711*, 134645. [[CrossRef](#)]
36. Zhang, P.; Sun, H.; Min, L.; Ren, C. Biochars change the sorption and degradation of thiacloprid in soil: Insights into chemical and biological mechanisms. *Environ. Pollut.* **2018**, *236*, 158–167. [[CrossRef](#)]
37. Yavari, S.; Sapari, N.B.; Malakahmad, A.; Yavari, S. Degradation of imazapic and imazapyr herbicides in the presence of optimized oil palm empty fruit bunch and rice husk biochars in soil. *J. Hazard. Mater.* **2019**, *366*, 636–642. [[CrossRef](#)]
38. Alvarez, D.O.; Mendes, K.F.; Tosi, M.; de Souza, L.F.; Cedano, J.C.C.; de Souza Falcao, N.P.; Tornisielo, V.L. Sorption-desorption and biodegradation of sulfometuron-methyl and its effects on the bacterial communities in Amazonian soils amended with aged biochar. *Ecotoxicol. Environ. Saf.* **2021**, *207*, 111222. [[CrossRef](#)] [[PubMed](#)]
39. Yu, X.Y.; Mu, C.L.; Gu, C.; Liu, C.; Liu, X.J. Impact of woodchip biochar amendment on the sorption and dissipation of pesticide acetamiprid in agricultural soils. *Chemosphere* **2011**, *85*, 1284–1289. [[CrossRef](#)] [[PubMed](#)]
40. Jones, D.L.; Edwards-Jones, G.; Murphy, D.V. Biochar mediated alterations in herbicide breakdown and leaching in soil. *Soil Biol. Biochem.* **2011**, *43*, 804–813. [[CrossRef](#)]
41. Muter, O.; Berzins, A.; Strikauska, S.; Pugajeva, I.; Bartkevics, V.; Dobeles, G.; Steiner, C. The effects of woodchip-and straw-derived biochars on the persistence of the herbicide 4-chloro-2-methylphenoxyacetic acid (MCPA) in soils. *Ecotoxicol. Environ. Saf.* **2014**, *109*, 93–100. [[CrossRef](#)]
42. Zhelezova, A.; Cederlund, H.; Stenström, J. Effect of biochar amendment and ageing on adsorption and degradation of two herbicides. *Water Air Soil Pollut.* **2017**, *228*, 216. [[CrossRef](#)] [[PubMed](#)]
43. Kah, M.; Sigmund, G.; Xiao, F.; Hofmann, T. Sorption of ionizable and ionic organic compounds to biochar, activated carbon and other carbonaceous materials. *Water Res.* **2017**, *124*, 673–692. [[CrossRef](#)]
44. Sousa, R.N.; Soares, M.B.; dos Santos, F.H.; Leite, C.N.; Mendes, K.F. Interaction mechanisms between biochar and herbicides. In *Interactions of Biochar and Herbicides in the Environment*; Mendes, K.F., Ed.; CRC Press: Boca Raton, FL, USA, 2022; pp. 79–130.
45. Frimpong, K.A.; Abban-Baidoo, E.; Marschner, B. Can combined compost and biochar application improve the quality of a highly weathered coastal savanna soil? *Heliyon* **2021**, *7*, e07089. [[CrossRef](#)] [[PubMed](#)]
46. Mendes, K.F.; Furtado, I.F.; Sousa, R.N.D.; Lima, A.D.C.; Mielke, K.C.; Brochado, M.G.D.S. Cow bonechar decreases indaziflam pre-emergence herbicidal activity in tropical soil. *J. Environ. Sci. Health Part B* **2021**, *56*, 532–539. [[CrossRef](#)]
47. Cheng, J.; Lee, X.; Gao, W.; Chen, Y.; Pan, W.; Tang, Y. Effect of biochar on the bioavailability of difenoconazole and microbial community composition in a pesticide-contaminated soil. *Appl. Soil Ecol.* **2017**, *121*, 185–192. [[CrossRef](#)]
48. Jenkins, J.R.; Viger, M.; Arnold, E.C.; Harris, Z.M.; Ventura, M.; Miglietta, F.; Taylor, G. Biochar alters the soil microbiome and soil function: Results of next-generation amplicon sequencing across Europe. *GCB Bioenergy* **2017**, *9*, 591–612. [[CrossRef](#)]
49. Noyce, G.L.; Winsborough, C.; Fulthorpe, R.; Basiliko, N. The microbiomes and metagenomes of forest biochars. *Sci. Rep.* **2016**, *6*, 26425. [[CrossRef](#)]
50. Zhu, X.; Chen, B.; Zhu, L.; Xing, B. Effects and mechanisms of biochar-microbe interactions in soil improvement and pollution remediation: A review. *Environ. Pollut.* **2017**, *227*, 98–115. [[CrossRef](#)] [[PubMed](#)]
51. Sharma, N.; Kaur, P.; Jain, D.; Bhullar, M.S. In-vitro evaluation of rice straw biochars' effect on bispyribac-sodium dissipation and microbial activity in soil. *Ecotoxicol. Environ. Saf.* **2020**, *191*, 110204. [[CrossRef](#)] [[PubMed](#)]
52. Egamberdieva, D.; Jabbarov, Z.; Arora, N.K.; Wirth, S.; Bellingrath-Kimura, S.D. Biochar mitigates effects of pesticides on soil biological activities. *Environ. Sustain.* **2021**, *4*, 335–342. [[CrossRef](#)]
53. Graber, E.R.; Harel, Y.M.; Kolton, M.; Cytryn, E.; Silber, A.; David, D.R. Biochar impact on development and productivity of pepper and tomato grown in fertigated soilless media. *Plant Soil* **2010**, *337*, 481–496. [[CrossRef](#)]
54. Kumar, A.; Joseph, S.; Tschansky, L.; Privat, K.; Schreiter, I.J.; Schüth, C.; Graber, E.R. Biochar aging in contaminated soil promotes Zn immobilization due to changes in biochar surface structural and chemical properties. *Sci. Total Environ.* **2018**, *626*, 953–961. [[CrossRef](#)]
55. Palansooriya, K.N.; Wong, J.T.F.; Hashimoto, Y.; Huang, L.; Rinklebe, J.; Chang, S.X.; Ok, Y.S. Response of microbial communities to biochar-amended soils: A critical review. *Biochar* **2019**, *1*, 3–22. [[CrossRef](#)]
56. Gorovtsov, A.V.; Minkina, T.M.; Mandzhieva, S.S.; Perelomov, L.V.; Soja, G.; Zamulina, I.V.; Yao, J. The mechanisms of biochar interactions with microorganisms in soil. *Environ. Geochem. Health* **2020**, *42*, 2495–2518. [[CrossRef](#)]
57. Islam, K.R.; Weil, R.R. Land use effects on soil quality in a tropical forest ecosystem of Bangladesh. *Agric. Ecosyst. Environ.* **2000**, *79*, 9–16. [[CrossRef](#)]
58. Wardle, D.A.; Ghani, A.A. A critique of the microbial metabolic quotient (qCO_2) as a bioindicator of disturbance and ecosystem development. *Soil Biol. Biochem.* **1995**, *27*, 1601–1610. [[CrossRef](#)]
59. Lacerda, K.A.P.; Cordeiro, M.A.S.; Verginassi, A.; Salgado, F.H.M.; Paulino, H.B.; Carneiro, M.A.C. Organic carbon, biomass and microbial activity in an Oxisol under different management systems. *Amaz. J. Agric. Environ. Sci.* **2013**, *56*, 249–254. [[CrossRef](#)]
60. Kaschuk, G.; Alberton, O.; Hungria, M. Three decades of soil microbial biomass studies in Brazilian ecosystems: Lessons learned

- about soil quality and indications for improving sustainability. *Soil Biol. Biochem.* **2010**, *42*, 1–13. [[CrossRef](#)]
61. Perucci, P.; Dumontet, S.; Bufo, S.A.; Mazzatura, A.; Casucci, C. Effects of organic amendment and herbicide treatment on soil microbial biomass. *Biol. Fertil. Soils* **2000**, *32*, 17–23. [[CrossRef](#)]
 62. Liao, H.; Li, Y.; Yao, H. Biochar amendment stimulates utilization of plant-derived carbon by soil bacteria in an intercropping system. *Front. Microbiol.* **2019**, *10*, 1361. [[CrossRef](#)] [[PubMed](#)]
 63. Liao, N.; Li, Q.; Zhang, W.; Zhou, G.; Ma, L.; Min, W.; Hou, Z. Effects of biochar on soil microbial community composition and activity in drip-irrigated desert soil. *Eur. J. Soil Biol.* **2016**, *72*, 27–34. [[CrossRef](#)]
 64. Hardy, B.; Sleutel, S.; Dufey, J.E.; Cornelis, J.T. The long-term effect of biochar on soil microbial abundance, activity and community structure is overwritten by land management. *Front. Environ. Sci.* **2019**, *7*, 110. [[CrossRef](#)]
 65. Hamer, U.; Marschner, B.; Brodowski, S.; Amelung, W. Interactive priming of black carbon and glucose mineralisation. *Org. Geochem.* **2004**, *35*, 823–830. [[CrossRef](#)]
 66. Mašek, O.; Budarin, V.; Gronnow, M.; Crombie, K.; Brownsort, P.; Fitzpatrick, E.; Hurst, P. Microwave and slow pyrolysis biochar—Comparison of physical and functional properties. *J. Anal. Appl. Pyrolysis* **2013**, *100*, 41–48. [[CrossRef](#)]
 67. Sam, A.T.; Asuming-Brempong, S.; Nartey, E.K. Microbial activity and metabolic quotient of microbes in soils amended with biochar and contaminated with atrazine and paraquat. *Acta Agric. Scand. B Soil Plant Sci.* **2017**, *67*, 492–509. [[CrossRef](#)]
 68. Ge, X.; Cao, Y.; Zhou, B.; Wang, X.; Yang, Z.; Li, M.H. Biochar addition increases subsurface soil microbial biomass but has limited effects on soil CO₂ emissions in subtropical moso bamboo plantations. *Appl. Soil Eco.* **2019**, *142*, 155–165. [[CrossRef](#)]
 69. INMET—Instituto Nacional de Meteorologia. Available online: <http://www.inmet.gov.br/portal/> (accessed on 18 April 2022).
 70. Mehdizadeh, M.; Izadi-Darbandi, E.; Yazdi, M.T.N.P.; Rastgoo, M.; Malaekheh-Nikouei, B.; Nassirli, H. Impacts of different organic amendments on soil degradation and phytotoxicity of metribuzin. *Int. J. Recycl. Org.* **2019**, *8*, 113–121. [[CrossRef](#)]
 71. ANVISA—Agência Nacional de Vigilância Sanitária. Resolução RDC N°. 166, 24 July 2017. Provides for the Validation of Analytical Methods and Makes Other Provisions. Available online: http://antigo.anvisa.gov.br/documents/10181/2721567/RDC_166_2017_COMP.pdf/d5fb92b3-6c6b-4130-8670-4e3263763401 (accessed on 18 April 2023).
 72. Ananyeva, N.D.; Susyan, E.A.; Gavrilenko, E.G. Determination of the soil microbial biomass carbon using the method of substrate-induced respiration. *Eurasian Soil Sci.* **2011**, *44*, 1215–1221. [[CrossRef](#)]
 73. Stotzky, G. Microbial respiration. In *Methods of Soil Analysis: Part 2 Chemical and Microbiological Properties*; Norman, A.G., Ed.; ACS: Madison, WI, USA, 1965; pp. 1550–1572.
 74. Islam, K.R.; Weil, R.R. Microwave irradiation of soil for routine measurement of microbial biomass carbon. *Biol. Fertil. Soils* **1998**, *27*, 408–416. [[CrossRef](#)]
 75. Anderson, T.H.; Domsch, K.H. Soil microbial biomass: The eco-physiological approach. *Soil Biol. Biochem.* **2010**, *42*, 2039–2043. [[CrossRef](#)]

Disclaimer/Publisher’s Note: The statements, opinions and data contained in all publications are solely those of the individual author(s) and contributor(s) and not of MDPI and/or the editor(s). MDPI and/or the editor(s) disclaim responsibility for any injury to people or property resulting from any ideas, methods, instructions or products referred to in the content.

Article

Cellulose Acetate Film Containing Bonechar for Removal of Metribuzin from Contaminated Drinking Water

 Kamila C. Mielke , Gustavo F. Castro  and Kassio F. Mendes 

Department of Agronomy, Federal University of Viçosa, Viçosa 36570-900, Brazil

* Correspondence: kamila.mielke@ufv.br

Abstract: Bonechar presents high sorption capacity for mobile herbicides retained in soil and water. However, its use in a granulated and/or powder form makes it difficult to remove water. The objective of this study was to produce a cellulose acetate film with bonechar as a viable alternative to remove metribuzin from water. The treatments were composed of 2 and 3 g of bonechar fixed on a cellulose acetate film, pure bonechar, and a control (no bonechar). The sorption and desorption study was carried out in the equilibrium batch mode with five concentrations of metribuzin (0.25, 0.33, 0.5, 1, and 2 mg L⁻¹). The water used in the experiment was potable water. Herbicide analysis was performed by High-Performance Liquid Chromatography (HPLC). The addition of 2 and 3 g of the bonechar fixed on the acetate film sorbed 40% and 60%, respectively, of the metribuzin at the lowest concentrations (0.25, 0.33, and 0.5 mg L⁻¹). For both additions, desorption was low, being 7% and 2.5% at 24 and 120 h, respectively. There are still no reports of the production of cellulose acetate film with bonechar for herbicide removal in water, considered an alternative of easy handling and indicated for water treatment plants.

Keywords: environmental remediation; herbicide; natural polymer; carbonaceous material



Citation: Mielke, K.C.; Castro, G.F.; Mendes, K.F. Cellulose Acetate Film Containing Bonechar for Removal of Metribuzin from Contaminated Drinking Water. *Processes* **2023**, *11*, 53. <https://doi.org/10.3390/pr11010053>

Academic Editor: Mostafa Y. Nassar

Received: 11 November 2022

Revised: 21 December 2022

Accepted: 23 December 2022

Published: 26 December 2022



Copyright: © 2022 by the authors. Licensee MDPI, Basel, Switzerland.

This article is an open access article distributed under the terms and conditions of the Creative Commons Attribution (CC BY) license (<https://creativecommons.org/licenses/by/4.0/>).

1. Introduction

Herbicides are initially used to ensure better crop productivity; however, they can lead to the contamination of aquatic ecosystems through retention-related processes (adsorption, absorption, and precipitation), transformation (decomposition or degradation) and transport (drift, volatilization, leaching, and runoff), and by the interactions of these processes [1]. Herbicides applied directly to the soil have the greater potential for ground-water contamination [2]. The mobility of herbicides in soil is coordinated by the movement of water in different directions, being vertical (leaching) and horizontal (runoff and/or running) [3,4]. The physicochemical characteristics of herbicides influence the behavior of the herbicide in the soil and interfere with the final destination of the water. Herbicides with high solubility (S_w) indicate the greater potential for leaching according with the soil water flow. Herbicides that have low S_w also have higher persistence in soil, which reduces groundwater contamination via leaching, but increases surface water contamination by runoff at high rainfall [2,5].

The increasing number of cases of herbicides detection in water is alarming [6]. Atrazine, simazine, diuron, terbuthylazine, ametryne, clomazone, imazapyr, sulfentrazone, and glyphosate have been found in water resources most frequently in Brazil [7–12]. Clomazone, sulfentrazone, diuron, and hexazinone were quantified at concentrations of 56.9, 31.9, 18.8, and 18.8 $\mu\text{g L}^{-1}$, respectively, by means of multiresidue analysis in water samples collected from semi-artesian wells in a rural area of the municipality of Jaboticabal, São Paulo State, Brazil [11]. In water samples collected from 20 farms in the Midwest region of Brazil, including surface water and groundwater, glyphosate herbicide was detected in 3.4% of the samples; however, only two were at levels higher than the limit of quantification (LoQ) of 1.2 $\mu\text{g L}^{-1}$ determined by the chromatographic method [13].

Metribuzin (4-amino-6-tert-butyl-4,5-dihydro-3-methylthio-1,2,4-triazin-5-one) is classified as a potential contaminant of groundwater and surface water [14] and its maximum residue limit (MRL) in drinking water is $25 \mu\text{g L}^{-1}$ [15]. Metribuzin presents high S_w (10.700 mg L^{-1} at 20°C), high mobility in soil (sorption coefficient normalized by organic carbon content (K_{oc}) from 38 mg L^{-1}), high leaching potential (groundwater ubiquity score (GUS) of 2.96), and low persistence (degradation half-life (DT50)) of ~ 20 days [16–18]. This is the main herbicide used in vegetables, applied pre-emergence, in systems with exhaustive soil preparation, such as plowing and harrowing, which can favor herbicide losses by leaching and surface runoff. Metribuzin residues were analyzed in water samples from Samambaia River sub-basin at the Federal District and Eastern Goiás State, Brazil [13]. Metribuzin was detected at concentrations above the LoQ of $2.37 \mu\text{g L}^{-1}$ in 73.2% of the water samples.

The use of carbonized organic waste is being evaluated as an alternative for the removal of contaminants from water and soil. Biochar, also called “charcoal”, is a carbon-abundant material from the partial carbonization of plant residues under controlled conditions with no or little oxygen and relatively low temperatures [19]. The main benefits of biochar-based materials lie in their high porosity, specific surface areas, improved ion exchange capacity, and abundant functional groups [20]. Other factors, such as the pH of the biochar (resulting from the pyrolysis condition), the residence time of the biochar in contact with the contaminant, the application rate of the biochar, and the type of contaminant can also affect the sorption of the herbicides [21].

Sorbents of natural origin (e.g., plant biomass) have become attractive due to the availability of abundant inputs, high sorption capacity, and low cost [2]. For example, bonechar (animal-based biochar) is derived from carbonizing animal bones by heating them at $500\text{--}800^\circ\text{C}$ in an airtight iron retort for 4–6 h [22]. Bonechar showed high removal capacity for diuron, ametryn, sulfometuron-methyl, and hexazinone in drinking water [23]. Removal for all herbicides was $\sim 100\%$ at the highest application rate of bonechar (1 g) added to 1 L of water. However, the use of pure bonechar in its granulated and/or powder form makes it difficult to remove it from the water, requiring a centrifugation step to remove the matrix after the herbicide is removed. In addition, the direct application of carbonaceous materials to water can increase the dissolved carbon content, affecting aquatic ecosystems through increased turbidity and metal toxicity [24].

An alternative is the use of a mixed material, in which fine bonechar particles can be added to solid particles by means of biopolymer, which can facilitate the collection and/or reuse of the material after the removal of the herbicide from the water. Cellulose acetate is a natural thermoplastic and biodegradable polymer that is prepared by acetylating cellulose [25]. The way cellulose acetate is processed influences its use, and it can be used for a wide variety of applications, such as for films, membranes, or fibers [26]. Cellulose acetate, being biodegradable, from the natural origin and abundant in the environment, is an environmentally viable alternative to be used as a support material for the doll making. A hybrid film of cellulose acetate with biochar was studied for the sorption ability of phosphorus in water [27]. However, there are still no reports of the production of cellulose acetate films and bonechar for the removal of herbicides in water, being a technological alternative of easy management. Different sorbents have been developed, such as polymer resins [28], particulate carbon [29], nanotubes [30], and mineral materials [31]. Some of these materials have been used to remove herbicides from wastewater, but the high costs limit their use [32].

Thus, the objective of this study was to produce a cellulose acetate film with bonechar as a viable alternative for immobilization and removal of metribuzin from water. The results determine the sorptive capacity of the acetate film and bonechar at different concentrations of metribuzin and that of pure bonechar powder.

2. Materials and Methods

2.1 Drinking Water Samples

The water used was potable and collected from a cold water tap in Viçosa, MG, Brazil, which is regularly used for human consumption. The water for the entire experiment was collected from the tap and stored in a 20 L closed barrel at room temperature. Water samples were used for the determination of the physicochemical properties (Table 1).

Table 1. Selected drinking water quality properties.

Properties	Values
Electrical conductivity ($\mu\text{S cm}^{-1}$)	117.20
Hardness ($\text{mg CaCO}_3 \text{ L}^{-1}$)	22.00
Alkalinity (mg L^{-1})	25.75
Total residual chlorine (mg L^{-1})	1.34
pH	7.25
Turbidity (uT)	0.18
Temperature ($^{\circ}\text{C}$)	16.90
Apparent color (uC)	3.60

Source: Water and Sewage Division of the Federal University of Viçosa, Viçosa, MG, Brazil.

2.2 Bonechar and Cellulose Acetate Film

Bonechar produced from ox bone raw material was purchased from Bonechar Carvão Ativado Ltd.a (Maringá, PR, Brazil) and was used as the sorbent material. The bonechar used had a granulometry of $40 \mu\text{m} \times 100 \mu\text{m}$. The selected properties of the bonechar are shown in Table 2. The surface morphology was performed by scanning electron microscopy (SEM) on a microscope of the brand JEOL (JSM-6010LA, Akishima, Tokyo, Japan). The resolution was 4 nm (with a beam at 20 kV), the applied magnification was from $8\times$ to $300,000\times$, and the acceleration voltage from 500 V to 20 kV. Biochar particles were attached to a metal surface by a conductive carbon tape (PELCO Tabs™, Ted Pella, Inc., Redding, CA, USA) and coated with gold (Leica EM ACE 600, Buffalo Grove, IL, USA) with a 120-nm-thick layer. The energy-dispersive X-ray spectrometry (EDS) of the doll was characterized by [33,34].

Table 2. Selected properties of the bonechar.

Properties	Values
Feedstock	Cow bone
Production temperature ($^{\circ}\text{C}$)	800
Total surface area ($\text{m}^2 \text{ g}^{-1}$)	200
Carbon surface area ($\text{m}^2 \text{ g}^{-1}$)	50
Carbon content (%)	11
pH (H_2O)	9.12
Soluble ash in acid (%)	<3
Insoluble ash content (%)	0.7
Tricalcium phosphate (%)	70
Calcium sulphate (%)	0.1
Iron (%)	<0.3
Pore size (nm)	7.5–60.000
Pore volume ($\text{cm}^3 \text{ g}^{-1}$)	0.225
Micropore area ($\text{m}^2 \text{ g}^{-1}$)	133
Humidity (%)	<5
Density (g cm^3)	0.65

Source: All information was provided by the manufacturer itself.

The cellulose acetate used had a degree of substitution of 2.5 [35]. To obtain a filmogenic solution, the cellulose acetate was solubilized in acetone (99.8%) at a ratio of 1:10 (w/v) and allowed to stand for 24 h in a completely sealed glass bottle at room temperature.

After this period, cellulose acetate films were produced with bonechar at a proportion of 13.3% (*w/v*) with a thickness of 0.45 mm. For the production of the cellulose acetate film, the filmogen solution with the bonechar was spread evenly over a petri dish with the aid of a glass rod. It was subsequently dried in natural air presenting a good adhesion of the bonechar particles to the film.

2.3 Sorption–Desorption Metribuzin

The methodology for the sorption and desorption study was established according to the OECD guidelines “106, Adsorption—Desorption Using a Batch Equilibrium Method” [36,37]. The stock solution was prepared at a concentration of 500 mg L⁻¹ of the standard Metribuzin-Pestanal™ (analytical standard, 98.8% purity; Sigma-Aldrich, San Luis, MO, USA) and the working solution at a concentration of 100 mg L⁻¹, both in acetonitrile (99.9% purity). Hereafter, five concentrations of metribuzin were prepared (0.25, 0.33, 0.5, 1.0, and 2.0 mg L⁻¹), where the highest concentration corresponded to the highest recommended field dose of the herbicide (1920 g a.i. ha⁻¹) for sugarcane cultivation.

The experiment design was entirely randomized with 3 replicates. The treatments were composed of 2 and 3 g of bonechar fixed on a cellulose acetate film, pure bonechar powder (2 g), and a control (no bonechar added). In a 200 mL Erlenmeyer flask, it was added to 150 mL of drinking water, followed by the concentrations of herbicides and the cellulose acetate film with bonechar. Then, the Erlenmeyer flasks were shaken on a shaking table (Tecnal TE-140; Piracicaba, São Paulo, Brazil) at 100 rpm for 24 h, until equilibrium concentration was reached [38,39]. The pH of the water was measured during the entire sorption and desorption study using a bench pH meter (Digimed, DM-22; Didática, São Paulo, Brazil). Subsequently, three 2 mL aliquots of the supernatant were filtered on a Millipore filter (PRFE membrane 0.45 µm) and placed in vials.

The desorption study was carried out under the same condition as the two-step sorption (24 and 120 h). The water from the sorption study was discarded from the Erlenmeyer flasks containing the films and 150 mL of drinking water, without herbicide, was added again and was stirred on a shaking table for 24 h. Subsequently, three 2 mL aliquots of the supernatant were filtered on a Millipore filter (PRFE membrane size: 0.45 µm) and placed in vials. The amount desorbed was calculated by the difference between the herbicides sorbed on the film and the amount remaining in the supernatant. The same procedure was repeated to analyze desorption at 120 h.

The quantification of metribuzin was performed on a High-Performance Liquid Chromatography (HPLC) system (LC 20AT, Shimadzu, Nagoya, Japan), with a photodiode array detector (SPD-M20A, Shimadzu, Japan) and stainless steel C18 column (Shimadzu VP-ODS Shim-pack 250 mm × 4.6 mm d.i., 5 µm of particle size).

The mobile phase was adapted from [38]. It was composed of acetonitrile/water (acidified with 0.01% phosphoric acid) in a ratio of 45/55 (*v v*⁻¹), an injection volume of 30 µL, a flow rate of 1.0 mL min⁻¹, a wavelength of 254 nm, and a column oven temperature of 30 °C. The mobile phase showed good linearity in the range from 0.05 to 2 mg L⁻¹ of metribuzin. The analytical curve showed a coefficient of determination (*R*²) equal to 0.9992. The limit of detection (LoD) and the limit of quantification (LoQ) were 0.0081 and 0.0289 mg L⁻¹, respectively.

2.4 Freundlich Model for Sorption–Desorption and Apparent Coefficient

The apparent sorption coefficient (*K*_{*d-app*}, L kg⁻¹) was calculated for all concentrations of metribuzin analyzed in the sorption and desorption study, using the following Equation (1):

$$K_{d-app} = C_s / C_e \quad (1)$$

where *C*_{*s*} is the amount of herbicide sorbed onto the bonechar film as Equation (2):

$$C_s = (C_i - C_e) \times V/M \quad (2)$$

where C_i is the initial liquid concentration (mg L^{-1}), C_e is the equilibrium liquid concentration (mg L^{-1}), V is the volume of herbicide solution added (mL), and M is the mass of bonechar (g) [40].

The Freundlich model and its distribution coefficient were determined from Equation (3):

$$K_f = C_s/C_e^{1/n} \quad (3)$$

where n (dimensionless value) can range from 0 to 1, depending on the heterogeneity of the sorption sites.

All isotherms were plotted in Sigma Plot® (version 14.0 for Windows, Systat Software Inc., Point Richmond, CA, USA), and parameter data were presented as means and the standard deviation of the mean ($n = 3$).

3. Results and Discussion

3.1 Synthesis of the Acetate Film with Added Bonechar

The physicochemical properties of the bonechar are presented in Table 2. The material presented a low ash content (0.7%) and a low carbon content (11%), a high tricalcium phosphate content (70%), pH (9.12), and a specific surface area (SSA) ($200 \text{ m}^2 \text{ g}^{-1}$). The surface of the material was irregular, rough and with a varying pore size (Figure 1). A lower surface area was observed for the bonechar produced at different pyrolysis temperatures ($350\text{--}700 \text{ }^\circ\text{C}$) [41]. The authors reported the surface area, the total pore volume, and the average pore diameter of $79.34 \text{ m}^2 \text{ g}^{-1}$, $0.041 \text{ cm}^3 \text{ g}^{-1}$, and 2.09 nm , respectively. Nigri et al. [42] observed a relatively high surface area ($140 \text{ m}^2 \text{ g}^{-1}$) with an irregular pore size and shape.

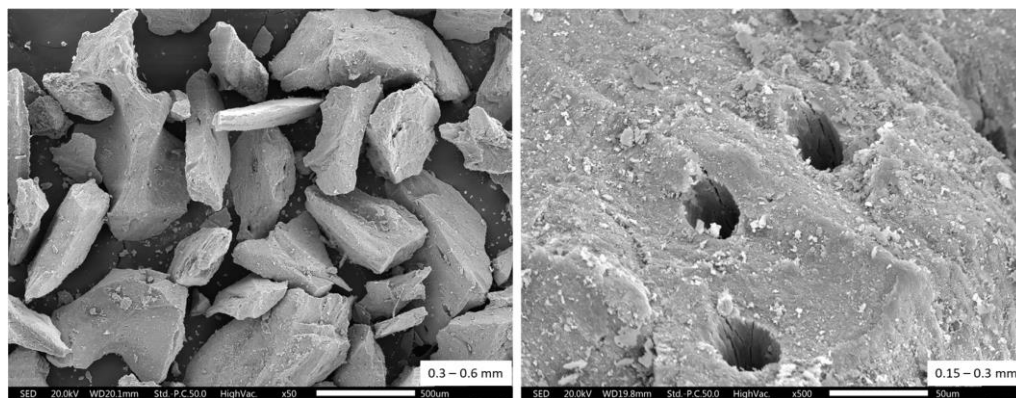


Figure 1. Scanning electron microscopy (SEM) images of the bonechar at two particle sizes: 0.3–0.6 mm and 0.15–0.3 mm at $50\times$ and $500\times$ magnifications, respectively.

The bonechar presents predominance of the elements oxygen (O), phosphorus (P), and calcium (Ca), totaling approximately 80% of the total composition, which is linked to the basic elemental composition of hydroxyapatite [33,41]. Analysis of the elemental composition of the bonechar was performed by energy-dispersive X-ray spectroscopy (EDS) by [33]. The authors reported that C and O appeared as dominant elements ($\sim 36\%$ each), with Ca and P also presented mass percentages of $\sim 18\%$ and 9% , respectively. The elements sodium (Na), magnesium (Mg), and chlorine (Cl) were also observed in the bonechar, however, at low concentrations. Bonechar is a material considered highly efficient in removing and immobilizing herbicides [23,33,34,43], as well as fluoride (F) [41], methylene blue [44], chromium (Cr) [45], and arsenic (As) [46] from water and soil. The use of ox bone waste for the production of bonechar not only reduces the risk associated with the waste, but also provides an environmental remediation solution as a potential sorbent for water and soil that can also be used as an alternative organic P [47].

The acetate film with bonechar is seen in Figure 2. The film produced presented good physical structure, with a complete coating of the bonechar granules avoiding

its dispersion in the water. Preliminary studies were necessary to determine the best proportion of the acetate film and the bonechar, since high ratios of the material result in a brittle film and make it difficult to remove from the water. A bonechar-free cellulose acetate film was previously tested for sorption potential of metribuzin and did not show sorptive capacity (unpublished data), so it did not enter into the study for removal of metribuzin from water.



Figure 2. (A) Cellulose acetate film without (pure) and with bonechar; (B) cellulose acetate film with bonechar; (C) visualization of the attachment of the material to the film (translucent water after 24 h of agitation).

3.2 Removal (Sorption/Desorption) of Metribuzin

The addition of 2 g of pure bonechar powder showed a high sorptive capacity (100%) for metribuzin at all concentrations studied, remaining lower than the LoQ (0.0289 mg L^{-1}). The sorption results for 3 g of the bonechar were not presented, since it was not possible to quantify them (Figure 3). In the control treatment (water + metribuzin only), the concentration of the herbicide remained stable throughout the study, excluding the hypothesis of metribuzin degradation. Bonechar is an excellent substitute for activated C due to its higher production and lower activation costs [47]. This material showed the potential for immobilization of different heavy metals in water [42,48–50] and herbicides in soil and water [23,33,34,43]. The bonechar has the high potential in the sorption of metribuzin when used in a powder form; however, it might have complications due to the difficulty in handling the material, such as the removal of the matrix after the removal of the herbicide. Another negative point is the change in the coloration of the water, becoming darker, observed in this study when the pure powdered material was added. For the cellulose acetate film with bonechar, no color change of the water was observed, and the filtration step can be discarded (Figure 2).

Sorption isotherms were fitted using the Freundlich model to describe the sorption of metribuzin on cellulose acetate and bonechar films, as indicated by the coefficients of determination of the equations ($R^2 \geq 0.98$) (Figures 4 and 5). The K_f of sorption was 19.09 and $53.68 \text{ mg}^{(1-1/n)} \text{ L}^{1/n} \text{ Kg}^{-1}$ with additions of film with 2 and 3 g bonechar, respectively. The degree of linearity ($1/n$) varied from 0.43 to 0.89, as the amount of bonechar in the acetate film increased, classifying the sorption isotherm as type L (Table 3). The L-type isotherms indicate that the sorption rate decreases as the herbicide concentration increases [51]. At low concentrations of metribuzin, the material showed higher availability of sorption sites, and at higher concentration, there was a reduction in the potential of the cellulose acetate film with bonechar to sorb metribuzin.

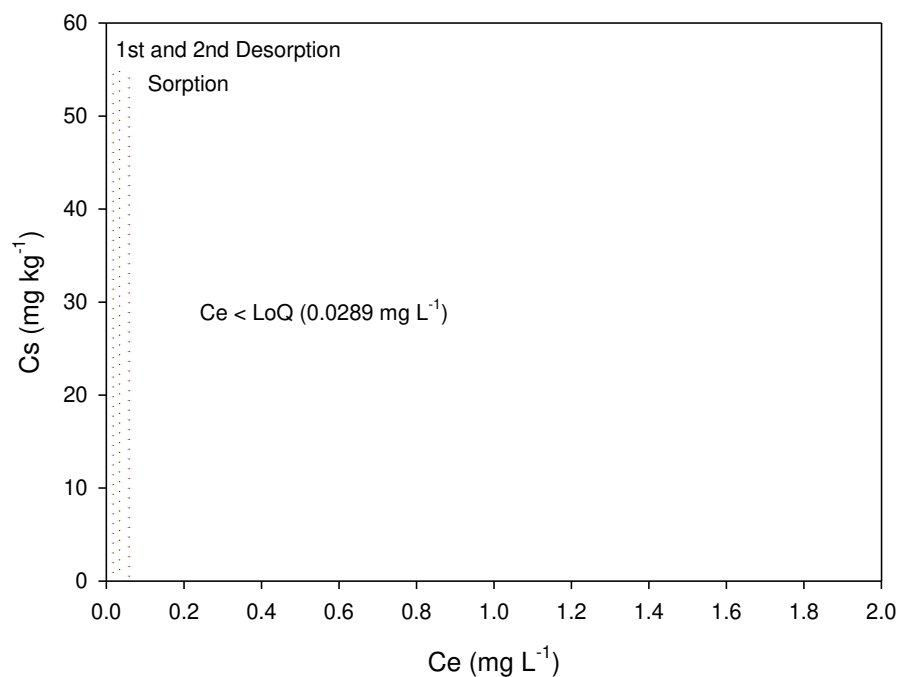


Figure 3. Sorption and desorption isotherms of metribuzin in pure bonechar powder (2 g) added in water. The x-axis indicates the C_e concentration at equilibrium, and the y-axis indicates the C_s concentration in the sorbent. Dotted lines show that no residues of the herbicide were detected (<limit of quantification (LoQ)). One-hundred percent sorption and 0% desorption of the herbicide were observed in the pure bonechar powder.

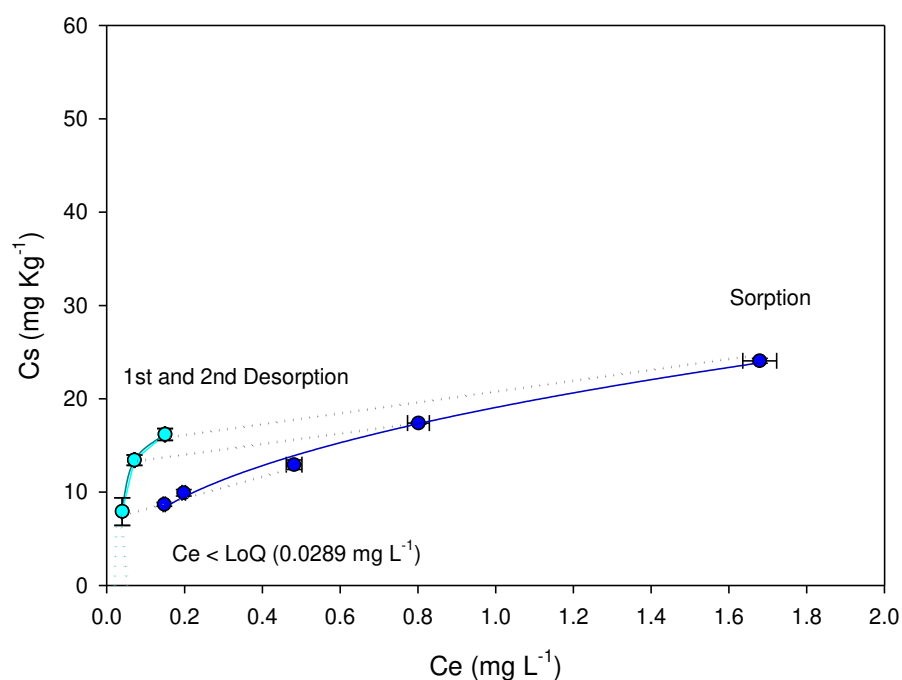


Figure 4. Sorption and desorption isotherms of metribuzin on cellulose acetate film and bonechar (2 g) added to water. The continuous lines in color correspond to the isotherms, and the dotted ones show that no residues of the herbicide were detected (<limit of quantification (LoQ)). The vertical and horizontal bars represent the standard deviation of the means ($n = 3$) of the C_e concentration at equilibrium and the C_s concentration in the sorbent, respectively. Symbols can cover the bars.

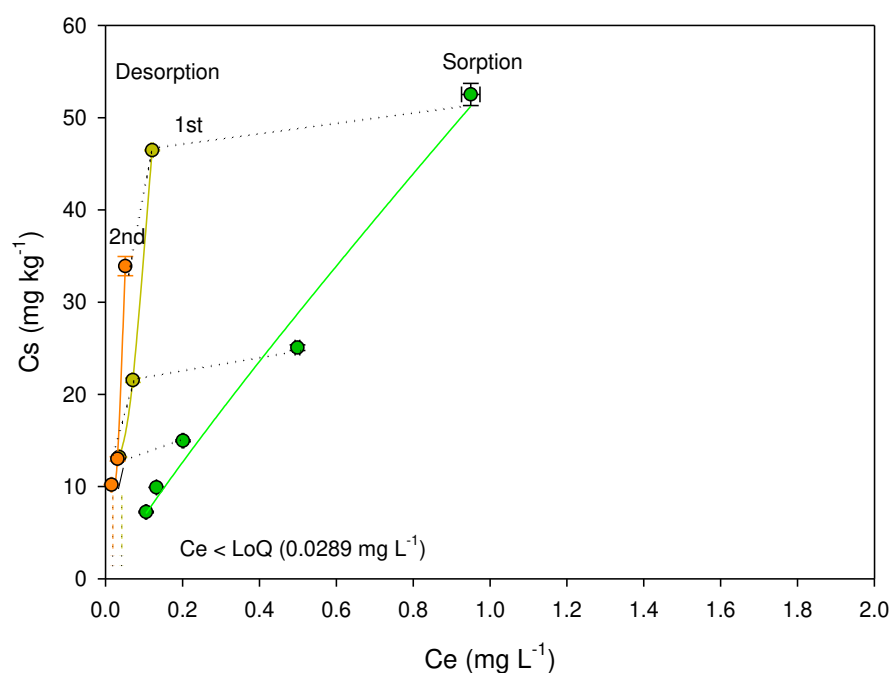


Figure 5. Sorption and desorption isotherms of metribuzin on the cellulose acetate film and the bonechar (3 g) added to water. The continuous lines in color correspond to the isotherms and the dotted ones show that no residues of the herbicide were detected (<limit of quantification (LoQ)). The vertical and horizontal bars represent the standard deviation of the means ($n = 3$) of the C_e concentration at equilibrium and the C_s concentration in the sorbent, respectively. Symbols can cover the bars.

Table 3. Freundlich model isotherm sorption parameters and sorption coefficients (K_{d-app}) of metribuzin on pure bonechar powder and on the cellulose acetate film with bonechar.

Carbonaceous material	K_f ($\text{mg}^{(1-1/n)} \text{L}^{1/n} \text{Kg}^{-1}$)	$1/n$	R^2	Metribuzin (mg L^{-1})				
				0.25	0.33	0.5	1.0	2.0
Bonechar pure powder (2 g)	< LoQ ^a	-	-	< LoQ	< LoQ	< LoQ	< LoQ	< LoQ
(%) sorbed	-	-	-	100	100	100	100	100
Acetate film with bonechar (2 g)	19.06 ± 0.07	0.43 ± 0.03	0.995	52.01 ± 0.02	51.21 ± 0.03	58.21 ± 0.03	18.58 ± 0.04	14.33 ± 0.04
(%) sorbed	-	-	-	40.95 ± 0.01	40.08 ± 0.05	43.70 ± 0.02	19.86 ± 0.03	16.04 ± 0.02
Acetate film with bonechar (3 g)	53.68 ± 0.05	0.89 ± 0.02	0.992	78.92 ± 0.03	75.05 ± 0.04	74.43 ± 0.04	50.23 ± 0.01	55.30 ± 0.03
(%) sorbed	-	-	-	67.95 ± 0.01	60.01 ± 0.03	59.81 ± 0.03	50.11 ± 0.02	52.51 ± 0.06

^a Limit of quantification. ^b Mean value of each parameter standard deviation of the mean ($n = 3$). (-) no data available.

The cellulose acetate film with bonechar showed an improvement in the sorption of metribuzin, however compared to that of the pure material, which showed 100% sorption, and the efficiency reduced to ~31% and 57% when adding 2 and 3 g of the bonechar, respectively, which indicates that the use of more films or even a film with a higher concentration of the carbonaceous material can improve the removal efficiency of metribuzin from water. These results were confirmed by the K_{d-app} values of the sorption at the five concentrations of metribuzin shown in Table 3. The acetate film with 2 g bonechar at the lowest concentrations of metribuzin (0.25, 0.33, and 0.5 mg L^{-1}) showed a sorptive capacity of ~40% and a K_{d-app} of ~55 L kg^{-1} . The sorptive capacity decreased to ~16% and the K_{d-app} reduced to ~16 L kg^{-1} , as the concentration of metribuzin increased to 2 mg L^{-1} . However, when 3 g of bonechar were added, the average K_{d-app} values were ~75 and 50 L kg^{-1} for the lowest (0.25, 0.33, and 0.5 mg L^{-1}) and highest (1 and 2 mg L^{-1}) concentrations of metribuzin,

respectively (Table 3).

The removal of metribuzin from water with carbonaceous materials was analyzed in different studies [29,52,53]. However, the materials used was in its granular form, which provided greater sorption potential, as observed in this study by the use of bonechar powder. The sorptive capacity of the bonechar is linked to the SSA properties ($200 \text{ m}^2 \text{ g}^{-1}$), C content (11%), and high Ca (18.3%) and P (8.5%) contents [33], which consequently increase the capacity to immobilize potentially toxic compounds [54].

The nature of the carbonaceous material versus herbicide interactions can be exclusively physical, chemical, or both and can result in the phenomenon of sorption. Physical sorption refers to the surface binding process related to the pore size of the carbonaceous material, and chemical sorption refers to binding forces involved, which operate in the formation of compounds [55]. Studies have reported that sorption by bonechar is associated with surface properties (chemical sorption) and carbon content and porosity (physical sorption) [33,34,42,46]. The sorption of metribuzin from aqueous solutions using magnetic and non-magnetic grass biochar was related to hydrogen bonds, Coulomb, van der Waals forces (physical sorption), and π - π interactions (chemical sorption) [56,57].

Bonechar powder had a high pH value (9.12), and it was observed that adding the material to the herbicide-added water increased the pH from 6.8 to an average value of 7.8. By adding bonechar to the cellulose acetate film, regardless of the application rate, the pH increased to 7.3 (Table 4).

Table 4. Changes in pH of the water during the sorption and desorption study of metribuzin in the water with bonechar.

Treatments	Sorption	1st Desorption (24 h)	2nd Desorption (120 h)
Water (with herbicide)	6.91	6.69	6.85
Bonechar pure powder (2 g)	8.72	8.59	7.87
Acetate film with bonechar (2 g)	7.14	7.22	7.39
Acetate film with bonechar (3 g)	7.72	7.25	7.02

Metribuzin is a strong acid (ionization constant, $\text{pK}_a = 1.3$), and its sorption gradually increases as the pH decreases towards the pK_a of metribuzin, which assumes its protonated (negatively charged) form [58]. The bonechar powder, despite changing the pH of the water, showed the ability to sorb 100% of metribuzin, which implicates that the physicochemical characteristics of the material provide high efficiency in the herbicide sorption. The acetate film with bonechar promoted a small pH increase; however, that may have influenced the sorption potential of the film, and further studies analyzing the pH change on the sorptive capacity of the cellulose acetate film with bonechar are needed. Grass biochar and modified (magnetic) grass biochar were analyzed to remove metribuzin from aqueous solutions [57]. These authors observed that low pH values (3–4) of the solution is beneficial for sorption of metribuzin on biochars when compared to high pH values (7) of the solution.

The desorption isotherms were not fitted to the Freundlich model (Figures 4 and 5), since it was not possible to detect the herbicide residues at the lowest concentrations (0.25 and 0.33 mg L^{-1}), as it was lower than the LoQ. Therefore, the model was carried out only from the K_{d-app} of each concentration. The percentage desorbed of metribuzin was $\sim 7\%$ at 24 h (1st desorption) and reduced to $\sim 2.5\%$ at 120 h (2nd desorption) of stirring, regardless of the concentration of bonechar added to the acetate film (Table 5). At 24 h, the K_{d-app} of desorption was $\sim 120 \text{ L kg}^{-1}$ and increased to $\sim 190 \text{ L kg}^{-1}$ at 120 h for the film with 2 g of the bonechar. The film with 3 g of the bonechar showed a desorption K_{d-app} of $\sim 350 \text{ L kg}^{-1}$ at 24 h. On the other hand, at 120 h, the K_{d-app} of desorption varied from 223.2 to 854.4 L kg^{-1} , as the concentration of metribuzin increased from 0.5 to 2 mg L^{-1} (Table 5). The desorption analyzed for 24 and 120 h at the metribuzin concentrations of 0.25 and 0.33 mg L^{-1} were less than the LoQ and less than the maximum residue limit (MRL) allowed for metribuzin in water (0.025 mg L^{-1}) [15], which demonstrates its availability for consumption. The highest concentrations of metribuzin (1.0 and 2.0 mg L^{-1}) presented greater desorption than the permitted MRL for both desorption steps. However, the highest dose of the herbicide tested in this study (2 mg L^{-1}) represented the highest commercial dose recommended in the field

for metribuzin (1920 g a.i. ha⁻¹), being 80 times higher than the MRL, and possibly only traces of the herbicide could be detected in the water. For the untreated surface and the ground water at Primavera do Leste, Mato Grosso State (Midwestern Brazil), metribuzin was detected at a maximum concentration of 0.00351 mg L⁻¹ [14]. In Portugal, surface waters are collected in river basins, and metribuzin is quantified at a concentration of 0.056 mg L⁻¹ [59].

Table 5. Desorption coefficients (K_{d-app}) of metribuzin on pure bonechar powder and on cellulose acetate film with bonechar at 24 and 120 h.

Carbonaceous Material	Metribuzin (mg L ⁻¹)					Metribuzin (mg L ⁻¹)				
	0.25	0.33	0.5	1.0	2.0	0.25	0.33	0.5	1.0	2.0
	K_{d-app} (L kg ⁻¹)—1st Desorption (24 h)					K_{d-app} (L kg ⁻¹)—2nd Desorption (120 h)				
Bonechar pure powder (2 g)	<LoQ ^a	<LoQ	<LoQ	<LoQ	<LoQ	<LoQ	<LoQ	<LoQ	<LoQ	<LoQ
(%) desorbed	0	0	0	0	0	0	0	0	0	0
Acetate film with bonechar (2 g)	<LoQ	<LoQ	113.65 ± 0.01 ^b	111.54 ± 0.04	135.27 ± 0.04	<LoQ	<LoQ	145.85 ± 0.02	194.83 ± 0.01	230.87 ± 0.04
(%) desorbed	0	0	7.50 ± 0.08	7.09 ± 0.05	7.47 ± 0.01	0	0	2.50 ± 0.04	2.93 ± 0.04	2.64 ± 0.07
Acetate film with bonechar (3 g)	<LoQ	<LoQ	373.65 ± 0.04	304.94 ± 0.04	384.40 ± 0.03	<LoQ	<LoQ	223.25 ± 0.06	384.40 ± 0.06	859.47 ± 0.08
(%) desorbed	0	0	6.50 ± 0.07	7.05 ± 0.03	6.04 ± 0.05	0	0	2.20 ± 0.01	3.06 ± 0.04	2.55 ± 0.06

^a Limit of quantification. ^b Mean value of each parameter ± standard deviation of the mean ($n = 3$). (-) no data available.

The films showed sorption potential and low desorption at lower doses of metribuzin, indicating that the greater the active surface area available for sorption of the herbicide, the greater the ability of the sorbent to remove contaminants. Cellulose acetate reduced the available surface area of the bonechar, which reduced the efficiency to ~31% and 57% when adding 2 and 3 g of the bonechar, respectively. A similar result was observed for cellulose acetate used to produce hybrid films with lamellar aluminum magnesium double hydroxides (HDL) as a sorbent for P uptake [60]. HDL incorporated into cellulose acetate had lower phosphate sorption values than HDL powder. The authors reported that a decrease in the sorption potential of the film occurred due to the lower amount of HDLs available for the sorption process.

Cellulose acetate is biodegradable, non-toxic and has the ability to absorb water [61], which makes it potential for use in agriculture, to improve water retention, manufacture of thin films on the surface of various materials. In addition, it has pharmaceutical and biomedical applications as a coating material [62,63]. The biomaterial is biodegradable in soil and can be especially useful in agricultural and horticultural applications [64].

The results are very relevant, when it comes to technologies for removing herbicides from water, presenting high practicality and easy handling. However, despite the film's potential for sorption of metribuzin, its low cost and easy incorporation into cellulose acetate, saturation of the sorptive surface may occur and reduce sorption efficiency when compared to pure bonechar. Strategies should be studied in order to improve the sorption potential of the acetate film with bonechar for higher doses of metribuzin. For example, increasing the amount of the cellulose acetate film with bonechar or successive stages of agitation of the film could contribute to a complete removal of the herbicide from the water. The use of a cellulose acetate film with bonechar for lower doses (0.25, 0.33, and 0.5 mg L⁻¹)

of metribuzin showed a high sorption capacity, and the adoption of the strategies mentioned above can provide complete sorption of metribuzin from water.

4. Conclusions

The use of cellulose acetate for bonechar attachment has not yet been reported in the scientific literature, being a technological innovation for herbicide removal from water. Pure bonechar powder showed a high sorptive capacity for metribuzin at all concentrations tested.

The cellulose acetate film with bonechar presented the higher sorption potential for the lower concentrations of metribuzin in drinking water. The bonechar added at the concentration of 2 and 3 g sorbed 40% and 60%, respectively, of the metribuzin at the concentrations of 0.25, 0.33, and 0.5 mg L⁻¹. For both films, desorption was low, being 7% and 2.5% at 24 and 120 h, respectively.

The film becomes an efficient and easy-to-handle alternative for decontaminating contaminated aquatic environments and can be an alternative for water and sewage treatment plants, as well as for use in spray tanks, washing personal protective equipment (PPE), and household filters.

Author Contributions: Conceptualization, K.C.M.; data curation, K.C.M.; investigation, methodology, and validation, K.C.M., G.F.C. and K.F.M.; writing—review and editing, K.C.M., G.F.C. and K.F.M.; project administration, formal analysis, and funding acquisition, K.F.M. All authors have read and agreed to the published version of the manuscript.

Funding: This research was funded by Coordination for the Improvement of Higher Education Personnel (CAPES—88887.479265/2020-00), National Council for Scientific and Technological Development (CNPq—404240/2021-6), and Foundation for Research Support of the State of Minas Gerais (FAPEMIG—2070.01.0004768/2021-84).

Data Availability Statement: Not applicable.

Acknowledgments: The authors thanks Federal University of Viçosa.

Conflicts of Interest: The authors declare no conflict of interest.

5. References

1. Vryzas, Z. Pesticide fate in soil-sediment-water environment in relation to contamination preventing actions. *Curr. Opin. Environ. Sci. Health* **2018**, *4*, 5–9. [[CrossRef](#)]
2. Mendes, K.F.; Régo, A.P.J.; Takeshita, V.; Tornisielo, V.L. Water resource pollution by herbicide residues. In *Biochemical Toxicology—Heavy Metals and Nanomaterials*; Ince, M., Ince, O.K., Ondrasek, G., Eds.; IntechOpen: London, UK, 2019; pp. 1–16.
3. Peña, A.; Delgado-Moreno, L.; Rodríguez-Liébaña, J.A. A review of the impact of wastewater on the fate of pesticides in soils: Effect of some soil and solution properties. *Sci. Total Environ.* **2020**, *718*, 134468. [[CrossRef](#)] [[PubMed](#)]
4. SDWF-Safe Drinking Water Foundation. Pesticides and Water Pollution. 2017. Available online: <https://www.safewater.org/factsheets-1/2017/1/23/pesticides> (accessed on 6 August 2022).
5. Giuliano, S.; Alletto, L.; Deswarte, C.; Perdrieux, F.; Daydé, J.; Debaeke, P. Reducing herbicide use and leaching in agronomically performant maize-based cropping systems: An 8-year study. *Sci. Total Environ.* **2021**, *788*, 147695. [[CrossRef](#)] [[PubMed](#)]
6. Palma, P.; Köck-Schulmeyer, M.; Alvarenga, P.; Ledo, L.; Barbosa, I.R.; López de Alda, M.; Barceló, D. Risk assessment of pesticides detected in surface water of the Alqueva reservoir (Guadiana basin, southern of Portugal). *Sci. Total Environ.* **2014**, *488*, 208–219. [[CrossRef](#)] [[PubMed](#)]
7. Wang, M.; Lv, J.; Deng, H.; Liu, Q.; Liang, S. Occurrence and removal of triazine herbicides during wastewater treatment processes and their environmental impact on aquatic life. *Int. J. Environ. Res. Public Health* **2022**, *19*, 4557. [[CrossRef](#)] [[PubMed](#)]
8. Zhang, R.; Du, J.; Dong, X.; Huang, Y.; Xie, H.; Chen, J.; Kadokami, K. Occurrence and ecological risks of 156 pharmaceuticals and 296 pesticides in seawater from mariculture areas of Northeast China. *Sci. Total Environ.* **2021**, *792*, 148375. [[CrossRef](#)]
9. Köck-Schulmeyer, M.; Ginebreda, A.; González, S.; Cortina, J.L.; De Alda, M.L.; Barceló, D. Analysis of the occurrence and risk assessment of polar pesticides in the Llobregat River Basin (NE Spain). *Chemosphere* **2012**, *86*, 8–16. [[CrossRef](#)]
10. Santos, E.A.; Correia, N.M.; Silva, J.R.M.; Velini, E.D.; Passos, A.B.R.J.; Durigan, J.C. Herbicide detection in groundwater in Córrego Rico-SP watershed. *Planta Daninha* **2015**, *33*, 147–155. [[CrossRef](#)]
11. Sousa, A.S.; Duaví, W.C.; Cavalcante, R.M.; Milhome, M.A.L.; Nascimento, R.F. Estimated levels of environmental contamination and health risk assessment for herbicides and insecticides in surface water of Ceará, Brazil. *Bull. Environ. Contam. Toxicol.* **2016**, *96*, 90–95. [[CrossRef](#)]

12. Pires, N.L.; Passos, C.J.S.; Morgado, M.G.; Mello, D.C.; Infante, C.M.C.; Caldas, E.D. Determination of glyphosate, AMPA and glufosinate by high performance liquid chromatography with fluorescence detection in waters of the Santarém Plateau, Brazilian Amazon. *J. Environ. Sci. Health Part B* **2020**, *55*, 794–802. [[CrossRef](#)]
13. Correia, N.M.; Carbonari, C.A.; Velini, E.D. Detection of herbicides in water bodies of the Samambaia River sub-basin in the Federal District and eastern Goiás. *J. Environ. Sci. Health Part B* **2020**, *55*, 574–582. [[CrossRef](#)] [[PubMed](#)]
14. Dores, E.F.G.C.; Navickiene, S.; Cunha, M.L.; Carbo, L.; Ribeiro, M.L.; De-Lamonica-Freire, E.M. Multiresidue determination of herbicides in environmental waters from Primavera do Leste Region (Middle West of Brazil) by SPE-GC-NPD. *J. Braz. Chem. Soc.* **2006**, *17*, 866–873. [[CrossRef](#)]
15. Brazil Ministry of Health. Office of the Minister. Ordinance nº. 888, of May 4, 2021. Amends Annex XX of the Consolidation Ordinance GM/MS nº. 5, of September 28, 2017, to Dispose on the Procedures for Control and Surveillance of the Quality of Water for Human Consumption and Its Potability Standard. *Diário Oficial da União*, Brasília, DF. 4 May 2021; p. 127. Available online: https://bvsms.saude.gov.br/bvs/saudelegis/gm/2021/prt0888_07_05_2021.html (accessed on 1 November 2022).
16. Saritha, J.D.; Ramprakash, T.; Rao, P.C.; Madhavi, M. Persistence of metribuzin in tomato growing soils and tomato fruits. *Nat. Environ. Pollut. Technol.* **2017**, *16*, 505.
17. Guimarães, A.C.D.; Mendes, K.F.; Campion, T.F.; Christoffoleti, P.J.; Tornisielo, V.L. Leaching of herbicides commonly applied to sugarcane in five agricultural soils. *Planta Daninha*. **2019**, *37*, e019181505. [[CrossRef](#)]
18. PPDB–Pesticide Properties Database. Footprint: Creating Tools for Pesticide Risk Assessment and Management in Europe. Developed by the Agriculture & Environment Research Unit (AERU), University of Hertfordshire, funded by UK National Sources and the EU-Funded FOOTPRINT project (FP6-SSP-022704). Available online: <https://sitem.herts.ac.uk/aeru/ppdb/en/Reports/469.htm> (accessed on 10 March 2022).
19. Lehmann, J.; Joseph, S. Biochar for environmental management: An introduction. In *Biochar for Environmental Management: Science, Technology and Implementation*; Lehmann, J., Joseph, S., Eds.; Routledge: New York, NY, USA, 2015; pp. 1–13.
20. Qiu, M.; Liu, L.; Ling, Q.; Cai, Y.; Yu, S.; Wang, S.; Fu, D.; Hu, B.; Wang, X. Biochar for the removal of contaminants from soil and water: A review. *Biochar* **2022**, *4*, 19. [[CrossRef](#)]
21. Li, L.; Zou, D.; Xiao, Z.; Zeng, X.; Zhang, L.; Jiang, L.; Liu, F. Biochar as a sorbent for emerging contaminants enables improvements in waste management and sustainable resource use. *J. Cleaner Product.* **2019**, *210*, 1324–1342. [[CrossRef](#)]
22. Chen, Y.N.; Chai, L.Y.; Shu, Y.D. Study of arsenic (V) adsorption on bone char from aqueous solution. *J. Hazard. Mater.* **2008**, *160*, 168–172. [[CrossRef](#)]
23. Mendes, K.F.; Freguglia, R.M.O.; Martins, B.A.B.; Dias, R.C.; Pimpinato, R.F.; Tornisielo, V.L. Cow bonechar for pesticide removal from drinking water. *J. Agric. Vet. Sci.* **2017**, *4*, 504–512.
24. Lipczynska-Kochany, E. Effect of climate change on humic substances and associated impacts on the quality of surface water and groundwater: A review. *Sci. Total Environ.* **2018**, *640*, 1548–1565. [[CrossRef](#)]
25. Da Ros, S.; Aliev, A.E.; del Gaudio, I.; King, R.; Pokorska, A.; Kearney, M.; Curran, K. Characterising plasticised cellulose acetate-based historic artefacts by NMR spectroscopy: A new approach for quantifying the degree of substitution and diethyl phthalate contents. *Polym. Degrad. Stab.* **2021**, *183*, 109420. [[CrossRef](#)]
26. Fischer, S.; Thümmel, K.; Volkert, B.; Hettrich, K.; Schmidt, I.; Fischer, K. Properties and applications of cellulose acetate. *Macromol. Symp.* **2008**, *262*, 89–96. [[CrossRef](#)]
27. Pinto, M.D.C.E.; Da Silva, D.D.; Gomes, A.L.A.; Leite, V.D.S.A.E.; Moraes, A.R.F.; De Novais, R.F.; Tronto, J.; Pinto, F.G. Film based on magnesium impregnated biochar/cellulose acetate for phosphorus adsorption from aqueous solution. *RSC Advances* **2019**, *9*, 5620–5627. [[CrossRef](#)] [[PubMed](#)]
28. Vinhal, J.; Lima, C.; Cassella, R. Sorption of the herbicides diquat and difenzoquat from aqueous medium by polymeric resins in the presence of sodium dodecylsulfate: Kinetic and mechanistic study. *J. Environ. Sci. Health B* **2016**, *51*, 482–489. [[CrossRef](#)]
29. Kumar, Y.; Singh, N.; Singh, S. Removal of herbicides mixture of atrazine, metribuzin, metolachlor and alachlor from water using granular carbon. *Indian J. Chem. Technol.* **2017**, *24*, 400–404.
30. Zhong, B.; Wang, S.; Dong, H.; Luo, Y.; Jia, Z.; Zhou, X.; Chen, M.; Xie, D.; Jia, J. Halloysite tubes as nanocontainers for herbicide and its controlled release in biodegradable poly(vinyl alcohol)/starch film. *J. Agric. Food Chem.* **2017**, *65*, 10445–10451. [[CrossRef](#)]
31. Shattar, S.; Zalzarria, N.; Foo, K. Preparation of a montmorillonite-derived adsorbent for the practical treatment of ionic and nonionic pesticides. *J. Mater. Res. Technol.* **2019**, *8*, 4713–4724. [[CrossRef](#)]
32. Liu, L.; Dai, Y. Strong adsorption of metolachlor by biochar prepared from walnut shells in water. *Environ. Sci. Pollut. Res.* **2021**, *28*, 48379–48391. [[CrossRef](#)]
33. Mendes, K.F.; Hall, K.E.; Takeshita, V.; Rossi, M.L.; Tornisielo, V.L. Animal bonechar increases sorption and decreases leaching potential of aminocyclopyrachlor and mesotrione in a tropical soil. *Geoderma* **2018**, *316*, 11–18. [[CrossRef](#)]
34. Mendes, K.F.; de Sousa, R.N.; Takeshita, V.; Alonso, F.G.; Régo, A.P.J.; Tornisielo, V.L. Cow bone char as a sorbent to increase sorption and decrease mobility of hexazinone, metribuzin, and quinclorac in soil. *Geoderma* **2019**, *343*, 40–49. [[CrossRef](#)]
35. Nilsson, R.; Olsson, M.; Westman, G.; Matic, A.; Larsson, A. Screening of hydrogen bonds in modified cellulose acetates with alkyl chain substitutions. *Carbohydr. Polym.* **2022**, *285*, 119188. [[CrossRef](#)]
36. OECD–Organisation for Economic Co-Operation and Development. *Adsorption—Desorption Using A Batch Equilibrium Method*; OECD: Paris, France, 2000; 44p, OECD, 106.

37. Mendes, K.F.; Sousa, R.N.; Soares, M.B.; Viana, D.G.; Souza, A.J. Sorption and desorption studies of herbicides in the soil by batch equilibrium and stirred flow methods. In *Radioisotopes in Weed Research*; Mendes, K.F., Ed.; CRC Press: Boca Raton, FL, USA, 2021; Volume 1, pp. 17–61.
38. López-Piñeiro, A.; Peña, D.; Albarrán, A.; Becerra, D.; Sánchez-Llerena, J. Sorption, leaching and persistence of metribuzin in Mediterranean soils amended with olive mill waste of different degrees of organic matter maturity. *J. Environ. Manag.* **2013**, *122*, 76–84. [[CrossRef](#)] [[PubMed](#)]
39. Loffredo, E.; Parlavecchia, M.; Perri, G.; Gattullo, R. Comparative assessment of metribuzin sorption efficiency of biochar, hydrochar and vermicompost. *J. Environ. Sci. Health Part B* **2019**, *54*, 728–735. [[CrossRef](#)] [[PubMed](#)]
40. Cabrera, A.; Cox, L.; Spokas, K.U.R.T.; Hermosín, M.C.; Cornejo, J.; Koskinen, W.C. Influence of biochar amendments on the sorption-desorption of aminocyclopyrachlor, bentazone and pyraclostrobin pesticides to an agricultural soil. *Sci. Total Environ.* **2014**, *470*, 438–443. [[CrossRef](#)] [[PubMed](#)]
41. Shahid, M.K.; Kim, J.Y.; Choi, Y.G. Synthesis of bone char from cattle bones and its application for fluoride removal from the contaminated water. *Groundw. Sustain. Dev.* **2019**, *8*, 324–331. [[CrossRef](#)]
42. Nigri, E.M.; Bhatnagar, A.; Rocha, S.D.F. Thermal regeneration process of bone char used in the fluoride removal from aqueous solution. *J. Clean Prod.* **2017**, *142*, 3558–3570. [[CrossRef](#)]
43. Mendes, K.F.; Furtado, I.F.; Sousa, R.N.D.; Lima, A.D.C.; Mielke, K.C.; Brochado, M.G.D.S. Cow bonechar decreases indaziflam pre-emergence herbicidal activity in tropical soil. *J. Environ. Sci. Health Part B* **2021**, *56*, 532–539. [[CrossRef](#)]
44. Jia, P.; Tan, H.; Liu, K.; Gao, W. Removal of methylene blue from aqueous solution by bone char. *Appl. Sci.* **2018**, *8*, 1903. [[CrossRef](#)]
45. Liu, K.; Li, F.; Tian, Q.; Nie, C.; Ma, Y.; Zhu, Z.; Liu, S. A highly porous animal bone-derived char with a superiority of promoting nZVI for Cr (VI) sequestration in agricultural soils. *J. Environ. Sci.* **2021**, *104*, 27–39. [[CrossRef](#)]
46. Alkurdi, S.S.; Al-Juboori, R.A.; Bundschuh, J.; Bowtell, L.; Marchuk, A. Inorganic arsenic species removal from water using bone char: A detailed study on adsorption kinetic and isotherm models using error functions analysis. *J. Hazard. Mater.* **2021**, *405*, 124112. [[CrossRef](#)]
47. Azeem, M.; Shaheen, S.M.; Ali, A.; Jeyasundar, P.G.; Latif, A.; Abdelrahman, H.; Li, R.; Almazroui, M.; Niazi, N.K.; Sarmah, A.K.; et al. Removal of potentially toxic elements from contaminated soil and water using bone char compared to plant-and bone-derived biochars: A review. *J. Hazard. Mater.* **2022**, *427*, 128131. [[CrossRef](#)]
48. Albatrni, H.; Qiblawey, H.; El-Naas, M.H. Comparative study between adsorption and membrane technologies for the removal of mercury. *Sep. Purif. Technol.* **2021**, *257*, 117833. [[CrossRef](#)]
49. Liu, J.; Huang, X.; Liu, J.; Wang, W.; Zhang, W.; Dong, F. Adsorption of arsenic (V) on bone char: Batch, column and modeling studies. *Environ. Earth Sci.* **2014**, *72*, 2081–2090. [[CrossRef](#)]
50. Hyder, A.H.M.G.; Begum, S.A.; Egiebor, N.O. Adsorption isotherm and kinetic studies of hexavalent chromium removal from aqueous solution onto bone char. *J. Environ. Chem. Eng.* **2015**, *3*, 1329–1336. [[CrossRef](#)]
51. Al-Ghouti, M.A.; Da'ana, D.A. Guidelines for the use and interpretation of adsorption isotherm models: A review. *J. Hazard. Mater.* **2020**, *393*, 122383. [[CrossRef](#)] [[PubMed](#)]
52. Ara, B.; Shah, J.; Jan, M.R.; Aslam, S. Removal of metribuzin herbicide from aqueous solution using corn cob. *Int. J. Sci. Environ. Technol.* **2013**, *2*, 146–161.
53. Cara, I.G.; Filip, M.; Bulgariu, L.; Raus, L.; Topa, D.; Jitareanu, G. Environmental remediation of metribuzin herbicide by mesoporous carbon rich from wheat straw. *Appl. Sci.* **2021**, *11*, 4935. [[CrossRef](#)]
54. Rojas-Mayorga, C.K.; Bonilla-Petriciolet, A.; Aguayo-Villarreal, I.A.; Hernandez-Montoya, V.; Moreno-Virgen, M.R.; Tovar-Gómez, R.; Montes-Morán, M.A. Optimization of pyrolysis conditions and adsorption properties of bone char for fluoride removal from water. *J. Anal. Appl. Pyrolysis* **2013**, *104*, 10–18. [[CrossRef](#)]
55. Sousa, R.N.; Soares, M.B.; Santos, F.H.; Leite, C.N.; Mendes, K.F. Interaction mechanisms between biochar and herbicides. In *Interactions of Biochar and Herbicides in the Environment*; Mendes, K.F., Ed.; CRC Press: Boca Raton, FL, USA, 2022; pp. 80–105.
56. Xiao, F.; Pignatello, J.J. $\pi^+ - \pi$ Interactions between (Hetero) aromatic Amine cations and the graphitic surfaces of pyrogenic carbonaceous materials. *Environ. Sci. Technol.* **2015**, *49*, 906–914. [[CrossRef](#)]
57. Essandoh, M.; Wolgemuth, D.; Pittman, C.U.; Mohan, D.; Mlsna, T. Adsorption of metribuzin from aqueous solution using magnetic and nonmagnetic sustainable low-cost biochar adsorbents. *Environ. Sci. Pollut. Res.* **2017**, *24*, 4577–4590. [[CrossRef](#)]
58. Landgraf, M.D.; da Silva, S.C.; Rezende, M.O.D.O. Mechanism of metribuzin herbicide sorption by humic acid samples from peat and vermicompost. *Anal. Chem. Acta.* **1998**, *368*, 155–164. [[CrossRef](#)]
59. Cerejeira, M.J.; Viana, P.; Batista, S.; Pereira, T.; Silva, E.; Valério, M.J.; Silva-Fernandes, A.M. Pesticides in Portuguese surface and ground waters. *Water Res.* **2003**, *37*, 1055–1063. [[CrossRef](#)]
60. Castro, G.F.; Ferreira, J.A.; Eulálio, D.; Moraes, A.R.F.; Regina, V.; Constantino, L.; Pinto, F.G.; Novais, R.F.; Tronto, J. Organic-Inorganic Hybrid Materials: Layered Double Hydroxides and Cellulose Acetate Films as Phosphate Recovery. *J. Agric. Sci. Technol. B* **2018**, *8*, 360–374. [[CrossRef](#)]
61. Kabiri, K.; Zohuriaan-Mehr, M. Superabsorbent hydrogel composites. *Polym. Adv. Technol.* **2003**, *14*, 438–444. [[CrossRef](#)]
62. Nazir, M.S.; Tahir, Z.; Hassan, S.U.; Ali, Z.; Akhtar, M.N.; Azam, K.; Abdullah, M.A. Remediation of pesticide in water. In *Sustainable Agriculture Reviews*; Lichtfouse, E., Ed.; Springer: New Delhi, India, 2021; pp. 271–307.
63. Mphateng, T.N.; Mapossa, A.B.; Wesley-Smith, J.; Ramjee, S.; Focke, W.W. Cellulose acetate/organoclay nanocomposites as controlled release matrices for pest control applications. *Cellulose* **2022**, *29*, 3915–3933. [[CrossRef](#)]

64. Wu, L.; Liu, M. Preparation and properties of chitosan-coated NPK compound fertilizer with controlled-release and water-retention. *Carbohydr. Polym.* **2008**, *72*, 240–247. [[CrossRef](#)]

GENERAL CONCLUSIONS

The results of this study demonstrated that sugarcane straw biochar has a direct impact on the sorption, desorption, and degradation of metribuzin in the soil, which is influenced by the application rate and pyrolysis temperature. However, it is important to highlight that the behavior of metribuzin in the soil is influenced by the physicochemical characteristics of the herbicide, soil, and biochar. This means that under field conditions, the observed results in this study may vary.

Application rates of 1% and 1.5% of BC350, BC550, and BC750 showed a lower impact on the sorption and desorption of metribuzin and can improve soil fertility by providing phosphorus (P), potassium (K), magnesium (Mg), iron (Fe), and manganese (Mn), as well as reducing potential acidity (H+Al) and increasing soil pH. Unlike sorption and desorption, higher degradation of metribuzin was observed for biochars produced at higher pyrolysis temperatures (BC550 and BC750) when added to the soil at lower application rates (0.1% to 1.5%).

From an environmental remediation perspective, soil modified with BC750 has a high potential to reduce the mobility and risks of environmental contamination of metribuzin, as well as mitigate issues related to the herbicide's persistence in subsequent crops. However, it is important to note that the sorption and degradation of metribuzin increase while desorption decreases with higher application rates of biochar, which may have a negative effect on the bioavailability of metribuzin in the soil solution. In agronomic terms, this can impact the residual effect of metribuzin in the soil and decrease its effectiveness in weed control.

When evaluating the efficiency of the cellulose acetate film with bone char, it was found that this approach could become a viable alternative for the removal of metribuzin from water. The addition of 2 g and 3 g of bone char sorbed 40% and 60% of metribuzin, respectively, at concentrations of 0.25, 0.33, and 0.5 mg L⁻¹. As for desorption, a low rate was observed, with 7% in 24 hours and 2.5% in 120 hours for both films. The use of cellulose acetate for bone char fixation has not been documented in the scientific literature, representing a technological innovation for herbicide removal from water.